UNIVERSITY OF CALIFORNIA, SAN DIEGO

# Tectonic and stratigraphic evolution of the Tjörnes Fracture Zone, Northern Iceland.

A Dissertation submitted in partial satisfaction of the
Requirements for the degree Doctor of Philosophy

in

Earth Sciences

by

Rebecca Ann Fenwick

Committee in charge:

Professor Neal Driscoll, Chair
Professor Kevin Brown
Professor Steve Cande
Professor Graham Kent
Professor Falko Kuester

2010

The Dissertation of Rebecca Ann Fenwick is approved, and it is acceptable in quality and form for publication on microfilm, and electronically:

_____

_____

_____

_____

_____

Chair

University of California, San Diego

2010

# DEDICATION

I dedicate this manuscript to all my family and friends who have helped, supported me and generally put up with me during my time in graduate school. You have no idea how much your support has meant to me,

Thanks and this one's for you!

TABLE OF CONTENTS

LIST OF FIGURES

LIST OF TABLES

ACKNOWLEDGEMENTS

I would like to acknowledge Professor Neal Driscoll, without whom none of this would have been possible. His support as the chair of my committee has been invaluable, but beyond that his support as my friend has made the process of obtaining my PhD possible. While working in Iceland Bryndis Brandsdóttir, Jeff Karsen and Krisjan Saemundsson were invaluable with their help, support and insight into Icelandic geology. Graham Kent has also been a fantastic source of support and has taught me an immense amount about seismic processing. I would also like to thank the “Party Lab” and all my friends at SIO for all their help in learning to play “fooze” and other life skills. Without those guys my time in grad school would not have been as productive or as much fun!

My family, as always, has been incredibly supportive of my plans, crazy schemes and goals. Thank you from the bottom of my heart for everything that you have done and all the opportunities that you have afforded me throughout my life. A special thank you goes to two of my professors from the University of Birmingham without whom none of this would have happened, to Dr Andy Chambers for offering me a place to pursue my love of earth science, and to Dr Graham Westbrook for introducing me to marine geology and geophysics and encouraging me to pursue a PhD here at SIO.

There are so many people to acknowledge and thank, but know that I appreciate everyone of you!

## MATERIAL SUBMITTED FOR PUBLICATION

Chapter 2 was submitted for publication in Marine Geology, 2009 as: Fenwick, Rebecca; Brandsóttir, Bryndís; Driscoll, Neal; Detrick, Robert; Kent, Graham; Babcock, Jeffrey; “Tectonic Deformation on the Húsavík-Flatey Fault, Northern Iceland”. The dissertation author was the primary investigator and author of this paper.

# VITA

## Education

2002 Master in Science, University of Birmingham, UK

2010 Doctor of Philosophy, University of California, San Diego

## Publications

Fenwick, R., Brandsdóttir, B., Driscoll, N., Detrick, R., Kent G., Tectonic Deformation on the Húsavík-Flatey Fault, Northern Iceland, *Marine Geology*, *accepted*

Fenwick R.A., Driscoll N.W., Detrick R., Brandsdóttír B., Fornari D., Richter B., 2006, Evidence for Fluid Flow Along the Húsavík Flatey Fault, Northern Iceland. American Geophysical Union, Spring Meeting 2006, abstract #T41A-06.

Fenwick R.A., Driscoll N.W., Babcock J.M., 2004, Transgressive Sequence Development on the Northern California Continental Shelf, American Geophysical Union, Fall Meeting 2004, abstract #OS1D-0522

ABSTRACT OF THE DISSERTATION

Tectonic and Stratigraphic evolution of the
Tjörnes Fracture Zone, Northern Iceland

by

Rebecca Ann Fenwick

Doctor of Philosophy in Earth Sciences

University of California, San Diego, 2010

Professor Neal Driscoll, Chair

Rifted margins and plate boundary tectonics dominate the surface morphology of the ocean basins, in particular the processes that occur in rifted margins and transform fault zones remain poorly understood. Northern Iceland is an ideal area to investigate distributed extensional deformation and the evolution of transform fault zones because of the repeated rift jumps eastward back to the Iceland plume. Studying this continually evolving system allows us the opportunity to understand better the complicated nature of evolving transform faults.

Using CHIRP subbottom, MCS, multibeam bathymetry, side-scan sonar, and towcam images we imaged the three basins that comprise the

Tjörnes Fracture Zone: Eyjafjördur, Skjálfandi, and Öxarfjördur bays. In the Tjörnes Fracture Zone, there appears to have been an initial stage of distributed extension accommodation: graben faulting with normal faults accommodating the extension between the newly formed North Volcanic Zone and the southern extent of the Kolbeinsey Ridge. This appears to have been followed and overprinted by more traditional oceanic transform faulting, with the development of the Húsavík-Flatey Fault and then the Grímsey Lineament that was subsequently formed with the northward propagation of the North Volcanic Zone.

Pockmarks are increasingly being commonly identified along margins, and our data allowed us to investigate controls over their occurrence, morphology and location in Skjálfandi Bay. In this area they have been observed in a band 15-22 km offshore, and in along the Húsavík-Flatey fault scarp near shore. Pockmarks along the fault scarp are easily attributed to fluid migration along the fault plan from depth, and we observed an increasing biota density and abundance within these pockmarks. This is likely due to either an increased nutrient flux from depth or increased detrital deposition within the pockmarks. Offshore pockmarks occur in a well-defined band determined by the interplay of the distribution of source material and the thickness of the overlying glacial sediments. The westward dipping layers at depth act as fluid flow pathways, resulting in linear pockmark chains on the seafloor. They are

further modified by sea floor currents creating an asymmetric profile with the long axis orientated with the current moving clockwise around the basin.

Through time as the North Volcanic Zone becomes more organized the extensional deformation was replaced by dextral strike-slip faults giving rise to the Húsavík-Flatey fault. The deformation along the Húsavík-Flatey fault is ongoing, albeit decreased from the maximum that occurred in the Miocene. This decrease in activity is the result of the North Volcanic Zone propagating past the Húsavík-Flatey fault and transferring a portion of the deformation to the Grimsey Lineament. Based on GPS data, the deformation is approximately equal between the Húsavík-Flatey fault and the Grimsey Lineament. This northward migration of the North Volcanic Zone is accompanied by the northward retreat of the Kolbeinsey Ridge imparting a clockwise rotation that reactivates the N-S normal faults as oblique slip sinistral strike-slip faults in the manner of bookshelf faulting.

# Chapter 1

# Introduction

In the last several decades, Earth and Ocean scientists have come to recognize a number of globally significant processes operating across many temporal and spatial scales within the ocean basins. Rifted margins and other interactions along plate boundaries dominate the surface morphology and deformational dynamics of our entire planet. Rifted margins and transform fault zones are areas of continued study, but many of the processes that shape them remain poorly understood. Understanding the evolution from continental rifting to seafloor spreading is a fundamental problem in the Earth Sciences, however, many of these transitions are obscured by thick wedges of sediment. Northern Iceland is an ideal area to examine distributed extensional deformation and the evolution of transform fault zones because of the eastward ridge jumps back to the  Iceland plume. Deformational and/or thermal processes that operate most intensely near plate margins and less intensely within plate interiors, result in a wide variety of fluid flow within the crust and between the crust and overlying ocean. The over arching goal of this thesis is to increase our understanding of the mechanics of transform fault evolution/formation and in addition, the specific neotectonic history of Northeastern Iceland.

Sedimentelogical records play a key role in teasing apart details and timelines and accommodation space for these sediments is governed by a complex interplay of tectonics, sea level fluctuations and climate. The time

frame that we are examining includes extensive glacial cycles, the Last Glacial Maximum (LGM) concomitant with a rapidly evolving plate boundary. The Northern Volcanic Zone (NVZ) is propagating northwards offshore, while the Kolbeinsey Ridge retreats northward, which creates a northward migrating zone of deformation. The changing tectonic and climatic conditions also directly effect the seafloor surface and through this the biota that inhabit the seafloor. Proximity to the plume head increases the thermal gradient, decreasing the depth of the hydrocarbon cracking window leading to thermogenic gases fluxing through the seafloor.

The research in this thesis primarily focuses on the tectonic and stratigraphic evolution of a migrating fracture zone driven by rift jumps and northward propagation using a variety of geophysical sampling tools (e.g. CHIRP subbottom data, side-scan sonar data, seafloor towcam images, multibeam bathymetry, sedimentary cores, and earthquake location data). In Chapter 2, we focus on the Húsavík-Flatey Fault, historically thought to be the main transform fault in the Tjörnes Fracture Zone. Onshore this fault system has large offsets where the fault trace joins the Theistareykir Fissure Swarm (vertical 200-1400 m, horizontal 5-60 km) and has been the site for large magnitude earthquakes. Borehole data near the 1872 ground break shows that the top 250 m sediments exhibit limited amounts of deformation. As the fault approaches the fissure swarm it changes character from a right lateral

strike-slip to an oblique normal fault. Offshore moving to the northwest towards the southern extent of the Kolbeinsey Ridge the CHIRP and MCS data show little offset in the transparent Holocene packages indicating that the dip slip component along the HFF has been insignificant in the last 3000 yrs. The large offset identified in the MCS at depth is consistent with considerable deformation and movement along the fault occurring in the Miocene, Pliocene and Pleistocene and with the deformation history observed in the Miocene basalts in the sea cliffs. Variation in the thickness of the sediments in the bay is controlled by differences in sediment supply and dispersal, not fault controlled accommodation differences. As the recent deformation appears to be decreasing along the HFF, we believe that some portion has been transferred north to the tectonically active Grímsey Lineament. This occurred primarily as a result of the propagation of the NVZ and retreat of the KR.

In Chapter 3, we focus in on the seafloor in Skjálfandi Bay and the fluid expulsion as recorded by pockmarks. There is a large pockmark field located in the central bay along with a smaller more localized field around the western HFF. Pockmarks are observed in the multibeam, sidescan, and CHIRP data as well as towcam images in several locations and scales. Central pockmarks are constrained to a band ~15-22 km from shore where the orientation of pockmarks consistently rotates around the bay, where the long axis it

interpreted to align with the bottom current flow direction. In plan view, these pockmarks are v shaped, some with a series of smaller pocks at the narrow deeper down current end. To explain the occurrence of the pockmarks, requires an interplay of organic source material and sediment over burden, we postulate that in this region the glacial/inter glacial sediments are thin enough not to act as a permeability barrier but is proximal enough to have organic rich sediments and also thick enough to allow some build up of fluids so as to create the pockmarks. Their exact distribution within this band is also governed by the west dipping strata that appear to control fluid migration pathways. Bottom currents then overprint the morphology of the linear chains of pockmarks by elongating their seafloor profile through erosion of the down current end.

Pockmarks along the HFF are tectonically controlled with the fault acting as a fluid pathway to the surface from depth. This focus of potentially nutrient rich fluids increases the biodiversity locally seen in the towcam photos of the seafloor. Pockmarks are only located along the fault in the western half of the bay where there is ~15 m of relief. The larger pockmarks are located on the uplifted side of the fault scarp and within them there are smaller pocks and a higher biodiversity. The biodiversity of the seafloor decreases away from the fault and away from the larger pockmarks.

Stepping back to investigate the larger tectonic picture of the TFZ, in Chapter 4 we examine the geologic and tectonic evolution. Using the dense grid of MCS data and swath bathymetry we observed a complex history of deformation that combines strike-slip faulting and block rotation with a small amount of early deformation accommodated by extension across Eyjafjördur, Skjálfandi and Öxarfjördur bays. Extension appears to have occurred only in the early stages of the NVZ establishing as a rift zone after the rift jump was completed at 3 Ma, while the Dalvík Lineament acts as the southern boundary of deformation. Once the NVZ propagated to the north and the Kolbeinsey Ridge retreats to the north, the Húsavík-Flatey Fault was established and was the main focus of dextral deformation. Once the ongoing propagation passes the Húsavík-Flatey Fault, a portion of dextral strike-slip deformation was relayed northward to the Grímsey Lineament. We predict that with continued propagation and retreat northward of the North Volcanic Zone and the Kolbeinsey Ridge respectively, more deformation will be accommodated by the Grímsey Lineament, and less by the Húsavík-Flatey Fault until a complete transfer of deformation has occurred.

# Chapter 2

# Tectonic Deformation on the Húsavík-Flatey Fault, Northern Iceland

## 2.1 ABSTRACT

CHIRP subbottom data, MCS seismic reflection and multibeam bathymetric data reveal the tectonic history of the Húsavík-Flatey Fault (HFF). MCS data across the HFF image significant deformation at depth with large fault offsets (>100 m) observed within basal sequences. The deformation diminishes up section as evidenced by the surficial CHIRP data, which imaged only minor vertical displacement with little to no evidence of fault growth. Onshore the deformation across the HFF is large, with vertical offsets of 200-1400 m and horizontal displacements on the order of 5-60 km. Borehole data acquired across the fault zone suggests that the deformation occurred predominantly during the late Miocene/Pliocene with only minimal offset of late Pleistocene and younger horizons. The onshore deformation records the last 7-9 Ma whereas the offshore stratigraphy imaged by the CHIRP and MCS data records only the last 20-45 kys and 300-500 kyrs respectively. The minor amount of Pleistocene to Recent deformation observed on the HFF both onshore and offshore is consistent with the northward propagation of the Northern Volcanic Zone (NVZ) at 1.5-2 Ma, which transferred the majority of deformation northward to the Grímsey Lineament.

## 2.2 INTRODUCTION

The westward migration of the North American-Eurasian plate boundary and the presence of a mantle plume beneath central, eastern Iceland results in the ridges to the north and south of Iceland (Kolbeinsey Ridge (KR), Reykjanes Ridge (RR)) being offset to the west with respect to the main volcanic rift zones across Iceland (Garcia et al., 2003, Rögnvaldsson et al., 1998, Einarsson 1991, Helgason 1985, Jancin et al., 1985, McMaster and Schilling, 1977, Saemundsson 1974). This offset has been evolving since ~6-7 Ma with the Tjörnes Fracture Zone (TFZ) accommodating the deformation between the northward propagating NVZ and the KR (Jancin et al., 1985, Saemundsson 1974, 1979)

The TFZ provides an ideal locale to examine how strain is accommodated and transferred between a transform fault and ridge segments (volcanic systems) as they propagate. Deformation along the 120 km long and 70-80 km wide TFZ has occurred in response to the eastward rift jumps, from the Húnaflói-Skagi zone via the Skagafjördur rift to the currently active NVZ. In addition, the NVZ has been propagating to the north, bypassing the HFF at about 2 Ma (Saemundsson 1974, 1978). Recent Ar-Ar dating (Garcia et al., 2003) indicates that the Skagafjördur rift zone and the NVZ coexisted for approximately 5-5.5 Ma until extension was fully transferred to the NVZ at 3 Ma.

Presently, the TFZ encompasses three major N-S striking extensional basins, Eyjafjördur, Skjálfandi and Öxarfjördur as well as three seismically active WNW-striking lineaments, the Grímsey Lineament (GL), Húsavík-Flatey Fault (HFF) and Dalvík Lineament (DL) (Saemundsson 1974, 1979 Fig. 2.1). The Grímsey Lineament is the offshore connection between the NVZ and the Kolbeinsey Ridge, whereas the right-lateral Húsavík-Flatey Fault connects the NVZ with the westernmost basin, Eyjafjördur, the magma starved southern extension of the Kolbeinsey Ridge. As the NVZ propagated northward, deformation within the TFZ shifted from predominately strike-slip motion along the Húsavík-Flatey Fault to strike slip and extension along four en-echelon rift segments (volcanic systems) within the GL (Sæmundsson, 1974, 1978). Based on the NUVEL-1A spreading model of DeMetz (1994) a fairly constant spreading rate of approximately 18 mm/yr along a 105° azimuth is inferred across the KR-TFZ-NVZ. Data from a continuous GPS station ARHO within the TFZ, suggests that at present a similar amount of strain is being accommodated at the HFF and the GL (Geirsson et al., 2006). Earthquake solutions indicate that the deformation in the TFZ is being accommodated by both extension and strike-slip motion (Rögnvaldsson et al., 1998; Porbjarnardóttir et al., 2003).

Onshore the HFF is manifested by a 25 km NW-trending scarp

exceeding 200-1400 m, with an inferred horizontal displacement of 5-60 km (Bergerat et al., 2000, Anglier et al., 2000, Fjäder et al., 1994, Gudmundsson et al., 1993, Jancin et al., 1985, Saemundsson 1974, Tryggvason 1973). Borehole data across the fault scarp north of Húsavík suggests there is little to no offset or rotation of the inter-glacial sediments at a depth of 250 m (Saemundsson 1974). Extensive conjugate faulting and dike intrusion along the HFF is also well documented on Flateyjarskagi Peninsula (Bergerat et al., 2000, Anglier et al., 2000, Jancin et al., 1985, Fjäder et al., 1994, Young et al., 1985), however, the majority of this deformation occurred in late Miocene and Pliocene time (Saemundsson 1974).

The HFF changes character along its length, at its western extent in the Eyjafjördur Bay it begins as several overlapping fault strands that bound an EW trending basin between Flateyjarskagi Peninsula and Flatey Island. Near the Flateyjarskagi Peninsula the HFF is characterized by one major fault strand dipping to the north. Upon entering Skjálfandi bay yet another fault strand becomes dominant, switching polarity to a south dipping fault. The surface expression of the fault decreases markedly from the Eyjafjördur to Skjálfandi bay, the relief created by the fault changing from 300 m in the west to little to no surface expression in the east.

The offshore section of the GL is seismically very active

(Porbjarnardóttir et al., 2003; Riedel et al., 2003, Rögnvaldsson et al., 1998). The Dalvík Lineament onshore is identified by morphologic features (e.g., river canyons) and limited seismic activity (Rögnvaldsson et al., 1998, Einarsson 1991, Mamula and Voight 1985). In an effort to further our understanding of tectonics and mechanics of strain partitioning within the TFZ, we acquired CHIRP subbottom and multi-channel seismic (MCS) data as well as multibeam bathymetry in 2001-2003 (Fig. 2.1).

## 2.3 DATA ACQUISITION

Data presented here were collected by two high-resolution seismic systems; a SUBSCAN CHIRP/Side Scan Sonar and a portable High-Resolution Multichannel Seismic Acquisition System (MCS) in 2001 and multibeam swath bathymetry in 2002 and 2003. The Lamont High-Resolution system is a portable multichannel seismic profiling system designed to image sediment structure to depths of more than 1 km depth with a vertical resolution of 2-5 m. The system consists of a 210 cubic inch Gas Injection (GI) gun by Seismic Systems Inc., a 600 m long ITI streamer with 193 hydrophones in 48 groups with a 12.5 m group interval and an OYO DAS-1 digital acquisition system. An air-cooled Price A-35 compressor can fire the GI gun at a shot interval of approximately 5 s (12.5 m). A Sun-based shipboard system running SIOSEIS was used to produce near-real-time brute stacks of each line. These

brute stacks were invaluable in assessing data quality and in making a preliminary interpretation of the deformation in the HFF.

The Edgetech SB0512 seismic sub-bottom CHIRP system used in the TFZ survey sweeps across 1.0 to 6.0 kHz in 50 ms. This yields subbottom penetration on the order of 30-40 m with sub-meter resolution. The remotely controlled system consists of a DF1000 side scan towfish and a X-Star subbottom sonar including a SB0516 tow fish and a real-time data display. Towfish navigation was obtained in relation to topside differential global positioning service (DGPS) receivers, and post processing alignment with bathymetric data. The MCS and CHIRP data were acquired concurrently at about 5 knots allowing a nested approach for high-resolution data collection both in the uppermost few tens of meters down to several hundred meters depth. Owing to favorable weather conditions throughout the cruise, more extensive reflection coverage was obtained than originally planned, a total of 1600 km acquired across the three bays (Eyjafjördur, Skjálfandi, and Öxarfjördur). Here, we present MCS and Chirp data from the Skjálfandi Bay, processed using the SIOSEIS (Henkart, 2003) and Seismic Unix (Cohen and Stockwell, 1999) processing software packages.

## 2.4 RESULTS

### 2.4.1 Sediment character variation

The insular margin of Iceland is incised by several major fjords, which occupy extensional basins, within which major ice streams flowed during recent glaciations. The iceberg scoured bank areas are nearly devoid of sediments that have accumulated within the fjords and basins. Our MCS and CHIRP data indicate that sediment thickness within the TFZ varies considerably within the area, the sediment carapace is underlain by a system of highly reflective basement ridges. Where visible at the surface, these basement ridges are V-shaped, characteristically up to 1 km long and 300-500 m wide, and are likely to be extensional features modified by glacial ice streams flowing seaward.

There are no cores from within Skjálfandi Bay itself, the closest being MD992275, located about 50 km north of central Skjálfandi Bay on CHIRP L7 (Fig. 2.1). The core was acquired for paleoclimate studies and thus sampled a region with a thick post-glacial sequence as imaged by the CHIRP data (Fig. 2.2). The tephra layers and biostratigraphy sampled in core MD992275 provide chronostratigraphic constraints for the sediment packages observed in Skjálfandi Bay (Knudsen and Eiríksson, 2002; Knudsen et al., 2008). Based on correlation of the CHIRP data with the core MD992275 (Fig. 2.3), the transparent acoustic section of the CHIRP data correlates with Holocene sediments overlying highly reflective late glacial and early post-glacial

diamictites and turbidites. Reflectors within the transparent layer may be generated by tephra layers or coarse sediment emplaced by jökulhlaups (large floods) associated with drainage of glacially dammed lakes and subglacial volcanic events.

Tephra layers already identified at core site MD992275 are Hekla 3 (2980 cal. year BP) at approximately 6.8 m depth, Hekla 4 (4200 cal. year BP) at 9.4 m, Hekla 5 (7100 cal. year BP) at 15.5 m, the Saksunarvatn tephra from Grímsvötn, Vatnajökull (~10200 cal. year BP) at 26 m, and the Vedde ash from Katla at 34.2 m (~12000 BP, corresponding to Ash Zone 1 in the N-Atlantic), constrain average sedimentation rates to vary from 2.1 to 3.5 m/kyr (Knudsen and Eiríksson, 2002; Knudsen et al., 2008). The basaltic Saksunarvatn tephra is a major sediment marker, traceable as a prominent reflector across the insular margin of Iceland. Being 6-8 cm thick at a depth of 35 m in MD992275 (Knudsen and Eiríksson, 2002) and 3-4 cm thick at a depth of 21 m ín MD992269 in Reykjarfjardaráll, offshore NW-Iceland (Andrews et al., 2002; Kristjánsdóttir et al., 2008). On the basis of acoustic character in the CHIRP data observed in the vicinity of core site MD992275 on CHIRP L7 and that observed on CHIRP L39 (Fig. 2.3), we interpret the prominent reflector at the base of the transparent layer within the Skjálfandi Bay to record the basaltic Saksunarvatn tephra. Given CHIRP line L39 is located in the center of Skjálfandi Bay it samples the thickest sediment preserved in this near shore

region. As this site is closer to land, during much of the glacial period it was ice covered, and during glacial retreat meltwater events and associated sediment-laden flows may have been bypassed the nearshore region, which may explain why the sedimentation rates in the bay are significantly less than those farther offshore (e.g., 0.9-1 m/kyr near shore compared to 2.75 m/kyr offshore). . The sedimentation rates observed near shore in Skjálfandi Bay are consistent with Holocene sedimentation rates of 0.5-1.5 m/kyr observed on the Northwestern shelf of Iceland, regions devoid of glacial river sediment input (core sites MD99-2264 and MD99-2265;Geirsdóttir et al., 2002; Ólafsdóttir et al., 2005), Skjálfandafljót, a major glacier river in Iceland, has been the main source of sediments into the Skjálfandi Bay in postglacial times entering Skjálfandi Bay in the southwest corner (Fig. 2.4). The subglacial Bárdarbunga system in NW-Vatnajökull lies within the Skjálfandafljót drainage system. Thus Holocene jökulhlaups associated with subglacial volcanism in Bárdarbunga provide an efficient transport mechanism for delivering sediments into the bay, most recently in 1902-03 and 1934 (Björnsson and Einarsson, 1990).

Given both CHIRP (~ 45 m depth resolution) and MCS (~500 m depth resolution) data are presented here we adopted the following labeling scheme to minimize confusion; CHIRP data are labeled using numbers (1-3), while the MCS data are delineated with letters (A-D). There appears to be two main depositional packages imaged in the CHIRP data, the upper 2-5 m of

sediments (Fig. 2.5, package 1, yellow: L42, L40, L39, L30, L38) and the underlying 5-20 m sediments (package 3, blue, on all lines). Package 1, where observed, is not displaced by the fault and drapes (i.e., mimics) underlying morphology. Package 2 (red) is only observed along the western section of the fault and exhibits a wedge shaped geometry thickening towards the fault (divergent wedge, Fig. 2.5). The thickness of the wedge also systematically thins to the NW with increasing distance from the sediment source. The main sediment source for the Skjálfandi Bay is presently from the southwest, along the Skjálfandafljót glacier river. Tides in the bay are anticlockwise resulting in the increased sediment thickness in the southern section of the bay south of the fault. Package 3 is clearly offset in all lines and in L39 and L30 there is some minor local deformation.

A Holocene sediment thickness of 10-25 m in the CHIRP records indicates an average sedimentation rate of 1-2 m/kyr, however there is significant spatial variations in sediment thickness across Skjálfandi Bay. Observed variations in Holocene sediment thickness across the Skjálfandi Bay are most likely caused by tidal currents (traveling clockwise around Iceland) and proximity to the sediment source. Based on the observed deformation and fault offset as well as the stratal geometry across the HFF, three depositional packages have been identified in the CHIRP data. In the upper 15-20 m there is evidence for one large event that offset the stratigraphy; Package 3 on

CHIRP Line L35 is offset ~15 m across the HFF and this offset systematically decreases toward the east to >1 m on CHIRP line L42 (Fig. 2.5).

The MCS data images the older deformation along the fault, (Fig. 2.6). Four stratigraphic units are identified on the basis of their acoustic and deformational character. Unit A (purple) is the basal sequence and is interpreted to be upper Tertiary basaltic basement, with the top of sequence marked by a pronounced angular unconformity. The section (Unit B, orange) overlying the basement dips toward the fault, exhibits divergence, and is preferentially deposited south of the fault scarp. This unit appears to thicken towards the east and is absent north of the fault and has a chaotic acoustic character, which may be indicative of glacial sediments (Fig. 2.6). Moving up section, Unit C, green, is offset across the fault with a marked increase in thickness on the down-thrown block. Unit C is more acoustically chaotic than the overlying section (Unit D, pink) and unit C becomes less chaotic toward the NW away from the sediment source region. Unit D is more acoustically laminated, indicative of a lower energy depositional environment. The vertical displacement across the fault in Unit D is minor compared to the offset at depth, and there is little to no evidence of growth structures across the fault in Unit D within the resolution of the data. All three packages identified within the CHIRP profile are contained within the upper third of Unit D, and show offset on the fault because of the higher vertical resolution (< 1 m) of the data. The

overall structure of the bay is illustrated in Figures 1.7a, 1.7b, with Units C and D thinning to the north, and Unit A dipping to the west.

Within the limits of the CHIRP penetration (45 m), only one potential divergent wedge (a localized triangular wedge of sediment located at the base of the scarp) is observed (Fig. 2.5, L30, L38, L35). The fault relief exhibits variability from west to east, a 15 m throw along L35 diminishes to 0-2 m just west of the town of Húsavík. As the fault trace (heavy black Fig. 2.4) jumps to the north it creates a constraining bend that results in a compressional popup structure at 66°06'N, 34°25'W. To the north and east of the high another set of faults is observed and extends eastward (L39) as four fault splays that coalesce into one trace by L40. In the east there is very little vertical displacement; the largest of which is on L40 (>1 m). There is little to no surface expression of the fault approaching the coast. The basement high reaches a maximum height of 50 m above the surrounding seafloor on L30, it extends north where it is mantled by sediments on L39. One divergent wedge is observed in the CHIRP data, indicating only one major deformation episode within the temporal resolution of the data. In the southeast corner of the bay, the transparent layer (presumably postglacial sediment) reaches a thickness of 15 m, and thins dramatically to the north and west (2-5 m). Sediment thickness varies across the HFF, with the greatest thickness observed south of the fault on the hanging wall in Skjálfandi Bay near the sediment source

region. Continued creep and elastic deformation might explain the microseismicity and lack of pronounced fault offset. The divergent wedge only exists to the west of the popup structure, as this is where the fault has the largest throw and the best conditions for slumping across the fault. The sediment thins away from the
southeastern source. East of the constraining bend a fault system is observed to the north with four splays, which coalesce into one trace towards the east.

Within the resolution of the CHIRP data there appears little or no sign of fault growth. The variability in sediment thickness along the fault reflects the southeast source region and the dispersal patterns from the bay. Deeper in the MCS section (Fig. 2.6,) there is clearly growth on the fault but it is confined to the Pliocene fill (Unit C) and the underlying Miocene strata (Unit B). In addition to the accommodation engendered by the ongoing deformation, Unit C appears to be infilling accommodation created by previous deformation across the fault. Unit D (Pleistocene and Holocene) also exhibits minor offset across the fault.

## 2.5 DISCUSSION

Characteristics of the HFF observed in CHIRP and MCS are consistent with the minor recent deformation observed onshore (Fig. 2.3; Rögnvaldsson et al., 1998, Gudmundsson et al., 1993). The lack of offset in the transparent

Holocene package (CHIRP package 1, L42, 3 m thick) indicates that the dip slip component of movement on the HFF has been insignificant in the last 3000 years, given a sedimentation rate of ~1 m/kyr (Knudsen and Eiriksson 2002, Andrews el. 2000, Eiriksson et al. 2000).

The large offsets observed in the MCS data indicate that there has been significant displacement during the Pleistocene and is consistent with the large deformation and offset observed onshore. The offshore data and onshore boreholes allow a temporal separation of the deformation history that is very difficult to achieve onshore in regions devoid of sediment. The Pleistocene to Recent differential sediment thicknesses observed along the strike of the fault and within the basin reflect differences in sediment supply and dispersal not fault control. Furthermore, there is little to no growth observed across the HFF fault within the late Pleistocene and Recent sediments. As previously mentioned, growth is observed mainly in the Miocene, Pliocene, and early to middle Pleistocene sediments, consistent with the HFF being the main transform during this time frame.

Observations of the HFF on the Tjörnes Peninsula document 200-1400 m vertical displacement from the shoreline to where the HFF coalesces with the Theistareykir fissure swarm (Garcia et al., 2002, Gudmundsson et al., 1993, Jancin et al., 1985, Tryggvason 1973). The deformation and

displacement both increase with greater proximity to the fissure swarm, and the orientation of the fault plane also rotates to that of the rift zone. As the fault approaches the fissure swarm the fault is re-characterized from a right lateral strike slip to an oblique normal fault. Onshore boreholes (Saemundsson, 1974 see their Fig. 2.5) drilled just north of Húsavík Village shows that the top 250 m of material (Foreset breccia of Grjóthváls (interglacial) and Morainic cover (present) only exhibits minor signs of deformation, even though there is at least 500 m vertical displacement between the Tertiary basalts. In summary, the boreholes that sampled across the three fault splays reveal that the upper Pleistocene and younger units have minimal offset with no syn-tectonic thickening.

The sea cliffs and rocks onshore around Húsavík show extensive deformation recording movement along the HFF, but the majority of deformation is observed within older strata (Fig. 2.8a, 1.8b). There are obvious offsets on the NS trending faults to the north of Húsavík (Fig. 2.8a) that occur in Pliocene sandstones, and to the south of Húsavík there are large faults in Pliocene/Miocene basalts (Fig. 2.8b) with up to 50 cm fault gouge. In the more recent Pleistocene strata, the fault offset is much smaller. In an exploratory trench across the HFF ground break of 1872, there were three terraces of basalts that were each offset by 1.5-2m down to the south. The faults offsetting these blocks extended to within 20-50 cm of the surface and were

both filled in with colluvium or were partially open (Fig. 8c). Nevertheless, just to the north of the fault, in a gravel quarry, the recent glacial/postglacial sediments have only limited offsets (Fig. 8d) and show minimal displacement.

If recent displacement has not been primarily accommodated along the HFF, it raises the question, where is the differential displacement accommodated? We return to concepts by Saemundsson (1974; 1979), outlining the northward propagation of the NVZ into Öxarfjördur Bay and along Malrakkaslétta, Peninsula bypassing the HFF fault system by ~1.5 Ma. Since this northward migration, the Grímsey Lineament is now the main transform fault, with decreasing amounts of deformation and reactivation along the HFF. This is consistent with the offshore data, with only small amounts of deformation observed on the HFF for last 300-500 kyrs.

Our working model (Fig. 2.9) has the rift jump occurring in several stages, with the paleo rift located in Skagafjördur, spreading in concert with the NVZ until 3 Ma (Jancin et al 1985, Garcia et al 2003). The three N-S extensional basins along the northern margin (west to east; Eyjafjördur, Skjálfandi, and Öxarfjördur) would have formed during the eastward migration of the rift zone. At this time, the Dalvík lineament was the transform fault, accommodating the motion between the NVZ and KR. Around ~2.5 Ma the NVZ propagated farther north, at the same time forming the HFF, where the

majority of the transform motion was focused until ~1.5 Ma. At which time, the NVZ propagated north of the HFF forming the GL. The exact date of this propagation is difficult to constrain due to the overprinting of the lavas (Saemundsson 1979). Because the faults are not orthogonal to the spreading direction, all three still accommodate some portion of the movement (Jouanne et al. 2006). As these faults consist of overlapping fault segments this oblique extension results in small amounts of volcanic activity, as observed along the GL forming a “leaky transform”. The offset observed on the basin bounding normal faults reflects the reactivation of relic extensional structures as oblique slip faults, originally formed during the rift jump.

## 2.6 SUMMARY AND CONCLUSIONS

Our high-resolution seismic data have provided new insights into tectonic deformation across the Húsavík-Flatey fault system.

1) The deformation associated with the HFF changes both temporally and spatially exhibiting large offset in Miocene and Pliocene times with only minor deformation in the Pleistocene to Recent time. The Pleistocene to Recent deformation along the HFF is best developed along the western portion of the fault and diminishes eastward toward the village of Húsavík

2) Onshore borehole observations from just north of the village of Húsavík are consistent with the offshore data and indicate that the top 250 m of sediment have minimal offset and the majority of deformation across the HFF occurred during the Miocene, Pliocene and early to middle Pleistocene.

3) Active oblique slip faults observed in the offshore basins are reactivated normal faults that are a relic features formed during the rift jump that occurred 3 Ma.

4) The northward propagation of the NVZ and the dying out of the proto rift at Skagafjördur has resulted in the formation of a propagating transform fault system, with the main transform fault located along the southern Dalvík Lineament (3-~2.5 Ma), then along the central Húsavík Flatey Fault (~2.5-1.5 Ma), and finally along the Grímsey Lineament (1.5 Ma-present).

In summary, the HFF was the main transform fault between the NVZ and KR from ~2.5 – 1.5 Ma, resulting in the large displacements and deformation observed on land, however offshore the large, older deformation is obscured by thick Pleistocene glacial sediment. When the NVZ migrated northward past Húsavík at around 1.5 Ma the deformation between the NVZ and the KR shifted north with the deformation portioned between the HFF and the

Grímsey Lineament. Despite the northward propagation of the NVZ, the oblique nature of the transform zone accounts for the continued seismic activity on both the HFF and the DL.

## 2.7 ACKNOWLEDGEMENTS

This research was supported by a grant from the National Science Foundation, University of Iceland Research Fund and the Iceland Geosurvey. We also like to thank Kristján Sæmundsson and Jeff Karson for allowing us to participate in field work and trenching the 1872 ground break of the Húsavík-Flatey Fault. In addition we would like to thank our coauthors Bryndis Bransdottir, Neal Driscoll, Robert Detrick, Graham Kent, and Jeffrey Babcock. Their help in preparing this paper for submission was invaluable.

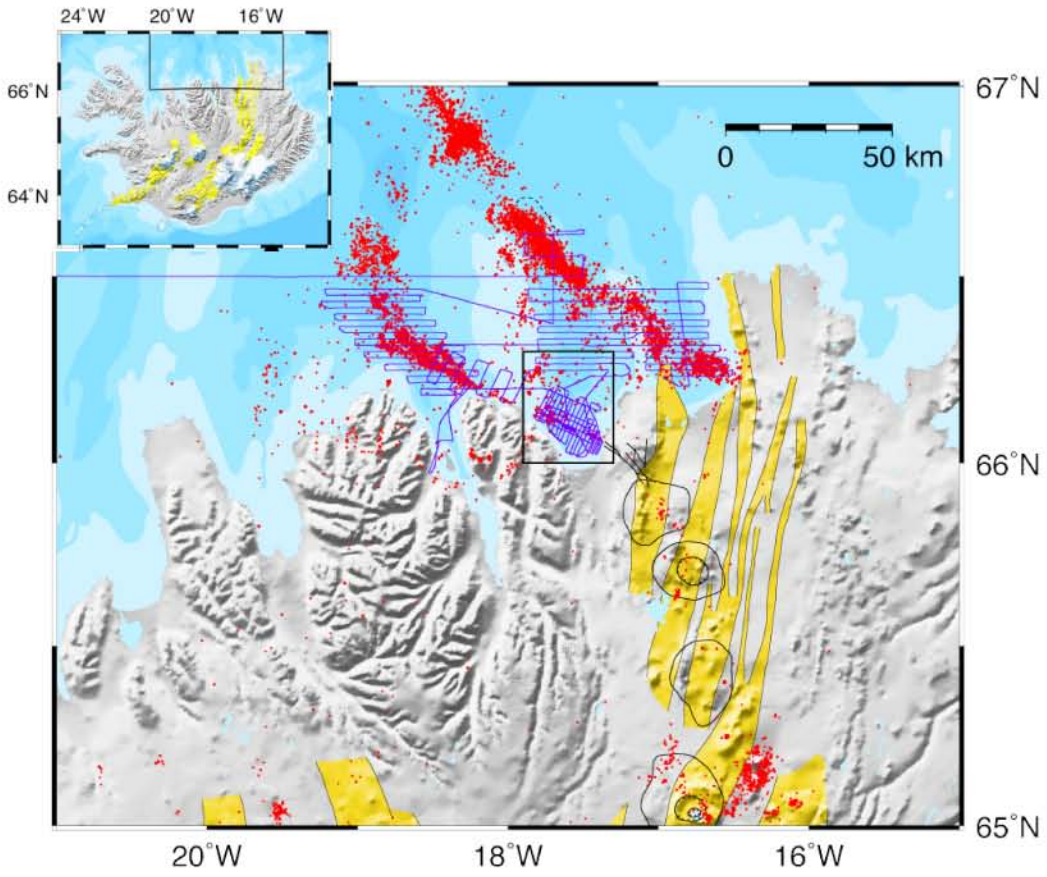


## Figure 2.1

Enlarged map of northern Iceland, focused on the Tjörnes Fracture zone (TFZ), with the modern rift zones of the North Volcanic Zone (NVZ) in yellow. The locations of the faults have been determined by both seismicity and surface expression, the Dalvík Lineament (DL) in the south, the Húsavík-Flatey Fault (HFF) in the center, and the Grímsey Lineament (GL) in the north. Offshore bathymetric data show some surface expression of the faults and also farther offshore the highs are associated with recent volcanic activity, trending to the Kolbeinsey Ridge (KR) in the north. Blue lines show the data coverage in the area, along with core locations (after Knudsen 2008). Line 7 is highlighted in red to give location of Fig 2.4. Inset is Iceland with the boxed region the location or the figure.

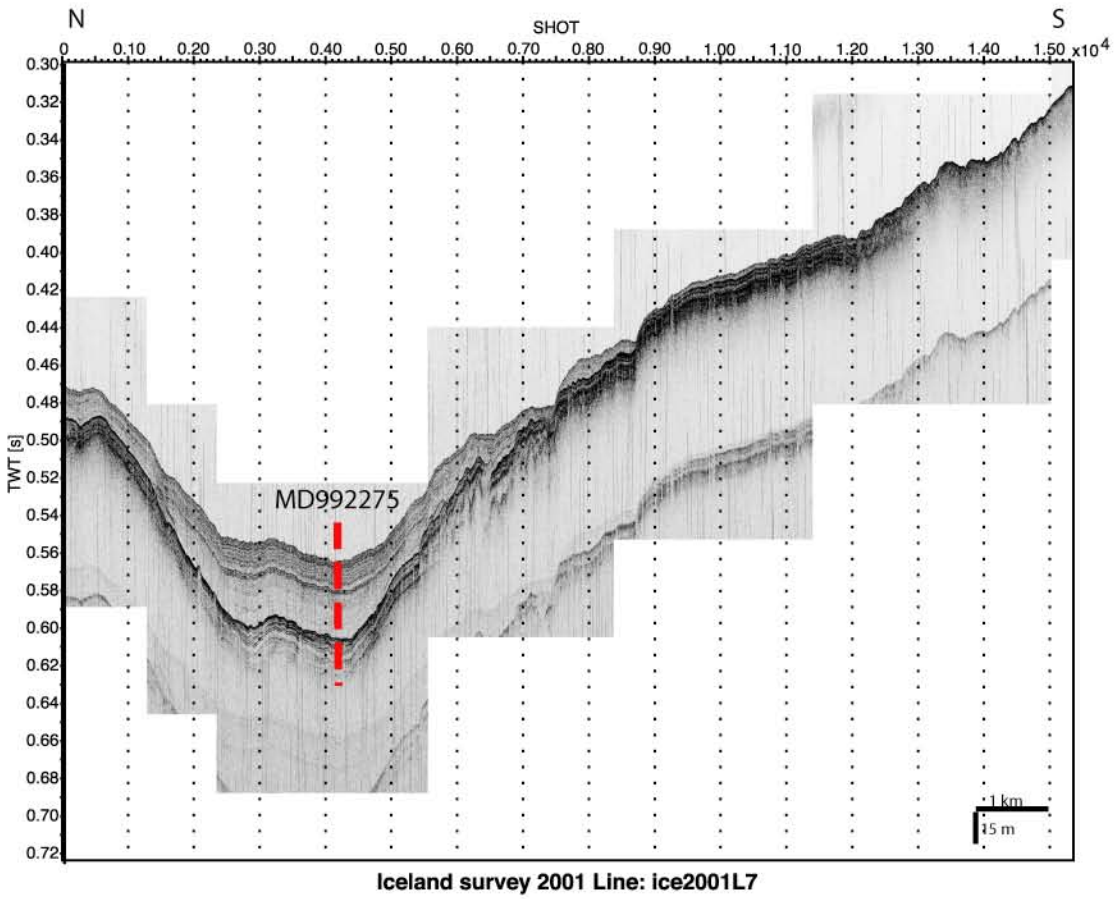


## Figure 2.2

CHIRP Line 7, for location see Fig. 2.1. L7 crosses the core site MD992275, and shows the thick basin deposits, from the core data (Knudsen 2008) the Holocene sediments are 12 m thick, and the Pleistocene sediments are 23 m thick.

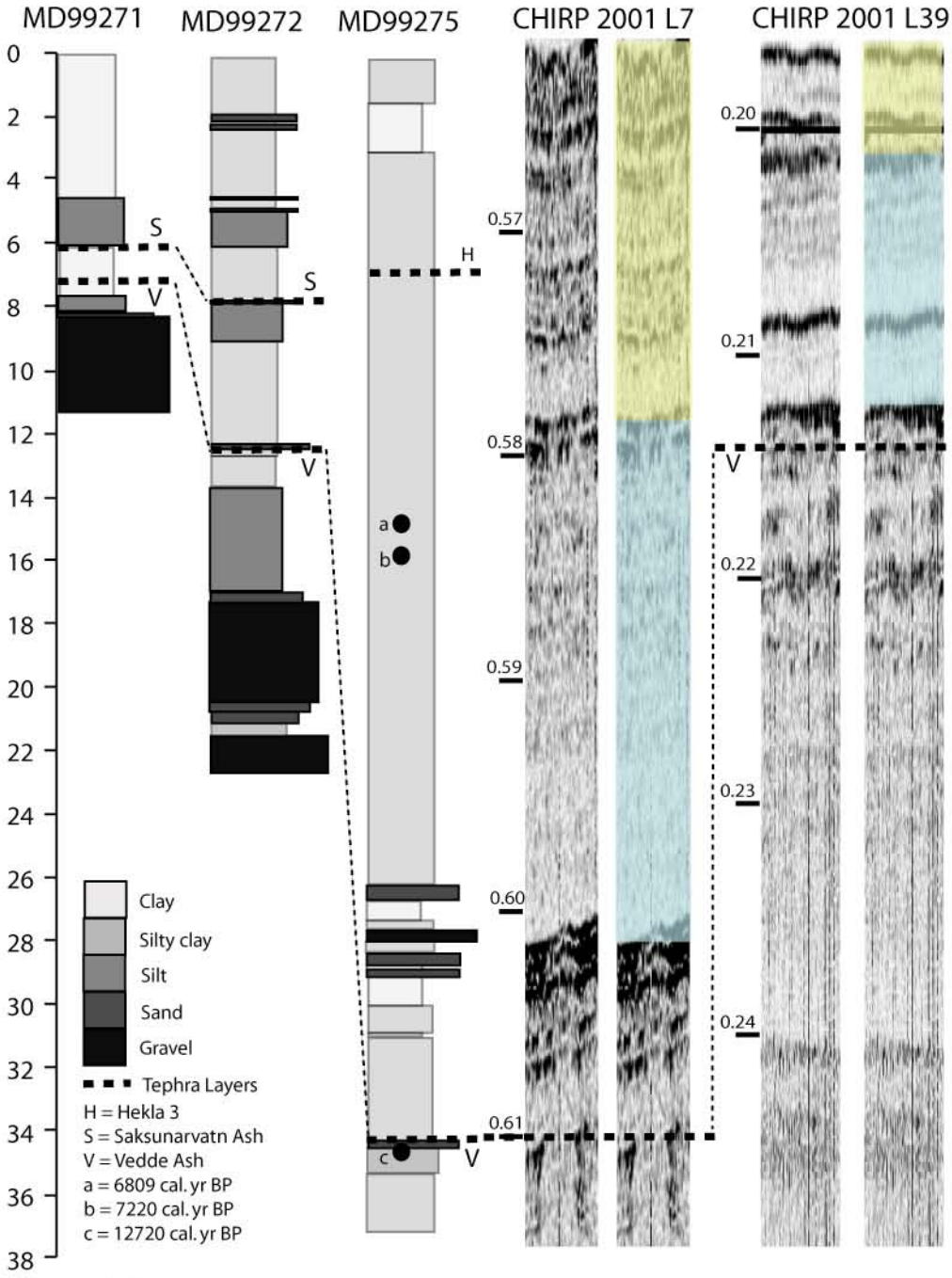


Figure 2.3

Core data after Knudsen (2002, 2008) correlated with CHIRP L7 and L39. L7 crosses the core site MD992275, allowing direct correlation to acoustic characteristics of the seismic data. Based on these acoustic characteristics, age constraints from core data are extrapolated to data in Skjálfandi Bay. L39 was used for this purpose as it is central to the bay and has average sediment thicknesses. Scale on CHIRP lines is two way travel time in seconds.

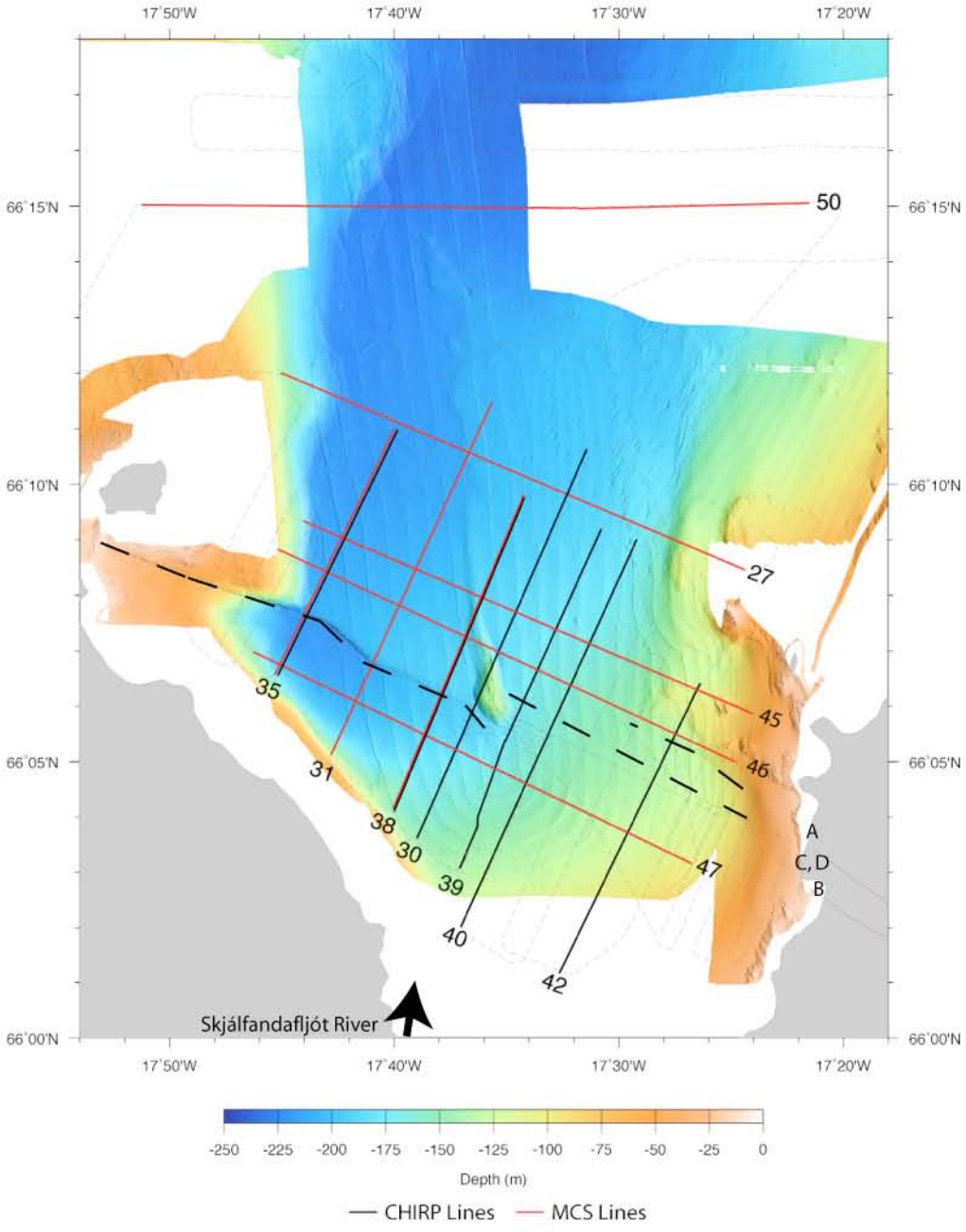


## Figure 2.4

Skjálfandi Bay data coverage: bathymetric data and seismic lines MCS in red and CHIRP in black. The dashed black line indicated the location of the HFF, determined from seafloor morphology and from seismic data. Skjálfandafljót glacier river enters the bay from the southwest (black arrow). Locations of photographs in Fig. 2.8 indicated by letters A-D.

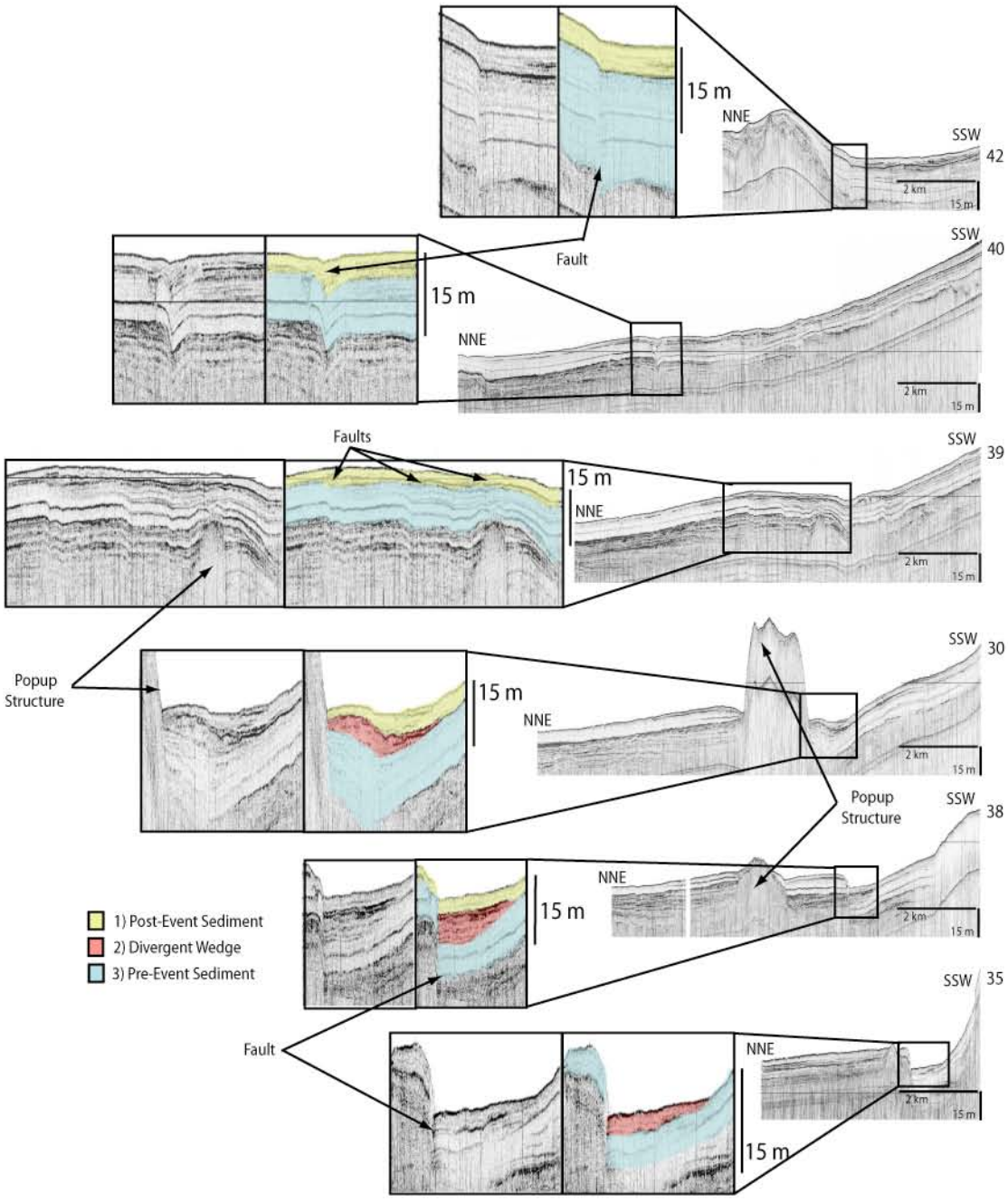


## Figure 2.5

CHIRP lines across the HFF . Lines run NNE SSW, L35 furthest to the west, L42 furthest to the east. The fault offset is largest to the west (15 m), diminishing to < 1 m in the east.

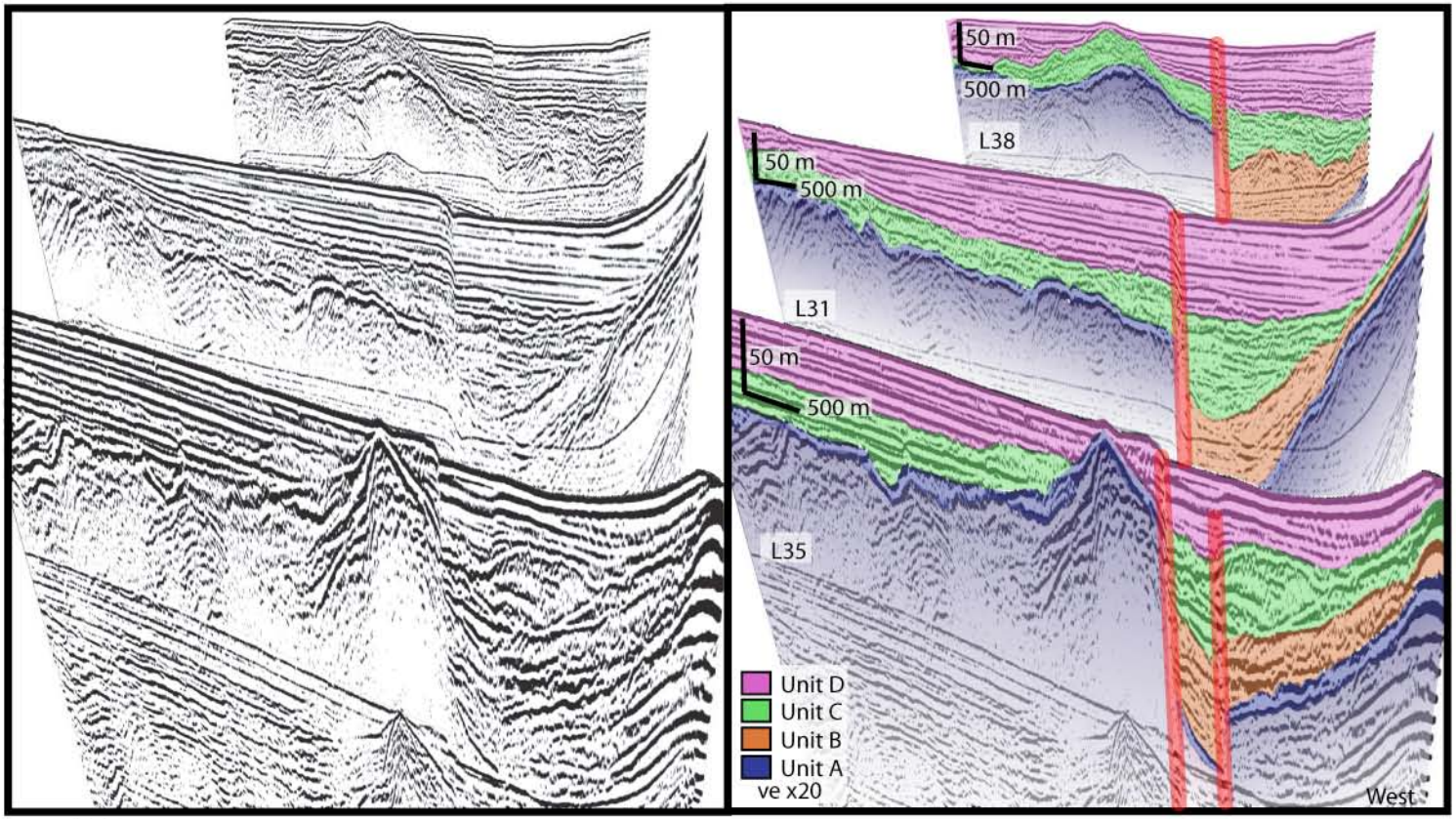


Figure 2.6

A perspective view of MCS L31, L35, L38 (Fig. 2.4 for location) showing both uninterrupted and interpreted profiles. Based on sedimentation rates of 1-2 m/kyr, Unit A and B are interpreted to be early to middle Pleistocene in age and record the large deformation associated with the HFF. Unit C is the sediment infilling the fault-generated accommodation created. Unit C is thought to be rapidly deposited glacial sediments associated with the last glacial event. Unit D is Pleistocene and recent sediments, with minor offset.

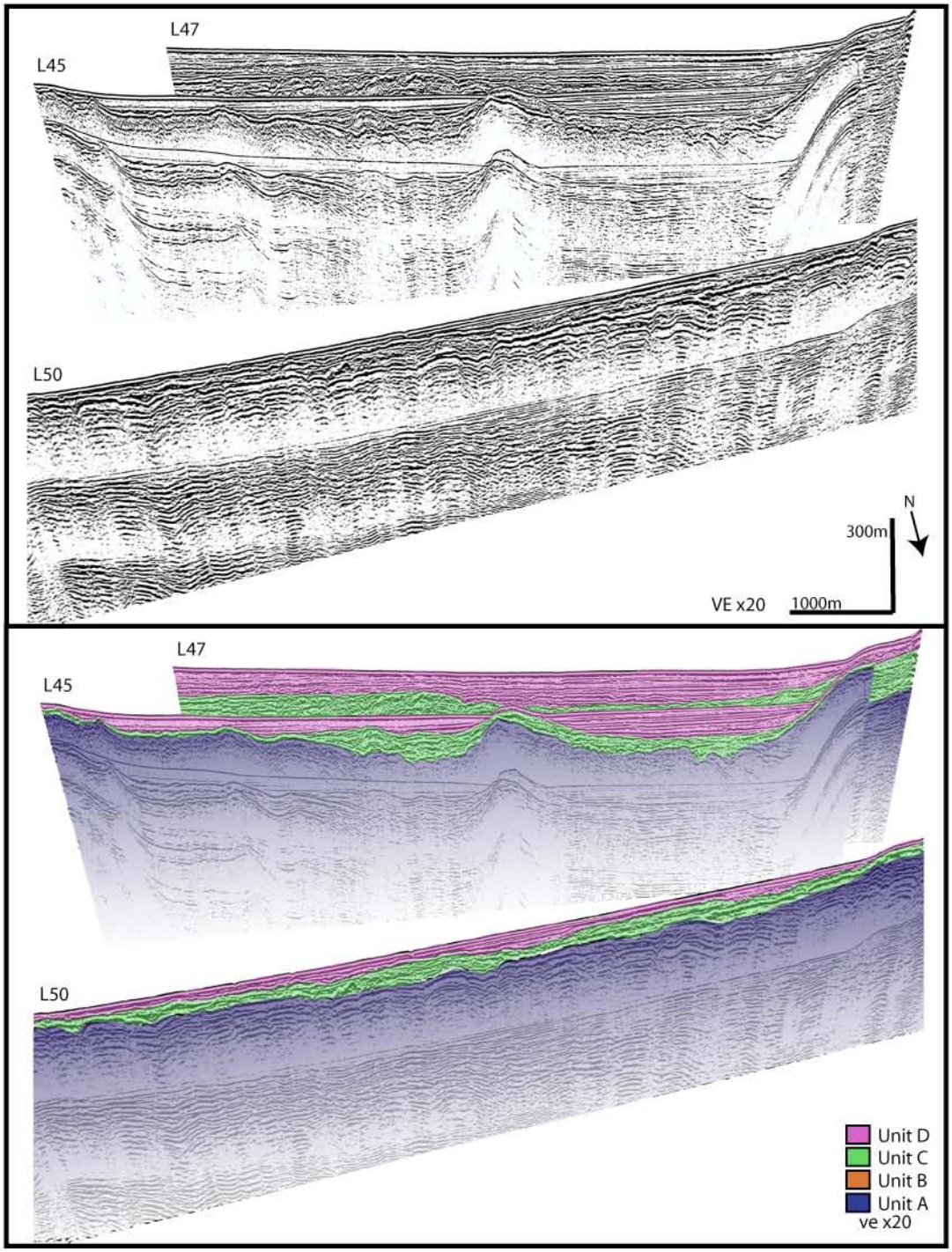


Figure 2.7a

Perspective view of MCS L50, L45, L47, both uninterrupted and interpreted profiles. The units are as Fig. 2.6, showing the structure of the bay viewed from the north, Unit A dipping to the west, Unit B and D thickening towards the south and the sediment source Skjálfandafljót river.

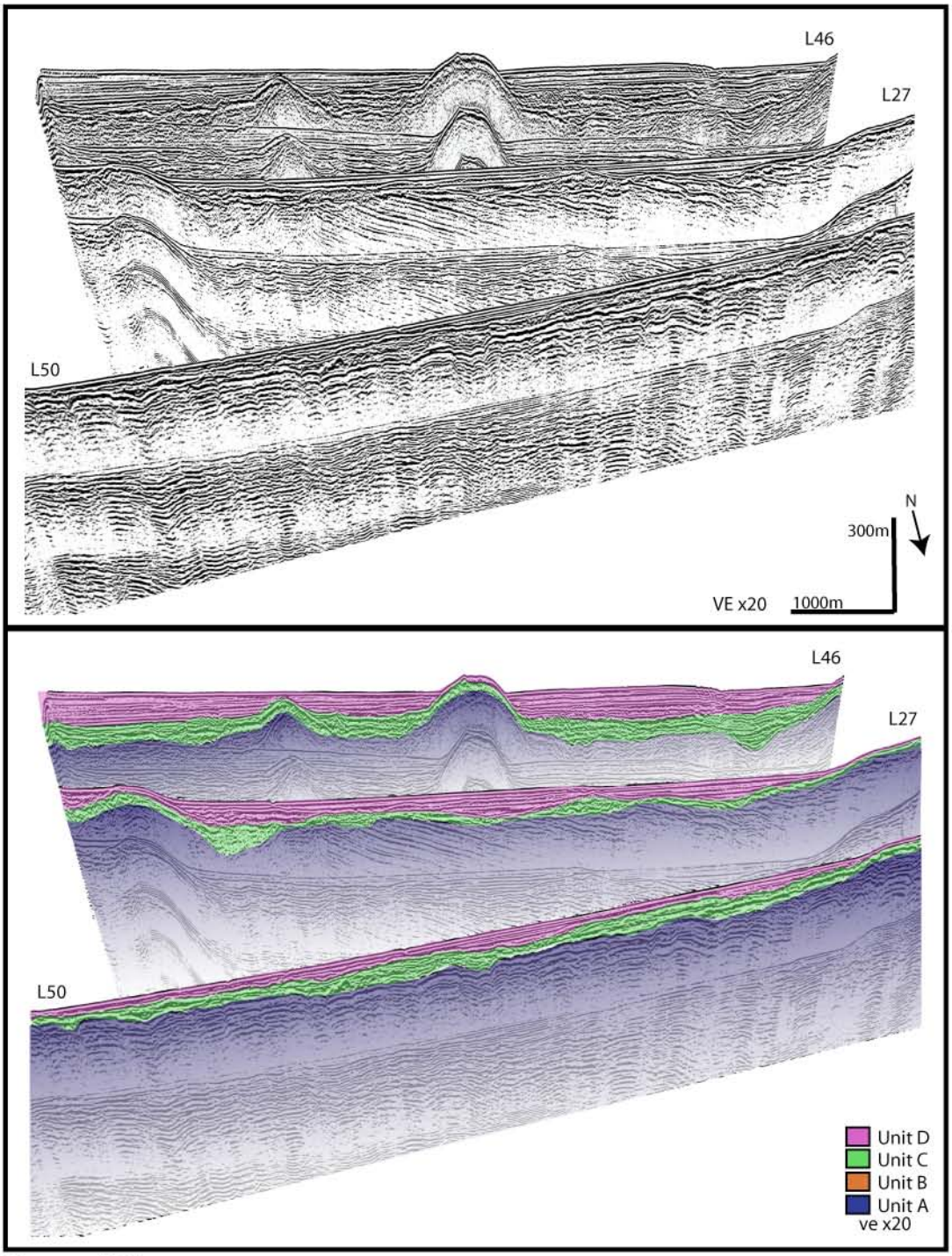


Figure 2.7b

Perspective view of MCS L50, L27, L46. , both uninterrupted and interpreted profiles. The units are as Fig. 2.6, showing the structure of the bay viewed from the north, Unit A dipping to the west, Unit B and D thickening towards the south and the sediment source Skjálfandafljót river.

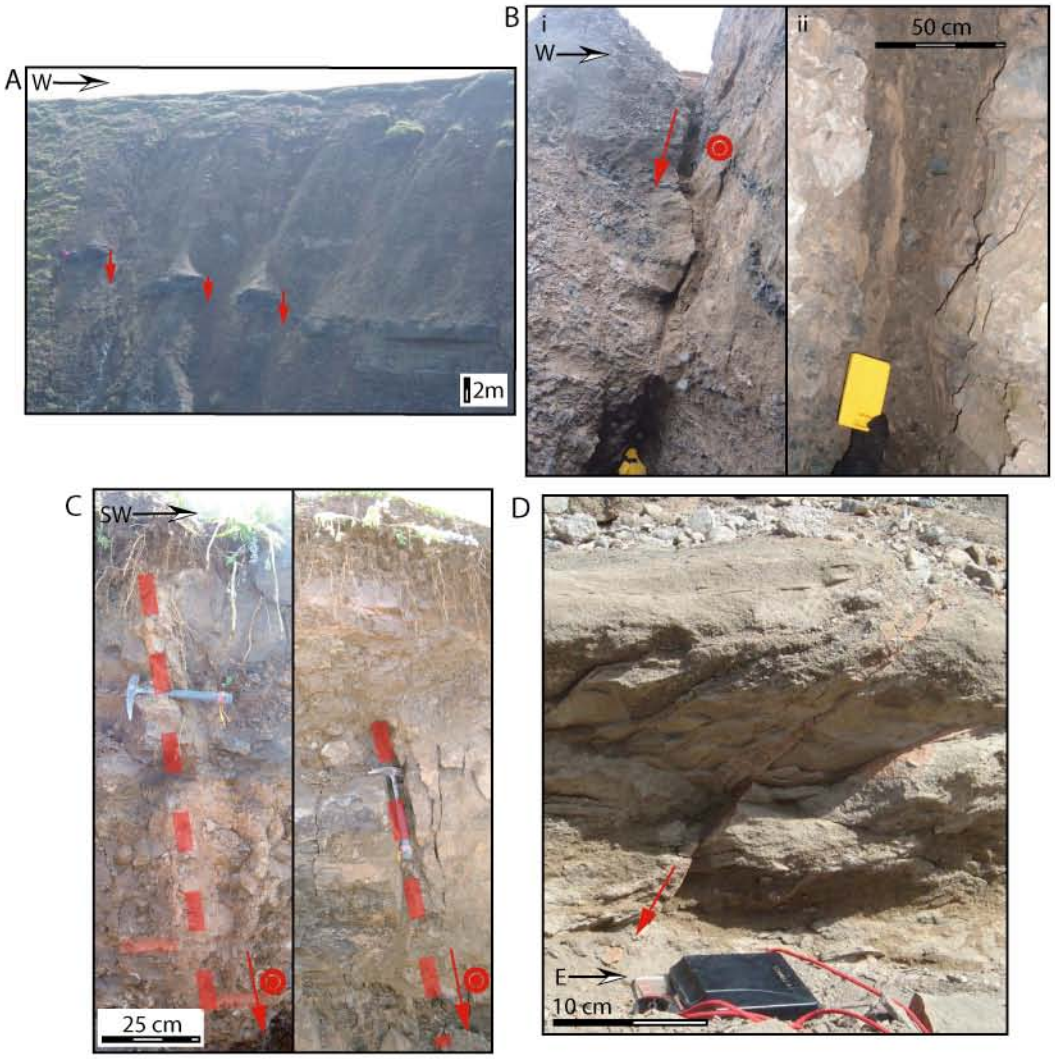


## Figure 2.8

A: Large massive Pliocene sandstone bed progressively down dropped to the west along several parallel ~20°N faults located to the north of Húsavík. Red arrows indicate sense of movement. B: (i) Large dextral strike slip fault with some dip slip component, identified from Riedal shears on the fault plane. This fault is located to the south of Húsavík. The fault cuts through late Pliocene flow basalts with a strike of 315° NW, and dip of 30° NE. (ii) Along the fault zone, a 50 cm fault gouge is observed consisting of clays and fault breccia, which has be eroded away near the base of the outcrop by wave activity. C: An exploratory trench was excavated across the HFF just north of Húsavík by Saemundsson & Karson , along the main strand of the 1872 ground break. Three basalt terraces were exposed and were offset by 1.5-2 m each. The faults shown here offset two of these terraces with strikes of 325°N and 310°N respectively. They stop within 20-50 cm of the surface and are partially to completely infilled with debris. Red arrows indicate dip-slip component, dashed line indicates location of fault. D: Small scale faulting, strike 010°N, dip 50°W, in recent glacial sediments located in a gravel quarry just to north of Húsavík. Faulting does not extend to the surface, and offsets are on the cm scale. Locations of outcrops are shown on Fig. 2.2.

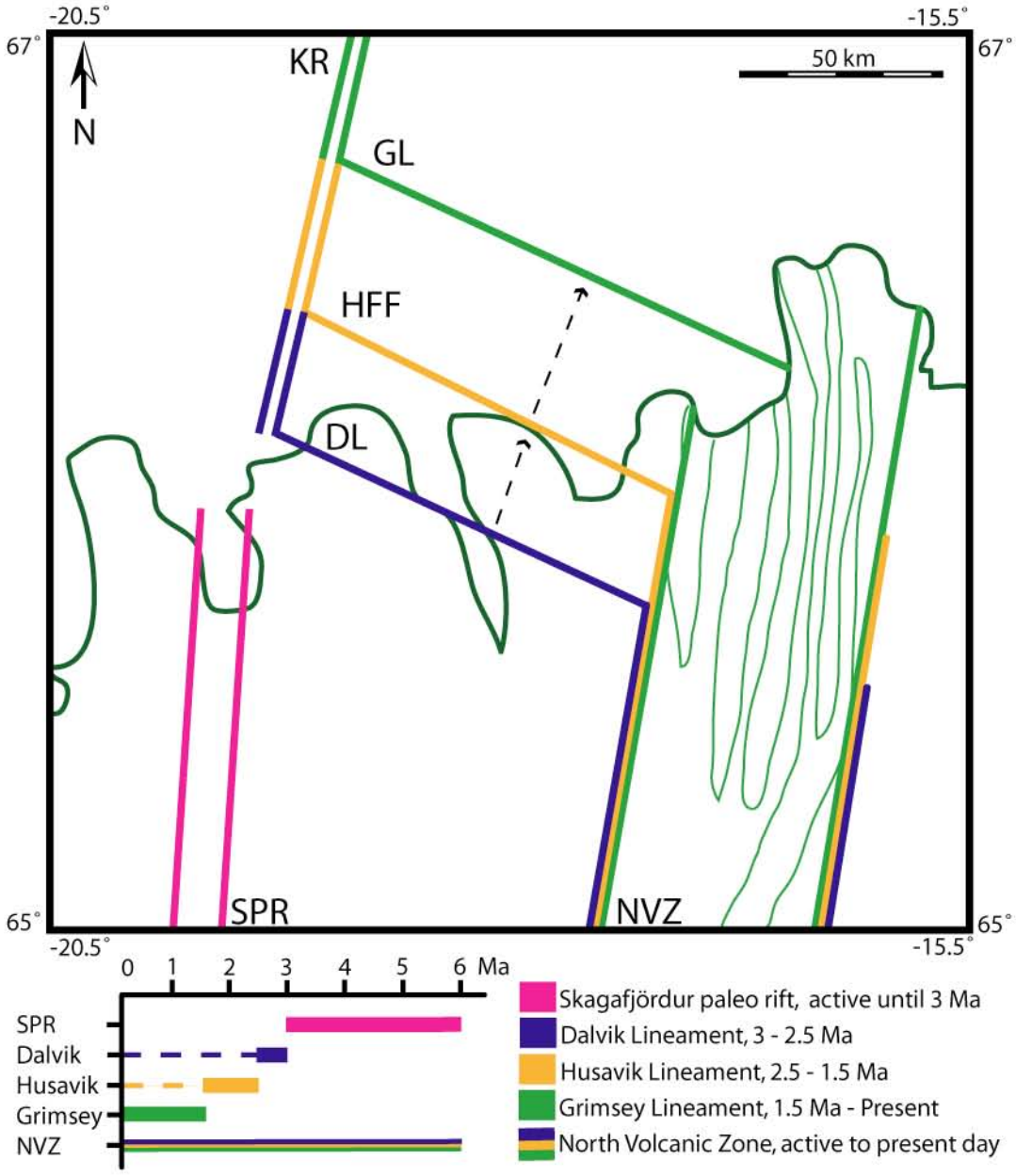


## Figure 2.9

A conceptual model for the transform fault migration through time. Until 3 Ma the Skagafjördur paleo rift (SPR) and the Northern Volcanic Zone (NVZ) were spreading in concert, and the Kolbeinsey Ridge (KR) extended farther to the south. As the KR has receded to the north and the NVZ has propagated to the north the transform fault has stepped northward and the majority of deformation now occurs along the GL with only minor deformation and reactivation along the HFF.

## 2.8 REFERENCES

Andrews J.T., Hardardòttir J., Helgadòttir G., Jennings A.E., Geirsdòttir A., Sveinbjörnsdòttir À., Schoolfield S., Kristjànsdòttir G.B., Smith L.M., Thors K., Syvitski J.P.M., 2000, The N and W Iceland Shelf: insights into Last Glacial Maximum ice extent and deglaciation based on acoustic stratigraphy and basal radiocarbon AMS dates, Quaternary Science Reviews, 19, 619-631.

Andrews, J.T., Á. Geirsdóttir, J. Hardardóttir, S. Principato, G.B. Kristjánsdóttir, G. Helgadóttir, K. Grönvold, J. Drexler and Á. Sveinbjörnsdóttir 2002. Distribution, sediment magnetism, and geochemistry of the Saksunarvatn (10.1809+/-60 cal. yr BP) tephra in marine, lake, and terrestrial sediments, northwest Iceland. Journal of Quaternary Science 17, 731 45.

Anglier J., Bergerat F., Homberg C., 2000, Variable coupling across weak oceanic transform fault, Flateyjarskagi, Iceland, Terra Nova, 12, 97-101.

Bergerat F., Angelier J., Homberg C., 2000, Tectontic analysis of the Húsavík-Flatey (northern Iceland) and mechanisms of an oceanic transform zone, the Tjörnes Fracture Zone. Tectonics, 19, 1161- 1177.

Björnsson, H., and P. Einarsson 1990. Volcanoes beneath Vatnajökull, Iceland: Evidence from radio echo-sounding, earthquakes and jökulhlaups. Jökull 40, 147-168.

Cohen, J. K., and J. W. Stockwell Jr., 1999, CWP/SU: Seismic Unix Release 33: A free package for seismic research and processing, software, Cent. for Wave Phenom., Colo. Sch. of Mines, Golden, Colo.

DeMets C.R., Gordon R.G., Argus F.D., Stien S., 1994, Effect of recent revisions to the geomagnetic reversal time scale on estimates of current motions, Geophys. Res. Letters, 21, 2191-2194.

Einarsson P., 1991, Earthquakes and present-day tectonism in Iceland, Tectonophysics, 189, 261-279.

Eiriksson J., Knudsen K.L., Haflidason H., Heinemeier J., 2000, Chronology of late Holocene climate events in the northern North Atlantic based on AMS $^{14}C$ dates and tephra markers from the volcano Hekla, Iceland, Journal of Quarternary Science, 15, 573-580.

Fjäder K., Gudmundsson A., Forslund T., 1994, Dikes, minor faults and mineral veins associated with a transform fault in North Iceland, Journal of Structural Geology, 16, 109-119.

Garcia S., Arnaud N.O., Angelier J., Bergerat F., Homberg C., 2003, Rift jump process in Northern Iceland since 10 Ma from 40Ar/39Ar geochronology, Earth and Planetary Science Letters, 214, 529-544.

Garcia S., Angelier J., Bergerat F., Homberg C., 2002, Tectonic analysis of an oceanic transform fault zone based on fault-slip data and earthquake focal mechanisms: the Húsavík-Flatey Fault zone, Iceland, Tectonophysics, 344, 157-174.

Geirsson H., Árnadóttir T., Völksen C., Jiang W. Sturkell E., Villemin T., Einarsson P.,
Sigmundsson F., and Stefánsson R., 2006, Current plate movements across the Mid-Atlantic Ridge determined from 5 years of continuous GPS measurements in Iceland, Journal of Geophysical Research, 111, B09407, doi:10.1029/2005JB003717.

Geirsdóttir, Á., J.T. Andrews, S. Ólafsdóttir, G. Helgadóttir and J. Hardardóttir, 2002. A 36 Ky record of iceberg rafting and sedimentation from north-west Iceland. Polar Research 21, 291-298.

Gudmundsson A., Brynjolfsson S., Jonsson M.T., 1993, Structural analysis of a transform fault-rift zone junction in North Iceland, Tectonophysics, 220, 205-221.

Helgason, J., 1985, Shifts of the plate boundary in Iceland: Some aspects of Tertiary volcanism, Journal of Geophysical Research, 90, B12 10084-10092.

Henkart, P., 2003, SIOSEIS, software, Scripps Inst. of Oceanogr., La Jolla,Calif. (available at http://sioseis.ucsd.edu).

Jancin M., Young K.D., Voight B., Aronson J.L., Saemundsson K., 1985, Stratigraphy and K/Ar ages across the west flank of the northeast Iceland axial rift zone, in relation to the 7 Ma volcano-tectonic reorganization of Iceland, J. Geophys. Res., 90, 9961-9985.

Jouanne F., Villemin T., Berger A., Henriot O., 2006, Rift-transform junction in North Iceland: rigid blocks and narrow accommodation zone revealed by GPS 1997-1999-2002, Geophys. J. Int, 167, 1439-1446.

Kundsen, K. L., Eirksson J., 2002, Application of tephrochronology to the timing and correlation of palaeoceanographic events recorded in Holocene and Late Glacial shelf deposites off North Iceland, Marine Geology, 191, 165-188.

Knudsen, K.-L., M.K.B. Sondergaard, J. Eiríksson and H. Jiang, 2008. Holocene thermal maximum off North Iceland: Evidence from benthic and planktonic foraminifera in the 8600-5200 cal year BP time slice. Marine Micropaleonotology, doi:10.1016/j.marmicro.2007.11.003

Kristjánsdóttir, G.B., J.S. Stoner, A.E. Jennings, J.T. Andrews and K. Grönvold 2007.
Geochemistry of Holocene cryptotephras from the North Iceland Shelf (MD99-2269): intercalibration with radiocarbon and palaeomagnetic chronostratigraphies. The Holocene 17, 155 DOI: 10.1177/0959683607075829

Mamula N., Voight B., 1985, Tectonic analysis of lineaments near a spreading axis, Northeastern Iceland, Tectonophysics, 116, 63-93.

McMaster R.L., Schilling J.E., 1977, Plate boundary within Tjörnes Fracture Zone on northern Iceland's insular margin, Nature, 269, 663-668.

Ólafsdóttir, S., J.S. Stoner, Á. Geirsdóttir, G.H. Miller and J.E. Channell 2005.

High-resolution Holocene palaeomagnetic secular variation records from Iceland: Towards marine-terrestial synchronization. Eos Transactions AGU, U43A-0820

Porbjarnardóttir, B.S., Gudmundsson G.B., 2003 Seismicity in Iceland 2002, Jökull, 53, 49-54.

Riedel, C., Petersen, T., Theilen, F. and Neben, S., 2003. High *b*values in the leaky segment of the Tjörnes Fracture Zone north of Iceland: Are they evidence for shallow magmatic heat sources? *J. Volcanol. Geotherm. Res.* **128**, 15–29.

Riedel, C., A. Tryggvason, T. Dahm, R. Stefansson, R. Bödvarson and G.B. Gudmundsson, 2005. The seismic velocity structure north of Iceland from joint inversion of local earthquake data. J. Seismology 9, 383–404.

Rögnvaldsson S.T., Gudmundsson A., Slunga R., 1998, Seismotectonic analysis of the Tjörnes Fracture Zone, an active transform fault in north Iceland, J. Geophys. Res., 103, 30117-30129.

Saemundsson K., 1974, Evolution of the axial rifting zone in Northern Iceland, Geol. Soc. of Am. Bull., 85, 495-504.

Saemundsson K., 1979, Outline of the geology of Iceland, Jökull, 29, 7-28.

Tryggvason E., 1973, Seismicity, earthquake swarms, and plate boundaries in the Iceland region, Bull. Seis. Soc. Am. 63, 1327-1348.

Young K.D., Jancin M., Voight B., Orkan N., 1985, Transform deformation of tertiary rocks along the Tjörnes fracture zone, north central Iceland, J. Geophys. Res., 90, 9986-10010.

\

# Chapter 3

## Pockmark Distribution and Seafloor Morphology in Skjálfandi Bay

## 3.1 ABSTRACT

Geophysical data collected offshore Northern Iceland (2001-3) reveal large pockmark fields in Skjálfandi Bay, the central basin of the Tjörnes Fracture Zone (TFZ). The distribution of the pockmarks observed in the bathymetry and side-scan sonar is predominantly clustered in a band ~15-22 km offshore. An additional zone of pockmarks is observed along the northern upthrown block of the Húsavík-Flatey Fault. To explain the offshore distribution of pockmarks, one has to invoke an interplay between organic source material and sediment overburden. Except for the pockmarks along the Húsavík-Flatey Fault, there are no pockmarks observed in the nearshore region. In the shallow inner bay, the thick glacial and post-glacial sequences overlying the organic source layer may form an effective permeability barrier that precludes pock formation. Farther offshore the occurrence of pockmarks also diminishes. The high organic sediments (e.g., estuarine) may not have been deposited in this region and thus there is no source for the gas to form the pockmarks.

We postulate that the pockmark field is formed in a region far enough offshore that the glacial/interglacial sequences are thin and do not act as permeability barriers, but proximal enough for deposition of organic-rich sediment layers. In such a scenario, the distribution of pockmarks would be controlled by the region of overlap, where organic-rich sediments are overlain by thin glacial/interglacial sequences. These conditions appear to exist ~15-22

km offshore, where the overlying sediments are thin, there is sufficient organic content, and the geothermal gradient is high resulting in the formation and migration of fluids (thermogenic) from depth producing a band of pockmarks across the bay. Their exact distribution within this band is also governed by the west dipping strata that appear to control fluid migration pathways. The morphology of the linear chains of pockmarks are then overprinted by bottom currents, elongating their seafloor profile. Pockmarks are also found along the western portion of the HFF, where the sidescan data imaged large elongate compound pockmarks at a high angle to the fault (10-50 m maximum length). This field of pockmarks appears to be tectonically controlled with fault-engendered deformation controlling the permeability pathway to the surface from depth.

## 3.2 INTRODUCTION

In the last several decades, Earth and ocean scientists have come to recognize a host of complex and globally significant processes operating across many scales of time and space within the ocean basins. Amongst these, interactions along plate boundaries dominate the surface morphology and deformational dynamics of our entire planet. Fluid expulsion patterns linked to these interactions have been identified along all three types of plate margins. Deformational and/or thermal processes that operate most intensely

near plate margins and less intensely within plate interiors, result in a wide variety of forced fluid migrations within the oceanic crust and between the crust and overlying ocean.

Fluid fluxes of these types may be steady state, episodic, or an admixture of both. Because of the profound effects fluids can have on the strength of rocks, geochemical mobility, and the nature of volcanism, these fluid and volatile fluxes may be both a cause and a consequence of the style and intensity of certain types of plate interaction. However, because of the submarine character of these largely inaccessible phenomena, the spatial patterns of fluid expulsion and their relationship to the tectonic environment, as well as the thermal and chemical fluxes associated with these fluid migrations, are very difficult to assess, let alone quantify. Large-scale fluid circulation is the most important chemical transport mechanism through margin sediments and crust. Fluids issuing from the vicinity of spreading centers and their flanks account for a large fraction of the global heat and chemical fluxes between the ocean crust/lithosphere and the overlying ocean. Fluid circulation patterns and the processes they represent in a transform fault environment are virtually unexplored territory. In part because they are not observable, these processes have been assumed to be relatively insignificant in oceanographic terms. In a sense this is a tacit hypothesis. It can only be tested with a long-term strategy

to measure time-integrated magnitudes of the steady state and episodic fluid input to the ocean from the crust.

In terms of subduction zone complexes, geochemical processes such as diagenesis and metamorphism are strongly controlled by fluid flow rate, fluid composition, and the rate of rock-fluid interactions. Flow-driving mechanisms include compaction and compression at active margins and gravitational circulation along passive continental margins. Water/rock/organic matter interactions change fluid composition and, by altering rock porosity and permeability, create a feedback mechanism affecting fluid pathways and flow rates. These fluid flow and diagenetic processes significantly influence the global geochemical inventory, yet many of these mechanisms, their rates, and the nature of fluid pathways are still largely unknown.

Within the past decade, we have come to recognize that these migrating fluids, whether operating at spreading centers, in mid plate, within subduction complexes, or along transform faults, expel heat and chemically active compounds that offer powerful constraints on lithosphere-ocean interactions. We have also come to recognize that many of these fluids provide nutritional support for a widespread, poorly characterized microbial biosphere within the oceanic crust and in the deep ocean. The fundamental role that fluid fluxes play in linking geologic, hydrologic, oceanographic and

biologic processes is emerging as a major intellectual driving force crossing traditional boundaries between and within the Earth and ocean sciences. Owing in part to the newness of the field and to the limits of past technologies, we have not yet been able to integrate local, regional, and global assessments of plate-modulated fluid fluxes or the microbial productivity linked to these transport phenomena across the water-rock interface at the bottom of the ocean. This tectonically, and perhaps tidally, forced fluid-expulsion/microbial-bloom relationship represents a newly recognized class of geobiological processes that are attuned to plate dynamics, to volcanism, and to deformation.

Injection of crustally derived, chemosynthetically active compounds into the overlying ocean is localized along faults, fissures, and other venting structures distributed at a variety of spatial-temporal frequencies. These venting fluids follow patterns that cannot now be predicted; they must be observed and mapped. We argue that assessing the effects of these phenomena requires a two-step approach. First, we must locate patterns of venting output along representative lengths of the different kinds of plate boundaries. Second, once the spatial distribution of venting sites is in hand, the temporal variation in output of a representative portion of these plate boundary injection fluxes must be measured directly, in situ, over significant

periods of time. The mapping goal is the thrust of this paper and the flux measurements should be an important focus of future research efforts.

We have mapped the TFZ (Fig. 3.1) at many scales to reveal an entire ensemble of plate tectonically generated pockmarks believed to be venting sites on, below, and immediately above the seafloor. Pockmarks have been identified along many margins around the world (Josenhans et al 1978, Hovland et al 1984, Hovland and Judd, 1988, Yun et al 1977, Voight et al 1999, Dimitrov and Woodside 2003, Judd and Hovland 2007), but when originally identified by King and McLean (1970) they were considered rare. As more high-resolution swath bathymetry data have been acquired, pockmarks have been found with greater frequency. They are considered characteristic of focused hydraulic activity at the seafloor. Pockmarks are usually approximately circular depressions ranging in diameter from tens of centimeters to hundreds of meters with a depth on the order of centimeters to tens of meters exhibiting a marked variability in size and shape as a result of different expulsion histories and activity levels (Josenhans et al 1978, Kelley et al., 1994, Driscoll et al., 2000). They tend to have slightly upward dipping sediments surrounding them as they are expulsion rather than collapse features (Dimitrov and Woodside 2003). Inclined bedding or other linear sub-seafloor structures can be exploited as fluid pathways (Josenhans et al., 1978, Judd 2003). In areas of active tectonics, fault planes tend to act as pathways

for the fluid migration, resulting in focused patterns of expulsion features on the seafloor (Hovland et al. 1984, Dimitrov and Woodside 2003, Judd 2003). Fluid that migrates along these pathways can be either thermogenic, biogenic or abiogenic in origin (Hovland and Judd 1988, Kvenvolden 1993, Judd 2003, Judd and Hovland 2007).

As outlined by Judd (2003) there are three types of methane sources in marine sediments: microbial, thermogenic, and abiogenic. Microbial methane is generated by microbial decomposition of organic material in the near surface sediments, and while some methane can be trapped in the sediments most will migrate to the surface. In areas of high microbial organic decomposition there is a high enough rate of methanogenesis for a portion of methane to reach the water column while most of the methane is oxidized by other microbes in the upper few cm's of sediment. Thermogenic methane is produced through thermocatalytic degradation at depth of organic matter not microbially decomposed in surfical sediments. Temperature, pressure and the starting organic materials govern the type of hydrocarbon compounds produced by this process resulting in anything from asphalt, crude oil, to hydrocarbon gas. Of these we are most interested in the hydrocarbon gas (methane is the most abundant) as it is mobile and can migrate to the seafloor and potentially result in the formation of pockmarks. Abiogenic methane is

inorganically derived from degassing/cooling mafic rocks or the serpentinization of ultramafic rocks within the ocean crust.

It is estimated that marine natural gas seeps are responsible for up to 20% of global methane emissions to the atmosphere (Fleischer et al., 2001), making them an important part of the carbon cycle (Judd, 2003). Methane seeps are present in every ocean and sea and in a variety of environments, including continental shelves, deep water and convergent and transform plate boundaries (Judd, 2003) with seep characteristics ranging from diffuse seafloor venting to more focused escape (Lonke et al., 2004). In addition to the environmental significance, gas in marine sediments may hold possible geohazard and resource significance (Driscoll et al., 2000; Fleischer et al., 2001, Geptner et al., 2006 a,b). Under normal circumstances (non-focused fluid flow) methane either in or moving through the sediments is oxidized by microbial activity. It is only in regions where the fluid flux rate exceeds the microbial oxidation rate that you have methane venting into the water column both as a gentle seepage or catastrophic release (Judd 2003). For methane to reach the atmosphere it either has to be a catastrophic release with some percentage reaching the atmosphere just by the shear volume of released gas or the gentle release of bubbles has to occur in shallow waters so that the methane bubbles reach the surface before dissolving in the water column. Methane not reaching the atmosphere is a significant contributor to the overall

amount of methane in the water column as on average, ocean water is methane deficient (Judd 2003). Impacts of increased levels of dissolved methane has not been quantified with respect to the fauna in the regions proximal to vents/pockmarks, although it is thought to be more significant below the photic zone.

Pockmarks associated with the venting of gasses and fluids have become widely observed seafloor features (Hovland and Judd, 1988) since their first discovery by King and McLean (1970) offshore Nova Scotia. The cross-sectional shape of these features varies from “u” shaped and “v” shaped seafloor depressions to truncated cones with steep, low angled or asymmetric walls; some are circular in plan view while others are elongate (Dimitrov and Woodside, 2003; Hovland et al., 2002). While most agree that pockmarks are the result of focused fluid flow (Hovland et al., 2002), the exact nature of venting remains poorly understood (Paull et al., 2002). Kelley et al. (1994) suggest two models for pockmark formation: 1) decomposition of organic matter deposited above a hard flat erosional surface releases gas that excavates the pockmark. The sediment is then carried away by currents creating a “v” shaped pockmark. Once the excavation extends down to the erosional surface, the pockmark spreads out laterally along that surface moving towards a more “u” shaped pockmark, and 2) a catastrophic event such as an earthquake or tsunami reduces the confining pressure in the area,

allowing gas and fluids to suddenly escape. Both models seem reasonable as the first can explain why “u” shaped, “v” shaped and flat-floored pockmarks are observed and the later why pockmark formation and increased methane venting have been documented to occur in response to earthquakes (Hovland et al., 2002; Christodoulou et al., 2003).

The morphology of the pockmark undergoes continual modification due to both subsequent fluid expulsion and bottom currents (Josenhans et al., 1978, Hovland et al., 1984). As the fluid escapes it displaces and slumps the surrounding sediment, which is in turn more susceptible to erosion, slumped sediment becoming suspended as the fluid rises. When a bottom current flows across an active or inactive pockmark it erodes the downcurrent side, elongating the pockmark so that the long axis is subparallel to the current direction (Fig. 3.2). If the pockmark is active the bottom current deflects the venting fluid and the down current side erodes the pockmark wall. An inactive pockmark also will erode preferentially on the down current side, as the current flows out of the pockmark the velocity increases eroding the wall sediments (Josenhans et al. 1978). The activity of the pockmark also contributes to it’s morphology, while the pockmark is active the walls of the pockmark maintain their steepness (“v” shape) and have little secondary modification (Kelley et al. 1994). When pockmark activity decreases the secondary modification and reworking on the sediment becomes the dominant

process transitioning to a “u” profile. Pockmarks can also be associated with brine pools or very dense liquids depending on the composition of the escaping fluids. Pockmarks identified in the Mediterranean have both brine pools located within and also show characteristic drainage channels where the dense/brine liquid has drained out of the pockmark (Dimitrov and Woodside 2003).

The TFZ, a northward migrating fracture zone, along northern Iceland is a region of active tectonic deformation. The TFZ connects the North Volcanic Zone (NVZ) with the Kolbeinsey Ridge (KR) and is an area of significant present-day fault activity (Fig. 3.1). High-resolution swath bathymetric maps reveal that the TFZ is right lateral transform  with three major N-S striking extensional basins, Eyjafjördur, Skjálfandi and Öxarfjördur, and three seismically active WNW-striking seismic lineaments, the Grímsey Lineament (GL), Húsavík-Flatey Fault (HFF) and Dalvík Lineament (DL), and numerous extensional NS normal faults (Garcia et al., 2003, Saemundsson 1974). The Grímsey Lineament connects the northern end of the NVZ and the Kolbeinsey Ridge, whereas the Húsavík-Flatey Fault connects the magma starved southern extension of the Kolbeinsey Ridge (westernmost basin, Eyjafjördur) to a portion of the NVZ. While the Dalvík Lineament connects the now extinct southern extension of the KR and a more southern section of the NVZ. Faulting in the TFZ is divided between NNE normal faults and WNW strike-slip

faults, the surface expression of these faults consisting of several overlapping fault strands, which in some locations coalesce at depth (1.5 km; Riedel et al 2001), and have small but varying amounts of dip slip motion.

The geothermal gradient in Iceland is on average higher than the average for oceanic crust of equivalent age due to the proximity of the plume head. This increased geothermal gradient decreases the depth at which diagenesis starts to occur. The temperature at 1000 m depth outside the geothermal areas usually is 50-100ºC, and 50-170ºC in our study area (Flóvenz and Sæmundsson 1993). This higher geothermal gradient results in the formation of high temperature water circulation and thermogenesis at depth sourcing the hydrothermal fields around Iceland. Samples taken in Öxarfjördur Bay, Northern Iceland represent slightly altered clastic deposits, along with hot water discharging from springs (Geptner et al 2006 a,b). In this and surrounding area there are networked interlinked faults that connect to deep-seated normal faults, creating pathways for fluid migration. The chemical signature (He, CO2, CH4 etc) of the fluids indicate that there is some component of lower crust/upper mantle, along with an isotopic composition of methane indicative of an abiogenic source mixed thermogenic hydrocarbons (Botz et al. 1999, Reidel et al. 2001). Hypocenters of earthquakes under Skjálfandi Trough are traceable down to 16km form a flower structure. This level of high seismic activity results in high permeability along some faults.

## 3.3 PREVIOUS WORK IN THE TJÖRNES FRACTURE ZONE

### 3.3.1 Fluid Flow in the Region: source and flow mechanisms

Fluid flow has been studied in the region, documenting a mixed origin for the fluids: thermogenic mixed with high temperature hydrothermal (Botz et al 1999). Previous work done on the Grímsey Hydrothermal Field (Reidel et al 2001) has shown that there is a significant amount of geothermal activity to the north of Manareyjar Ridge (Fig. 3.3), the seaward extension of the Theistareykir Fissure Swarm, at the northern extent of the NVZ. The fluids are of abiotic origin and are focused along west dipping normal faults that extend down to 1.5 km depth. Based on the chemical makeup, it appears that the fluids have some interaction with the mantle. In the vicinity of Grímsey Island fluid venting at the sea floor with temperatures up to 250˚C has been observed. The fluids venting in the Grímsey Hydrothermal Field have $CH_4/^3He$ ratios indicating a sedimentary source for some of the methane and the C1/C2+C3 value of $CH_4$ indicating a high temperature hydrothermal source along with some additions of thermally degraded organic sedimentary material. As a consequence of the local geothermal gradient unusually shallow depths can enter the cracking window (Botz et al 1999). Given the proximity and similarity in tectonic and sedimentary settings, we are likely to have similar sources for fluid in our area. On shore there are hot springs located along the

strike of the HFF near the town of Húsavík, indicating that there is active fluid flow in the area.

A detailed study of the components of the fluid upwelling in the southern portions of Öxarfjördur and Skjálfandi Bays was conducted by Geptner et al. 2006 (a, b), focused on the polycyclic aromatic hydrocarbons (PAH) composition. In fracture zones thermogenic fluids have 10-100 times the level of hydrocarbons found in pelagic marine sediments, along with characteristic molecular signatures (Chernova et al. 2001). PAH's are sourced either from sediments or synthesis from simple organic compounds and are transported by/related to the movement of thermal fluids. Across Iceland there is a strong correlation between hyrothermal upflow and higher than average concentrations of hydrocarbons. In Skjálfandi Bay samples were taken from in the pockmark field in the northern portion of the bay (Fig. 3.4 Site B, Table 1), and along the HFF (Fig. 3.4 Site A, Table 1). Cores 2 and 4 show high levels of PAH 58 ppb and 123 ppb respectively, comparable with hydrocarbon associations for high temperature oil fields. Samples taken in Öxarfjördur area were mainly from surfical lagoon sediments and coastal hot sand areas using diatomite absorbers in traps (Geptner et al. 2006 a,b). PAH levels vary widely from 9 to 925 ppb mainly consisting of naphthalene, benzofluorene, benzo(a)pyrene and benzo(ghi)perylene. Due to the geological and sedimentelogical similarities between Skjálfandi and Öxarfjördur Bays the

Table 3.1:

| Site | Core no. | Lat | Lon | Depth, m | Core length, cm | Cutter contents | Comments |
|---|---|---|---|---|---|---|---|
| Site A | A1 | 66º10.837 | 17º29.191 | 190 | 90.9 | Silty-clay | Pock site |
| | A2 | 66º10.873 | 17º29.191 | 190 | 120.0 | Silty-clay | Pock site |
| | A3 | 66º10.286 | 17º29.634 | 181 | 52.0 | Silty-clay | Non-pock site |
| | A7 | 66º10.496 | 17º33.553 | 196 | 75.5 | Silty-clay | Non-pock site |
| Site B | B2 | 66º06.961 | 17º41.308 | 204 | 37.5 | Coarser silt/clay | Pock site on HFF |
| | B3 | 66º06.688 | 17º40.146 | 204 | 63.0 | Coarser silt/clay | Pock site on HFF |
| | B4 | 66º06.500 | 17º39.193 | 202 | 16.5 | Coarser silt/clay | Pock site on HFF |

source and accumulation of hydrocarbon is though to be identical in both bays, with a large hydrocarbon reservoir at depth (Geptner et al. 2006 a,b).

Concentrated fluid flow can occur both along faults and bedding planes (Josenhans et al. 1978, Hovland et al. 1984, Dimitrov and Woodside 2003, Judd 2003). Different sedimentary units have differing porosity based on changes in the physical properties of the sediments, grain size, matrix material and compaction (Driscoll et al., 2000; Hill et al., 2004). Pathways commonly occur where there is a high porosity unit overlain by a significantly less porous unit or aquitard and when combined with a head or buoyancy gradient along dipping beds the fluid will flow (Fig. 3.5). Faults commonly act as pathways for fluid flow through two mechanisms; topographic driven groundwater flow (faults occurring in topographic lows and valleys because of preferential erosion along fault planes), and the high permeability that occurs in fault zones due to a concentration of stress and fault slip (Gudmundsson 2000). Fault zones consist of two contrasting permeability units, the core unit (the main fault slip zone) consisting of brecciated material, and the damage zone that has a much higher permeability than the host rock (highly faulted and fractured). High permeability in fault zones is maintained by concentrating stress, generating new fractures and reopening old ones in the fault zone itself (Gudmunsson 2000). Due to the focused nature of fluid expulsion, seafloor

environments can be significantly different within a small area, resulting in wide variation in habitat.

These differences in seafloor environment can lead to significant differences in biota distribution. This can either be because of active fluid flow potentially enhancing nutrient levels, or to increased detrital deposition occurring in divots and pockmarks enhancing nutrient levels (Judd and Hovland 2007).

### 3.3.2 Pockmark Classification

Hovland et al. 2002 outline the common morphological categories of pockmarks. Unit Pockmarks are small depressions (1-10 m x 0.5 m) commonly inside and near larger pockmarks. Circular depressions on the order of 10-700 m x 1-45 m are classified as Normal Pockmarks and can have cross sections basin shaped to asymmetric steep walled features. Elongate Pockmarks where one axis is disproportionately longer than the other. Strings of pockmarks can consist of unit or normal pockmarks in linear/curvilinear chains. Elongate pockmarks are thought to form in areas of strong currents and/or steep slopes (Driscoll et al., 2000, Hill et al., 2004). As the expulsion event occurs material is displaced, suspended and transported away by bottom currents or dominant tidal forces. This directional transportation results in preferential erosion in the down current direction of the pockmark elongating

the pockmark, resulting in potential pockmark growth and the long axis parallel to the dominant flow direction (Josenhans et al. 1978, Hovland et al., 1984, Judd & Hovland 2007). Strings of pockmarks are usually spatially associated with faults; the faults act as fluid pathways to the surface, focusing fluid expulsion in areas along curvilinear features (Fig. 3.5). The first expulsion event is thought to be reasonably violent and results in the initial evacuation of the pockmark, while subsequent events can be less energetic and pockmarks can continue to exist without continual fluid flow through preferential erosion. Pockmark size has also been inversely linked to sediment size, with large pockmarks only occurring in fine grain sediments (Judd & Hovland 2007). The pockmarks profile is indicative of the level of activity of the pockmark itself, a more “v” shaped profile indicated a more active pockmark, while pockmarks with a more “u” shape are likely to have been intermittently active (Hovland et al. 1984, Kelly et al. 1994)

## 3.4 DATA ACQUISITION

A dense grid of CHIRP lines and high-resolution bathymetry was acquired in Skjálfandi Bay documenting the high density of pockmarks in the outer bay and along the western portion of the Húsavík-Flatey Fault (HFF) (Fig. 3.4). Three cruises were conducted in the TFZ during the 2001, 2002, and 2003 field seasons, two high-resolution seismic systems were used; the

SUBSCAN CHIRP/Side Scan Sonar and a portable High-Resolution Multichannel Seismic Acquisition System (MCS) as well as EM300 and Reson 8010 multibeam. During the 2001 cruise the MCS and CHIRP were operated simultaneously allowing a nested approach for data interpretation and 1600 km of both CHIRP and MCS data were acquired across the three bays (Eyjafjördur, Skjálfandi, and Öxarfjördur). During the 2003 field season an additional 700 km of CHIRP was acquired just within Skjálfandi Bay generating an unprecedented density of seismic lines in this location. In addition, we acquired digital bottom photography using the WHOI TowCam system (Billings and Fornari 2002) and sediment cores (Fig. 3.4).

The Edgetech SB0512 seismic sub-bottom profiling and side scan imaging system used in the TFZ survey sweeps (chirps) across 1.0 to 6.0 kHz in 50 ms. With these operating frequencies we are able to obtain sub-meter resolution for a depth of 30-40 m. The remotely controlled system consists of a DF1000 side scan system operated in conjunction with an X-Star subbottom sonar with a shipboard real-time data display. Data display in real time allows fine tuning of the operational procedure with respect to fish depth and ship speed, an invaluable tool to improve the quality of the data. The Lamont High Resolution MCS system was used, it is designed to image structures > 1 km depth to a resolution of 2-5 m. It consists of a 210 cu. in. Gas Injection system by Seismic Systems, a 600 m long ITI streamer with 193 hydrophones in 48

groups with a 12.5 m group interval, a OYO DAS-1 a digital acquisition system, and a 5s shot spacing was used. SIOSEIS was used to provide brute stacks of the data in near real time so as to maximize data quality.

Due to the offset between the towed instrumentation and the shipboard GPS precise location of the data was obtained using differential global positioning service (DGPS) receivers, and post processing alignment with bathymetric data. The MCS and CHIRP were operated concurrently at about 5 kts allowing a nested approach for high-resolution data collection both in the uppermost 20-50 m and down to 500 m. A total of 1600 km acquired across the three bays (Eyjafjördur, Skjálfandi, and Öxarfjördur), here we present MCS and Chirp data from the Skjálfandi Bay, processed using the SIOSEIS (Henkart, 2003) and Seismic Unix (Cohen and Stockwell, 1999) seismic processing software packages.

## 3.5 DISSCUSSION

### 3.5.1 Pockmarks in Skjálfandi Bay

Pockmarks in Skjálfandi Bay occur in a band approximately 15 – 22 km offshore, along with some localized pockmarks along the HFF (Fig. 3.4). The subsurface structure in the region creates an interesting relationship between the most recent approximately horizontal postglacial sediments, the underlying

chaotic glacial sediments and the older westward dipping sediments (Fig. 3.6). The pockmarks in the outer bay are expressed on the seafloor where the recent sediments are ~ 30 m thick and the glacial sediments are ~50 m thick (Fig. 3.7). Assuming that the fluids in this area are of similar composition to those to the north, they are migrating from depth and require input of organic matter. The source for the upwelling fluids is likely to be the Tjornes beds (up to 1200 m thick onshore), which are made up of interbedded lava flows, fluvial, lacustrine and fossiliferous marine sediments, alternating with glacial tillites. This is consistent with the findings of Geptner et al. (2006 a,b) who showed that there is a strong hydrocarbon signal in the geothermal fluids. As described by Einarsson (1991) there are three main sedimentary groups separated by lava flows, acting as both sealing units and pathways. The units consist mainly of marine sediments rich in fossilized shells and gastropods and lignite, indicating that the sediments have both been below sealevel and at or near it. The oldest of which is the Tapes Layer, followed by the Mactra and the Serripes layers. Tapes and Mactra layers consist of alternating lignite and shell deposites, forming in shallow seas and coastal regions. Pollen analysis of the lignite deposites in the Mactra layers indicate that the lignite was formed during a time when there were coniferous forests mixed with other trees, suggesting a milder climate then present. The Serripes layers are just over half the total thickness of the whole sediment succession, and consist of

mainly marine sediments, with some thin lignite beds near the top, underlying these sediments are 8 Ma Tertiary volcanics.

During glacial times sea level was significantly lower, exposing large areas of the bay as coastal plains and estuarine regions. These were subsequently flooded as sea levels rose burying the organic rich sediments that through diagenetic processes can become hydrocarbon source rock. Sealevel and shoreline locations are tied to glacial extent, at the last glacial maximum glaciers filled Eyjafjördur fjord and extended north into Skjálfandi bay while Öxarfjördur bay was ice free (Norddahl et al 2005), during the preboral glaciation (9,800 B.P.) the whole region of study was ice free and was either estuarine or shallow marine environment.

A Holocene sediment thickness of 10-25 m in the CHIRP records indicates an average sedimentation rate of 1-2.5 m/kyr, however there is significant spatial variations in sediment thickness across Skjálfandi Bay caused by active sediment drifts and depositional environments within this region. Observed variations in Holocene sediment thickness across the Bay are most likely caused by currents that travel clockwise around Iceland (Jónsson and Valdimarsson 2005). Water circulation around Iceland is dominated by the interaction of two different water masses, the warm and saline Atlantic Water and the cold and fresh Polar Water. The Atlantic current

is the main current that influences the northeastern coastal region (Jónsson and Valdimarsson 2005). The Atlantic current flows north and splits as it hits southern Iceland, part of the current flow to the east towards the Iceland-Faroe Ridge, and the other portion flows west and north becoming the Irminger Current. The Irminger Current flows north clockwise around Iceland, it splits again at the western extreme of Iceland, with a small portion continuing to the east as the North Icelandic Irminger Current. It is this current that effects the currents in our area of interest. The interaction between the current and the tides is a key factor in the final morphology of the seafloor, and SPOT images of Skjálfandi Bay (Fig. 3.8) clearly show the effect of the tides on the distribution of sediment in the bay, circulating the input from Skjálfandafljót glacier river counter clockwise. Given the resulting morphology of the pockmarks we believe that it is likely that the current has a greater effect in the deeper northern section of the bay, decreasing to the south as the tidal and riverine input becomes more dominant.

The CHIRP data images the most recent sediments down to a depth of 35-40 m and the MCS data images older sediments in the bay, with three basin wide stratigraphic units identified on the basis of their acoustic and deformational character. The basal unit is interpreted to be the top of the Tertiary, topped by both on angular and erosive unconformity. This unit largely consists of beds that are dipping to the west, and are thought to perhaps

correspond to the Tjörnes Beds. Moving up section, the dipping beds are overlain by an acoustically chaotic unit 20-50 m that fills in the roughness of the unconformity. Above this acoustically chaotic unit there is an acoustically laminated unit 50-100 m thick, indicative of a calmer depositional environment and all of the CHIRP data lies within the top third of this unit.

The pockmarks occurrence in the outer bay is a tightly constrained band (15-22 km offshore) that is likely due to the interplay between the organic source material and the sediment overburden (Fig. 3.7). In the near shore region the thick glacial and postglacial sediments may form an effective permeability barrier above the source rocks preventing the formation of pocks apart from in proximity to the HFF, where the fault itself provides a permeability pathway to the surface. Slightly further offshore it is probable that the sediment overburden has thinned to a sufficient degree to allow the passage of gas to the surface. Farther offshore the organic rich sediments may not have been deposited, with no source rock for gas there will be no pockmarks. All of these factors combined give rise to the distribution of pockmarks that are observed on the seafloor in Skjálfandi Bay.

### 3.5.2 Linear pockmark chains

The detailed location of linear chains of pockmarks within the larger band of pockmarks is likely to be controlled by fluids migrating along dipping

units at depth. Several of these linear chains are highlighted in red on the MCS data in Fig. 6 and occur directly above the updip end of the beds. Fluid moving along these beds migrates up through overlying sediments, which gives rise to the linear chains of pockmarks observed on the seafloor. The orientation of the long axis of the individual pockmarks changes systematically around the bay (Fig. 3.9), with the eastern portion NE-SW, central EW and the western portion NW-SE. There is also an asymmetry in the excavated profile of these pockmarks, where the eastern wall of the pockmark is steep (5-12º) and the western wall of the pockmark much less steep (1-2º). Morphology of the pockmarks on the seafloor exhibit interesting features; most of them have a curious shape, a steep eastern wall, and an elongate “v” shaped tail. On both the eastern and western side of Skjálfandi Bay the pockmarks have a curious alignment, they occur in predominantly linear groups (Fig. 3.10). The fluid rising from the inclined bedding interacting with currents along the seafloor gives rise to these linear pockmark chains and their asymmetric seafloor morphology. The consistent morphological shape of the pockmarks; elongate, steep sided, and “v” shaped, shows that there are all governed by the same expulsion and activity regime. There are no areas that area obviously more or less active than others in the northern section of the bay.

Whether the fluid expulsion along the faults is either constant or episodic – the resulting pockmark would have surprisingly similar morphology

consisting of a “u” or “v” profile. The expulsion event would mobilize the sediment, which would be then transported by the bottom currents creating the v-shaped tail. This shape would be maintained by the continued current flow, either by transporting the sediment as it expelled or by eroding the sediment preferentially from the pockmark. If the pockmark is less active the unstable sides of the pockmark fail, filling and widening the pockmark enough to result in more of a “u” shaped profile. The location of the pockmarks is controlled by the fault distribution while the bottom currents control the surface morphology.

The seafloor around the HFF also exhibits pockmarks in a systematic way indicating that control on the occurrence and distribution of pockmarks may also be tectonic in origin in addition to the control from sediment distribution and current influence.

### 3.5.3 Pockmarks associated with the HFF

Those that occur closer to the HFF lack the elongate profile observed in the outer bay pockmarks, they are compound pockmarks consisting of 3 or more pockmarks that coalesce (~100 m x 20 m x 2-3 m). These larger pockmarks occur along the edge of the uplifted footwall block (Fig. 3.11). Within southern Skjálfandi Bay elongate pockmarks occur in groups along the HFF to the west of the popup structure where the vertical displacement of the HFF is the greatest (Fig. 3.12a,b). The western half has significant vertical

uplift, up to 15 m in places, decreasing to 0-1 m in the eastern half. This change dramatically occurs across the basement high (~40 m) resulting from a constraining bend in the strike slip fault. The eastern portion has little to no significant vertical offset with no observed pockmarks in the bathymetric data. The HFF has been traced in places to a depth of 1.5 km (Riedel et al. 2001) and at such depth it would cut through the postglacial and glacial sediments providing a pathway for hydrocarbon rich fluids to migrate to the surface. For a fault to act as a pathway there has to be continued activity or stress to increase the permeability in the fault zone, there is obvious activity on the western portion of the fault and very little to none on the eastern half. This dichotomy in fault characteristics is also observed in the distribution of pockmarks along the HFF. On the western portion they occur in groups that range from orthogonal to oblique with respect to the fault plane, their orientation influenced by the behavior of the hanging wall block during movement on the fault, fault movement and reactivation can cause slight fractures at high angles to the fault block, fractures that are exploited by fluid flow in this location.

### 3.5.4 Towcam and Sidescan images of the HFF pockmarks

The tow cam data shows that the seafloor in this area can be characterized in to three categories; a) hard grounds exposed at or on the fault scarp (Fig. 3.11, 2.13, yellow), b) normal soft grounds characteristic of the

average seafloor (Fig. 3.11, 2.13, blue), and c) soft grounds within the large pockmarks observed on the bathymetry and sidescan (Fig. 3.11, 2.13, red). These three types of seafloor have markedly different appearances and biota. The hard grounds consist of more indurated sediment that has been exposed at the seafloor through the vertical displacement of the fault. Many different types of fish, soft corals, urchins, starfish, sea cucumbers and other species populate the fault scarp. The soft grounds are all fine to medium grained sediment, inhabited by polychaete worms. Inside the large pockmarks the biota is significantly different than outside, with an increase in the density of polychaetes and the occurrence of small pocks, cm size features on the seafloor that could be either fluid expulsion features or burrows. Some of these pocks have small shrimp occupying them and it is difficult to determine if they are resident in these features or have taken refuge in them while being photographed. Occasional pocks have what appear to be excavation mounds located near the mouth of the feature that would tend to indicate a tenant inside (Fig. 3.13 #6, note the excavated sediment is a darker color), however as this is only observed infrequently, it is unclear how common is the occupation.

There is a clear linkage between the geology of the seafloor and faunal distribution. The large pockmarks that occur in close proximity to the HFF consist of multiple pockmarks. With seafloor photographs it is apparent that

these pockmarks are home to a variety of fauna that are not found on or in the unpockmarked seafloor. This increase in faunal diversity is thought to be because of an increase in nutrients at these locations, due either to active fluid flow or an increase in deposition of detrital material in the pockmark.

Temperature data was taken concomitantly with the Towcam photographs and there were no observed temperature anomalies associated with the pockmarks, with the temperature at the seafloor staying consistently around 5.5-6 ºC (Fornari D., personal communication). Other cold seeps (Gulf of Mexico, Paull et al. 1984) have large and vigorous biological communities closely resembling those observed at high temperature vents on the East Pacific Rise and other locations.

## 3.6 SUMMARY AND CONCLUSION

In the last few years, the impact and influence that migrating fluids have on the on the lithosphere-ocean interactions has started to be understood. Many of these fluids expel heat, along with chemically active compounds that can provide nutrients to the microbial biosphere impacting the entire system from a fundamental level. This introduction of fluids occurs in a variety of setting, notably along faults, fissures, and other venting structures. The pattern and distribution of venting fluids at the seafloor is not something that can be

predicted at this time. To do this their distribution needs to be mapped and observed, and then understood. Only then can the fluid flux be effectively measured and the direct impact be assessed and modeled. In this paper we mapped and explained the distribution of pockmarks in Skjálfandi Bay, and have furthered the understanding of the controlling mechanisms for the distribution of pockmarks. Some insight has also been gained into the interaction between seafloor processes, such as tides and currents, and the expulsion of fluid/sediments giving rise to unique pockmark morphology. The pockmarks in turn are exploited by biota in the region either because of nutrients being supplied by the fluid or detritus collecting in the pockmarks themselves, either way they provide a valuable habitat for the regional fauna.

In summary below:

- Pockmarks occur in a band across Skjálfandi Bay ~ 15-22 km from shore
- Where these pockmarks occur, the recent and glacial sediments are thin enough to allow fluid migration from depth along westward dipping bedding planes to reach the surface forming linear pockmark chains, < 30 m and < 50 m respectively.
- The seafloor morphology of the pockmark chains indicates modification by seafloor currents circulating through the bay clockwise.

- Pockmarks occur along the HFF because the fault plane breaks into the hydrocarbon/fluid reservoir at depth.
- Seafloor morphology of the elongate pockmarks in proximity to HFF appear to be controlled primarily through fluid flow along the fault plane or associated fractures.
- Unit pockmarks (~ 10-40 cm diameter) occur with significantly greater proportion within the elongate pockmarks near HFF.
- Faunal diversity is much higher with the elongate pockmarks on the HFF than outside them, indicating the biota is exploiting either increased nutrients due to active fluid flow, or due to increased detrital deposition.

We have demonstrated here the importance of combining observational tools of different scales they provide an unprecedented opportunity to integrate from multibeam and seismic data (10's m scale) down to towcam images (cm scale) and in doing so document the linkages between geologic processes and biological distribution. Without the ability to view the seafloor at such a variety of scales the linkage between elongate pockmarks and faunal distribution along the HFF would remain an unknown, and without the linkages of seismic data and bathymetric data the structural control of pockmark location in the outer Skjálfandi bay would be unexplained. Information at

different scales is key for gaining a full understanding of the processes and influences that shape the environment.

## 3.7 ACKNOWLEDGEMENTS

This research was supported by a grant from the National Science Foundation, University of Iceland and Iceland Geosurvey.

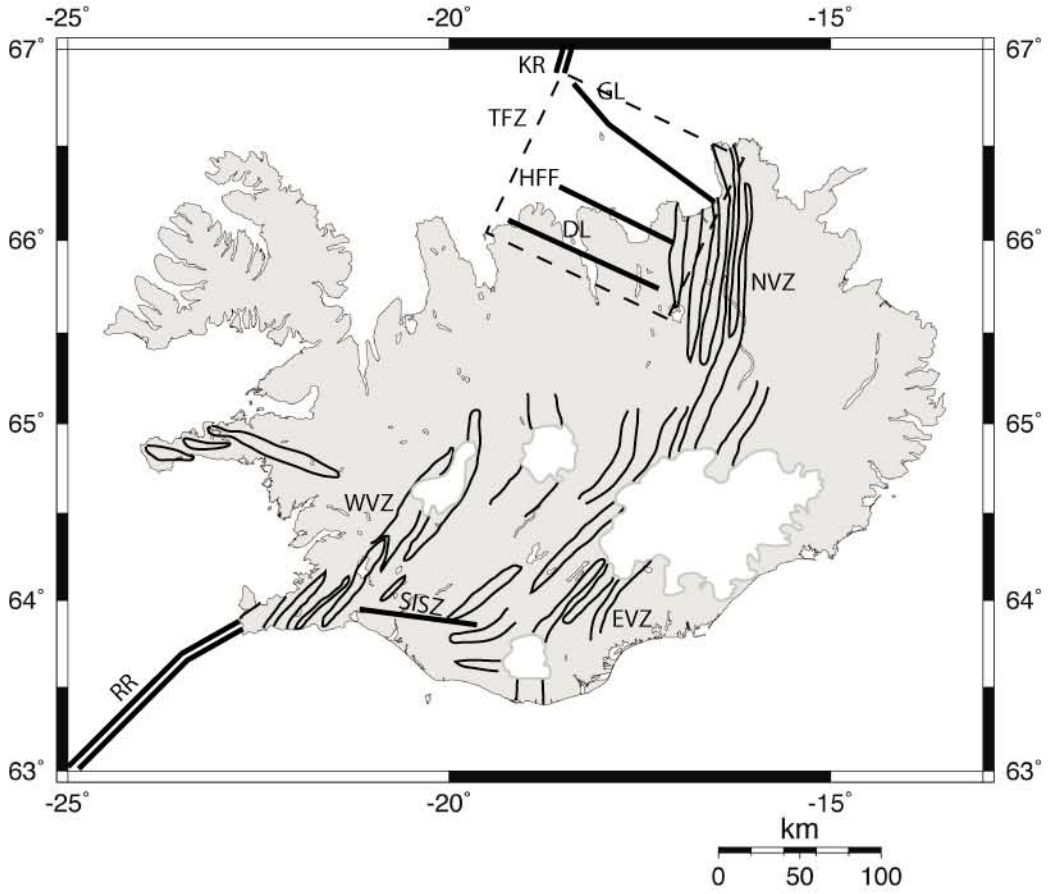


## Figure 3.1

Iceland location map detailing the Reykjanes Ridge (RR), and the Kolbeinsey Ridge (KR) offshore as double lines. The West Volcanic Zone (WVZ), East Volcanic Zone (EVZ) and the North Volcanic Zone (NVZ). The South Iceland Seismic Zone (SISZ) is indicated by a single line onshore. The Tjörnes Fracture Zone (TFZ) occurs within the dashed box and contains the Dalvík Lineament (DL), the Húsavík-Flatey Fault (HFF), and the Grímsey Lineament (GL).

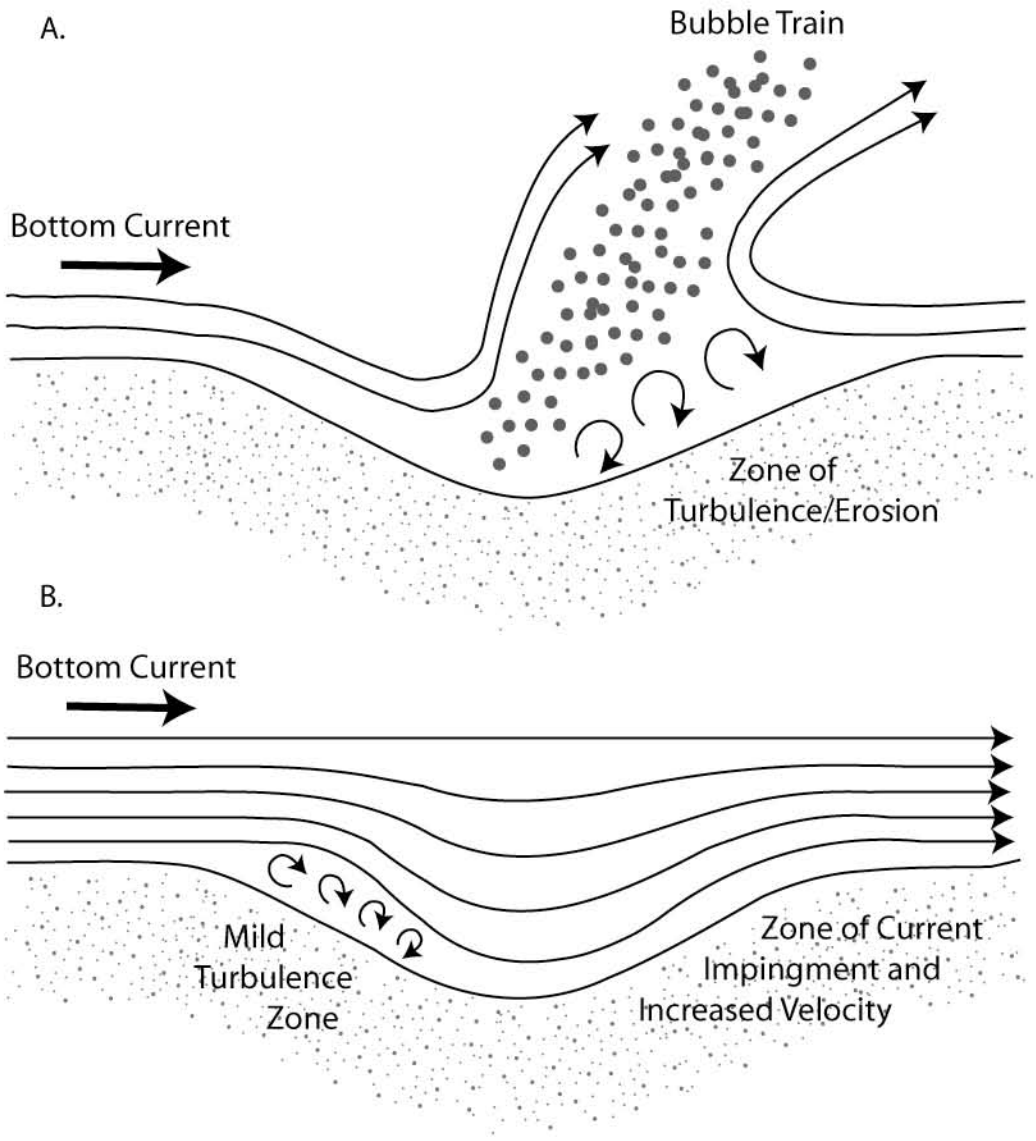


## Figure 3.2

A) Pockmark formation interaction with bottom currents or tides, arrows indicate current flow direction. Pockmark elongates through erosion caused by turbulence at the down stream wall.

B) Elongation of inactive pockmarks, some erosion on the upstream edge if the current is high enough to induce turbulence, main area of erosion is on the downstream side from current impingement and resulting in increased velocity and erosion. (Modified from Josenhans et al. 1978).

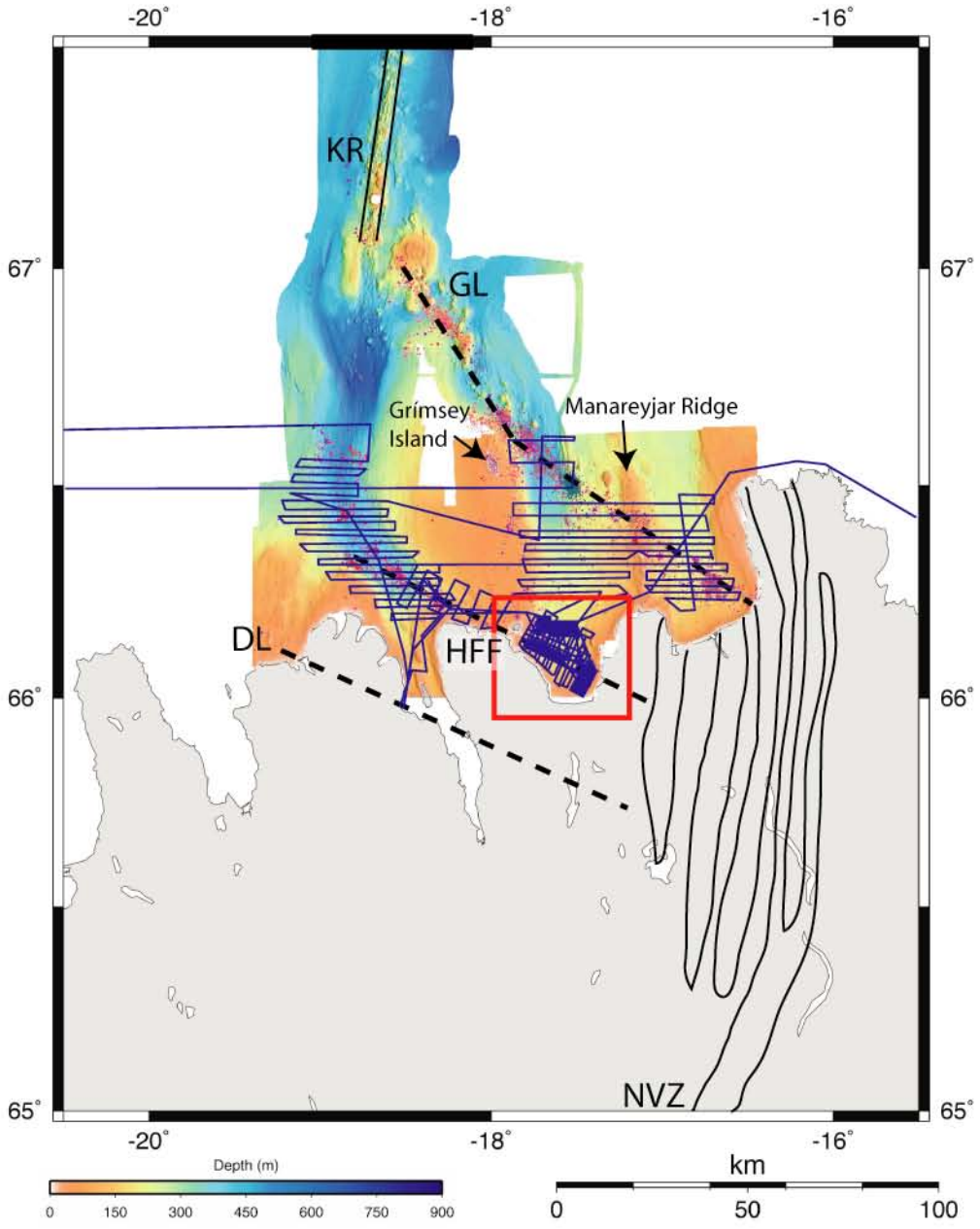


## Figure 3.3

Data coverage in the TFZ, colored areas are bathymetry (cooler = deeper), blue lines is the seismic data coverage, both CHIRP and MCS. This shows the bathymetry of Manareyjar Ridge, the offshore extension of the NVZ, Dalvík Lineament (DL), Húsavík-Flatey Fault (HFF), Grímsey Lineament (GL).

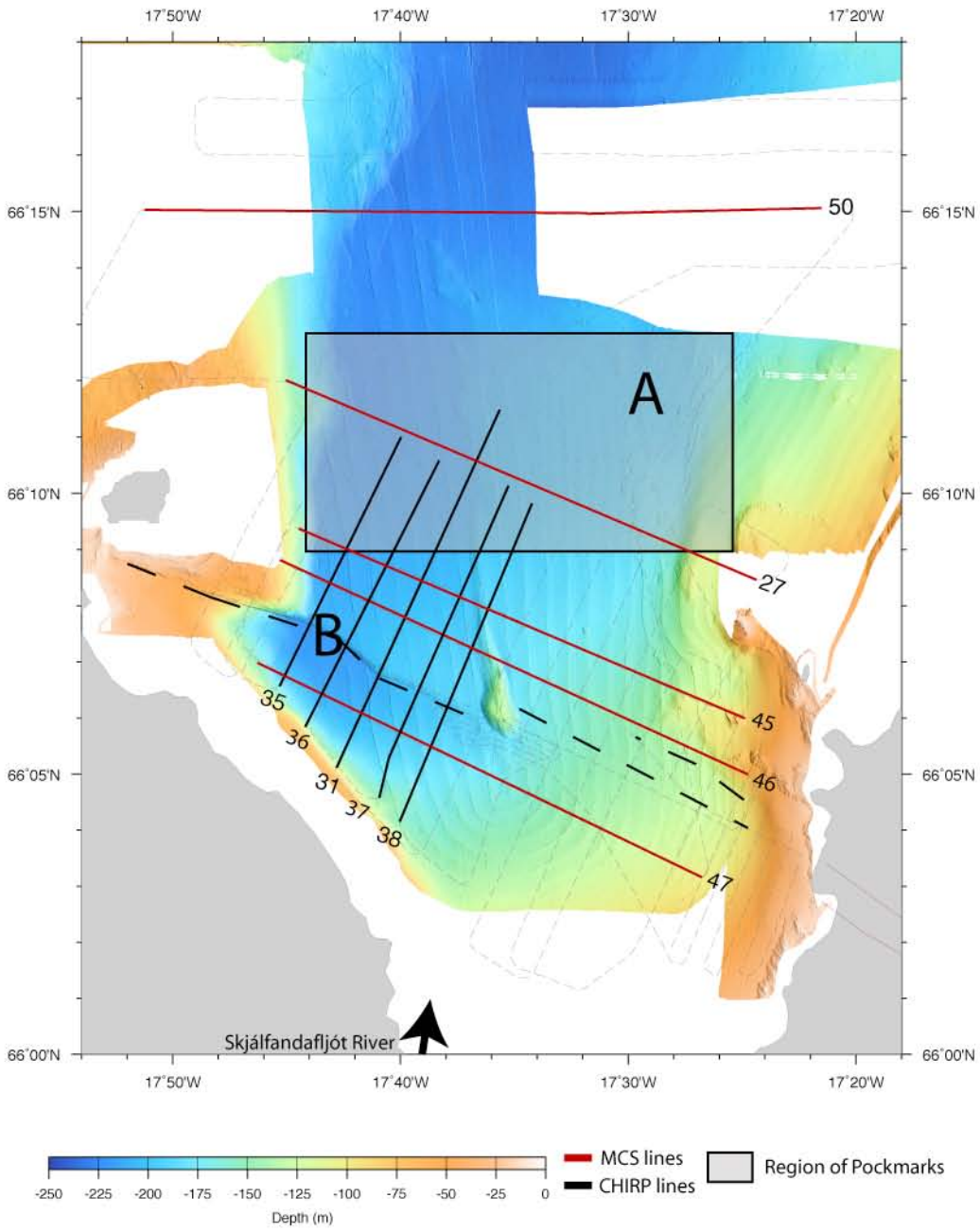


## Figure 3.4a

Map of Skjálfandi Bay, highlighted lines are the data presented in this paper CHIRP lines are black, MCS lines are red. Húsavík-Flatey Fault is the black dashed line. Site A and B are the locations of the cores and the stippled area is the band of pockmarks 15-22 km offshore.

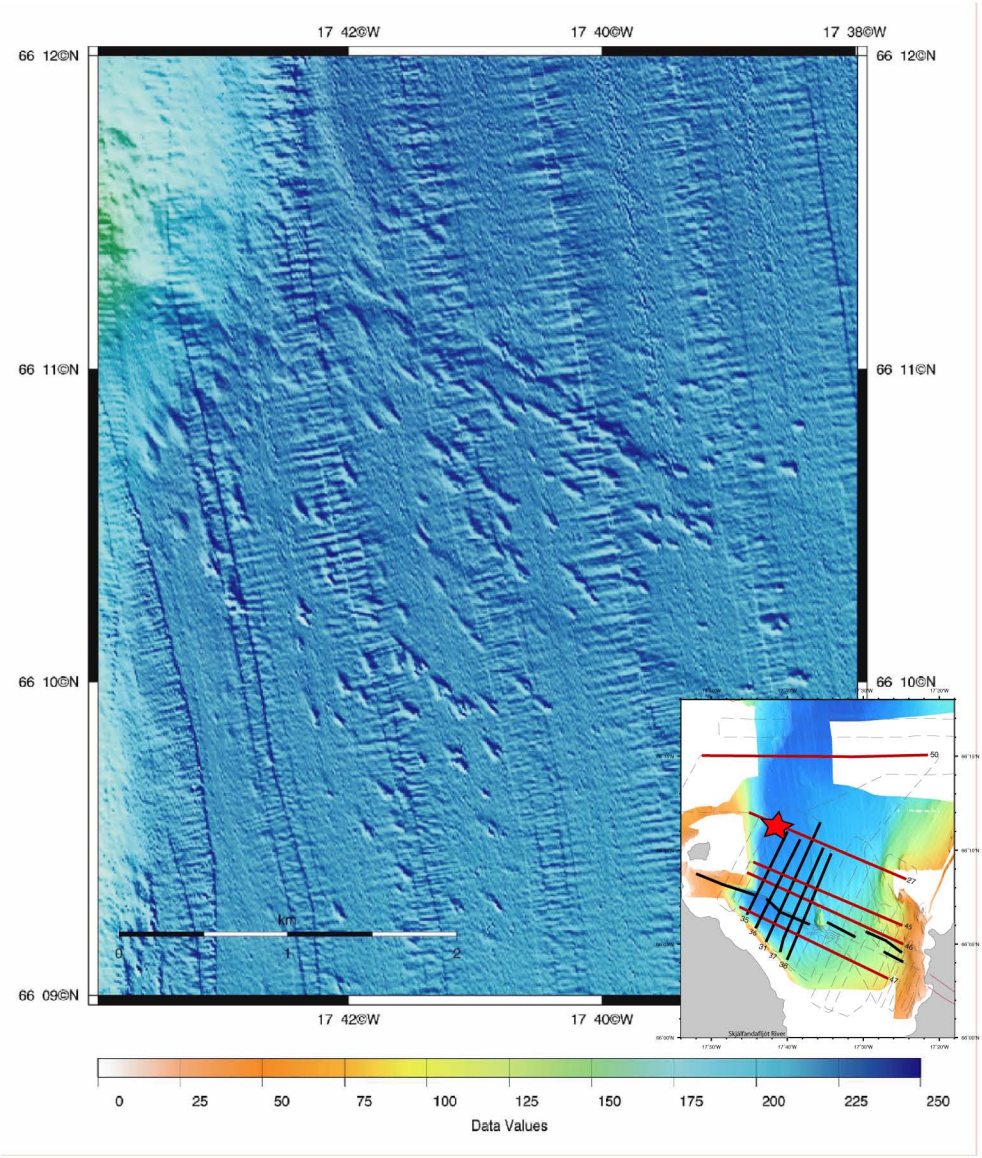


## Figure 3.4b

Elongate, assymetric pockmarks located on the western side of the bay, see map to left for locationindicated by red star. Orientation of the long axis of the pockmarks changes with proximity to the basin margin.

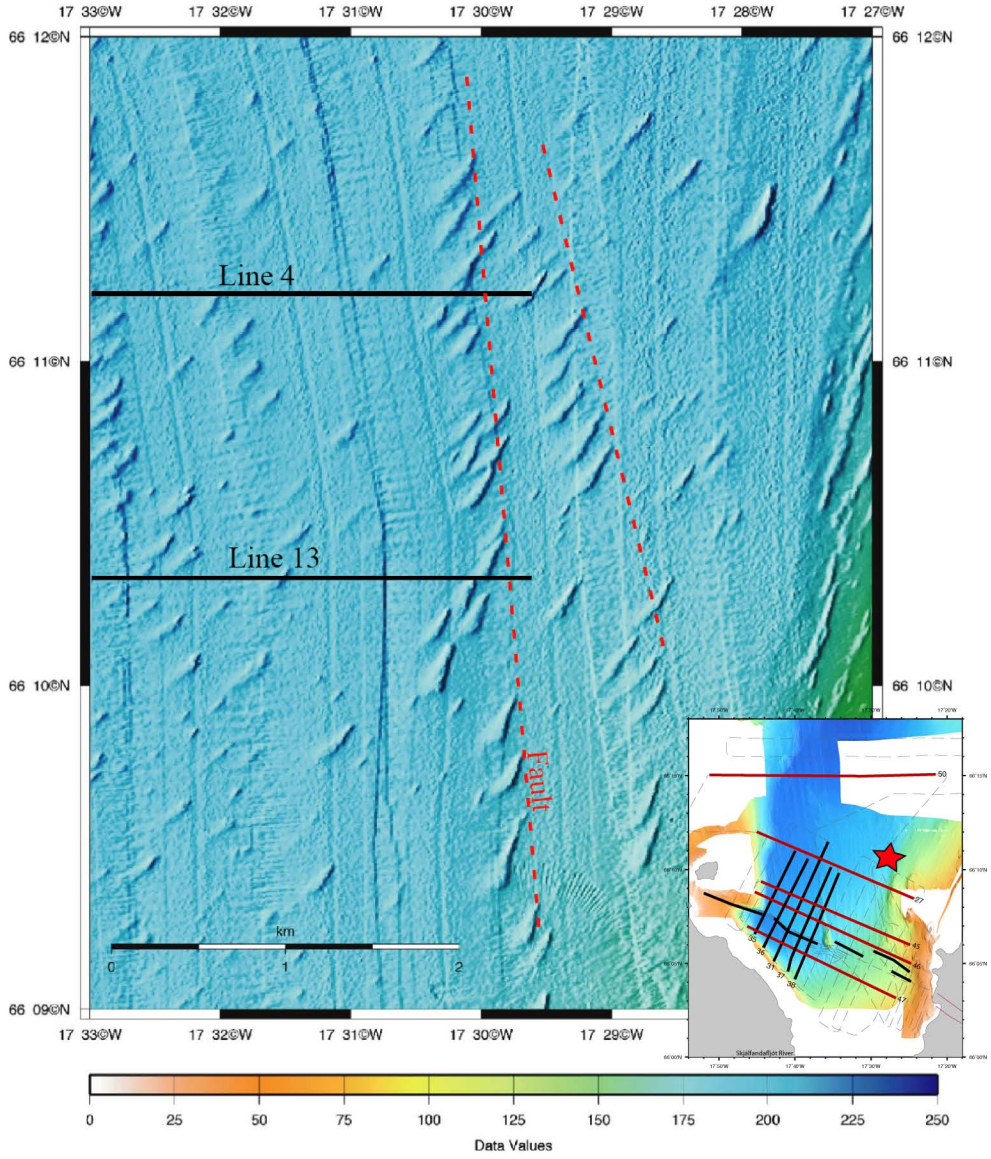


## Figure 3.4c

Elongate, assymetric pockmarks located on the eastern side of the bay, see map to left for location indicated by red star. Orientation of the long axis of the pockmarks changes with proximity to the basin margin.

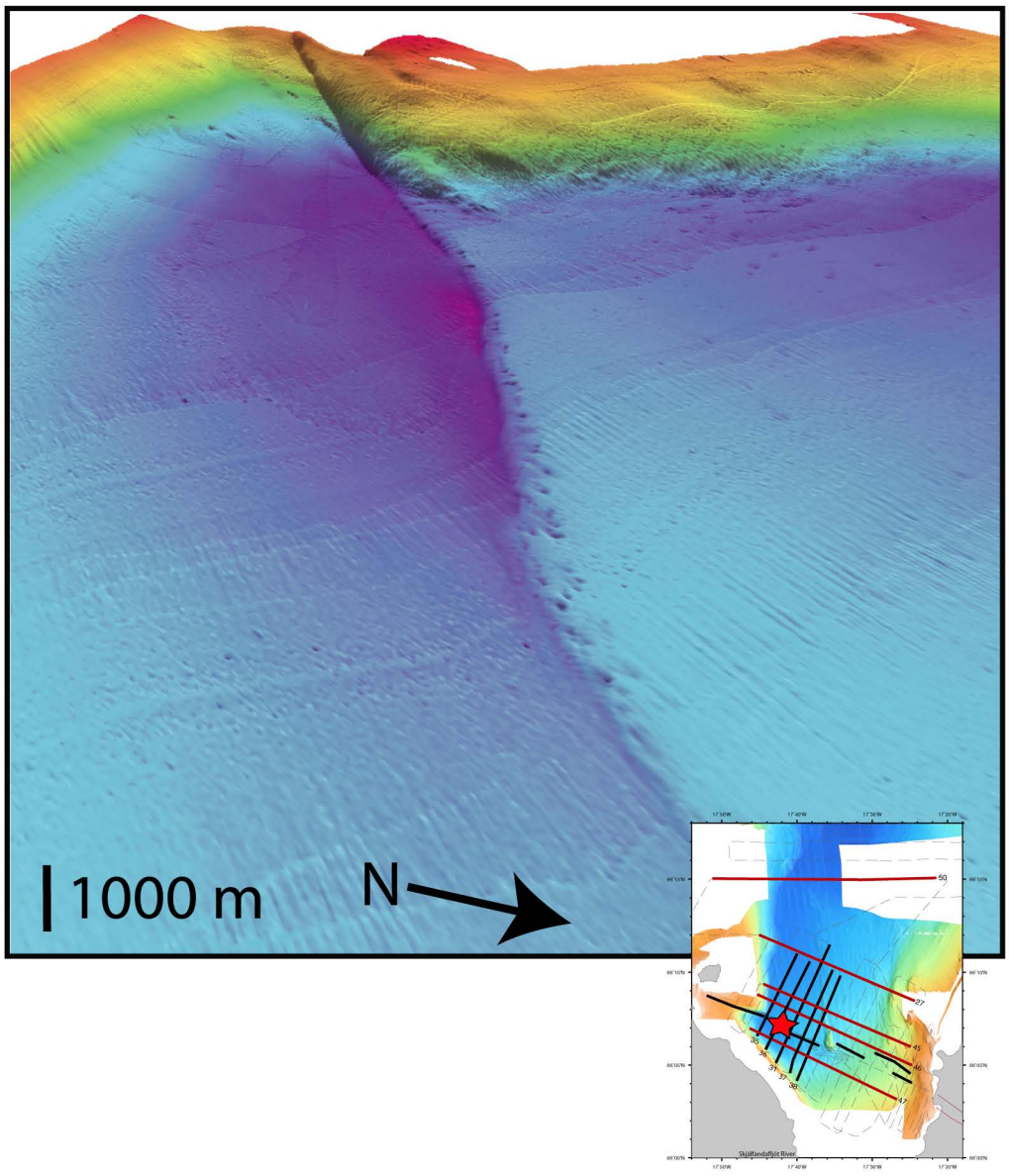


## Figure 3.4d

Prespective view of the pockmarks along the HFF, both single and compound pockmarks. Location of figure indicated by the red star on map to left.

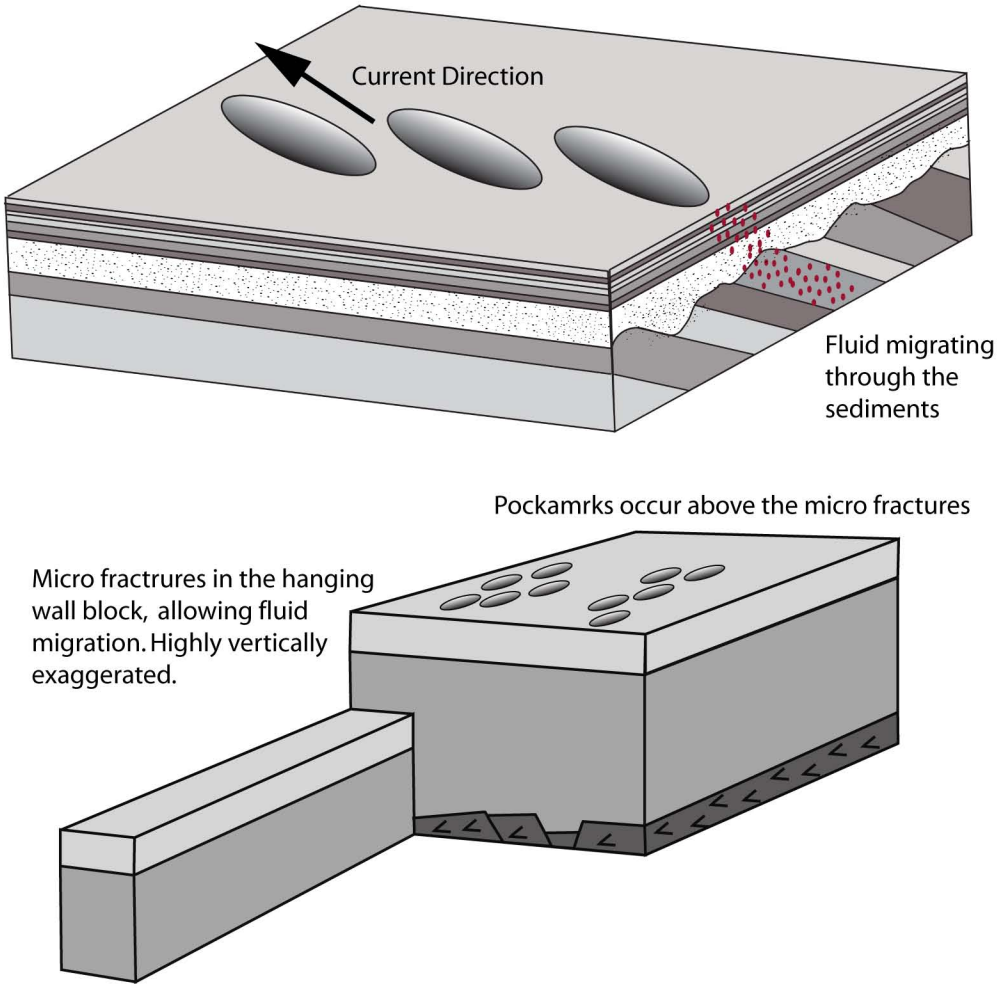


## Figure 3.5

Fluid migrating from depth (red dots), travels along the bedding planes and percolates through the overlying sediments, forming pockmarks at the seafloor. Concentrations of pockmarks occur in linear features above the updip limit of the inclined beds. Seafloor morphology is modified by bottom currents creating a systematic asymmetry.

Fluid migrates from depth along the small cracks that occur at a high angle to the fault (highly exaggerated in this figure) and pockmarks are located at or near these cracks.

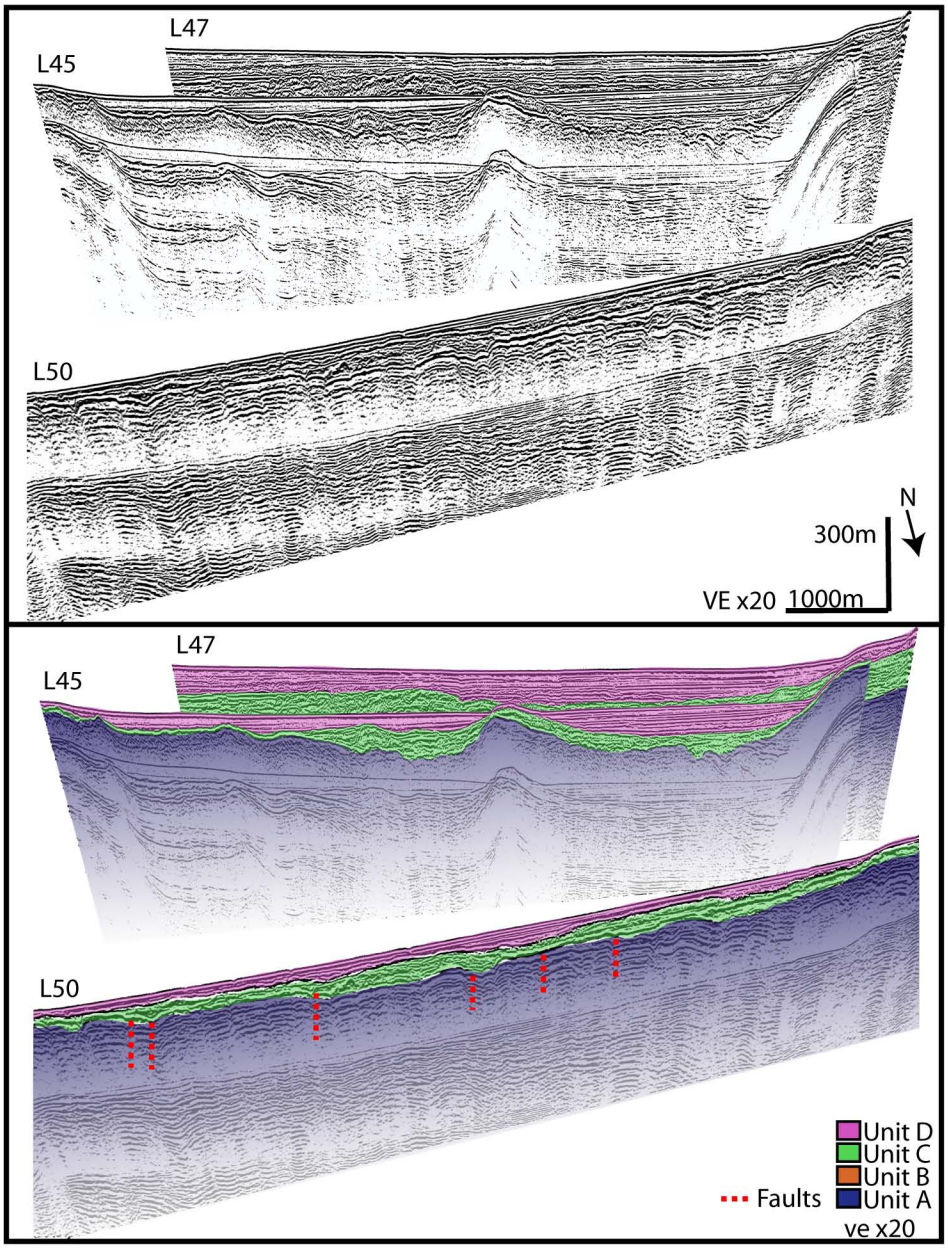


## Figure 3.6a

MCS lines L47, 27, 50 (for location see Fig. 2.4). L47 is near shore and has thick postglacial and glacial sediments, only a small section of the west dipping beds can been observed within the resolution of the data. L27 cuts through the band of pockmarks in the bay, solid red lines indicate linear chains of pockmarks, dashed red lines indicate possible faults. Note that the linear chains of pockmarks lie directly above the updip limit of dipping units. L50 is furthest off shore and is beyond the pockmark band, the postglacial and glacial sediments are thin, and the dipping units have decreased in dip and are highly faulted. 6b: is the interpreted seismic data; Unit A and B are interpreted to be early to middle Pleistocene in age, Unit D is Pleistocene and recent sediments, with minor offset.

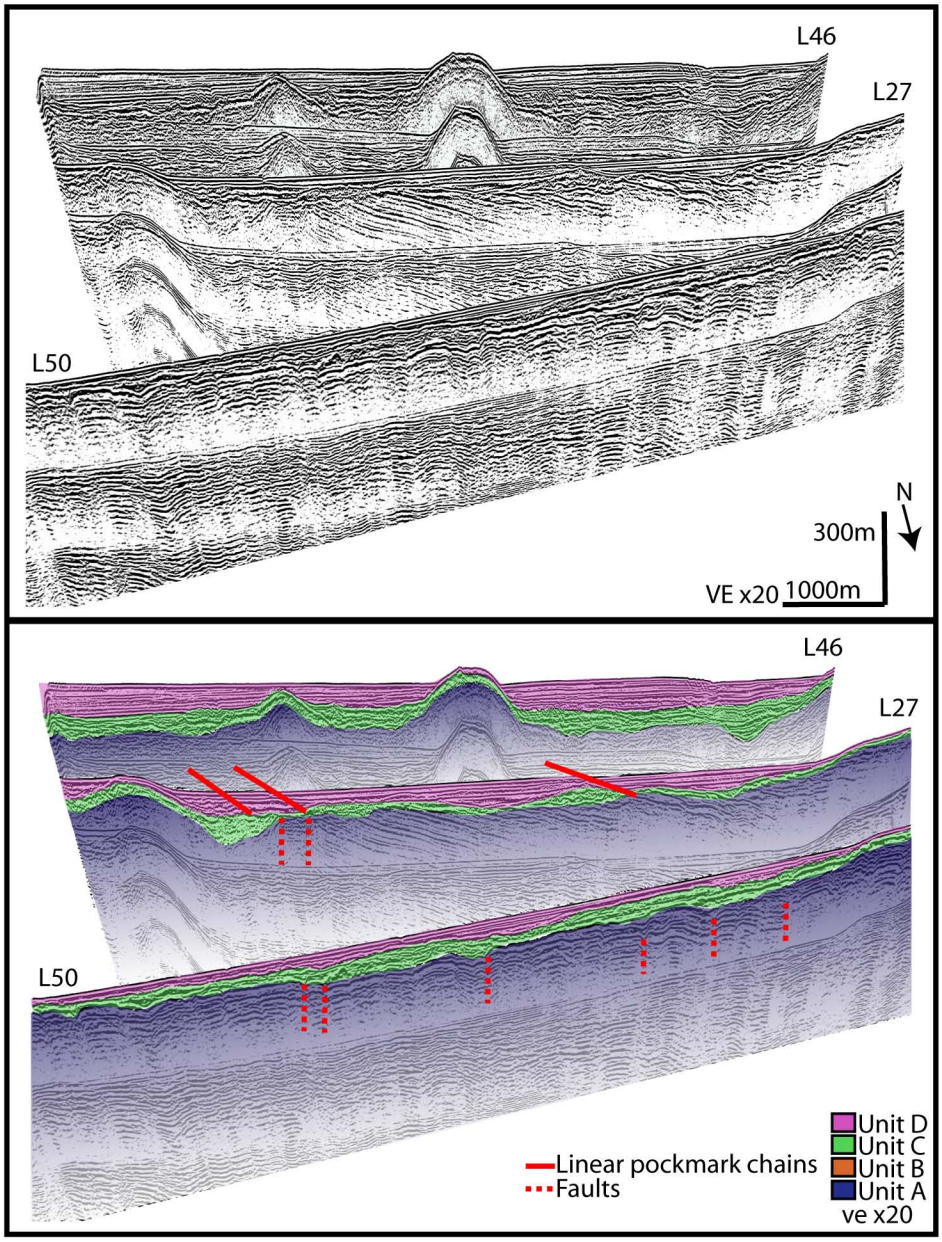


## Figure 3.6b

MCS lines L46, 27, 50 (for location see Fig. 3.4). L46 is near shore and has thick postglacial and glacial sediments, only a small section of the west dipping beds can been observed within the resolution of the data. L27 cuts through the band of pockmarks in the bay, solid red lines indicate linear chains of pockmarks, dashed red lines indicate possible faults. Note that the linear chains of pockmarks lie directly above the updip limit of dipping units. L50 is furthest off shore and is beyond the pockmark band, the postglacial and glacial sediments are thin, and the dipping units have decreased in dip and are highly faulted. 6b: is the interpreted seismic data; Unit A and B are interpreted to be early to middle Pleistocene in age, Unit D is Pleistocene and recent sediments, with minor offset.

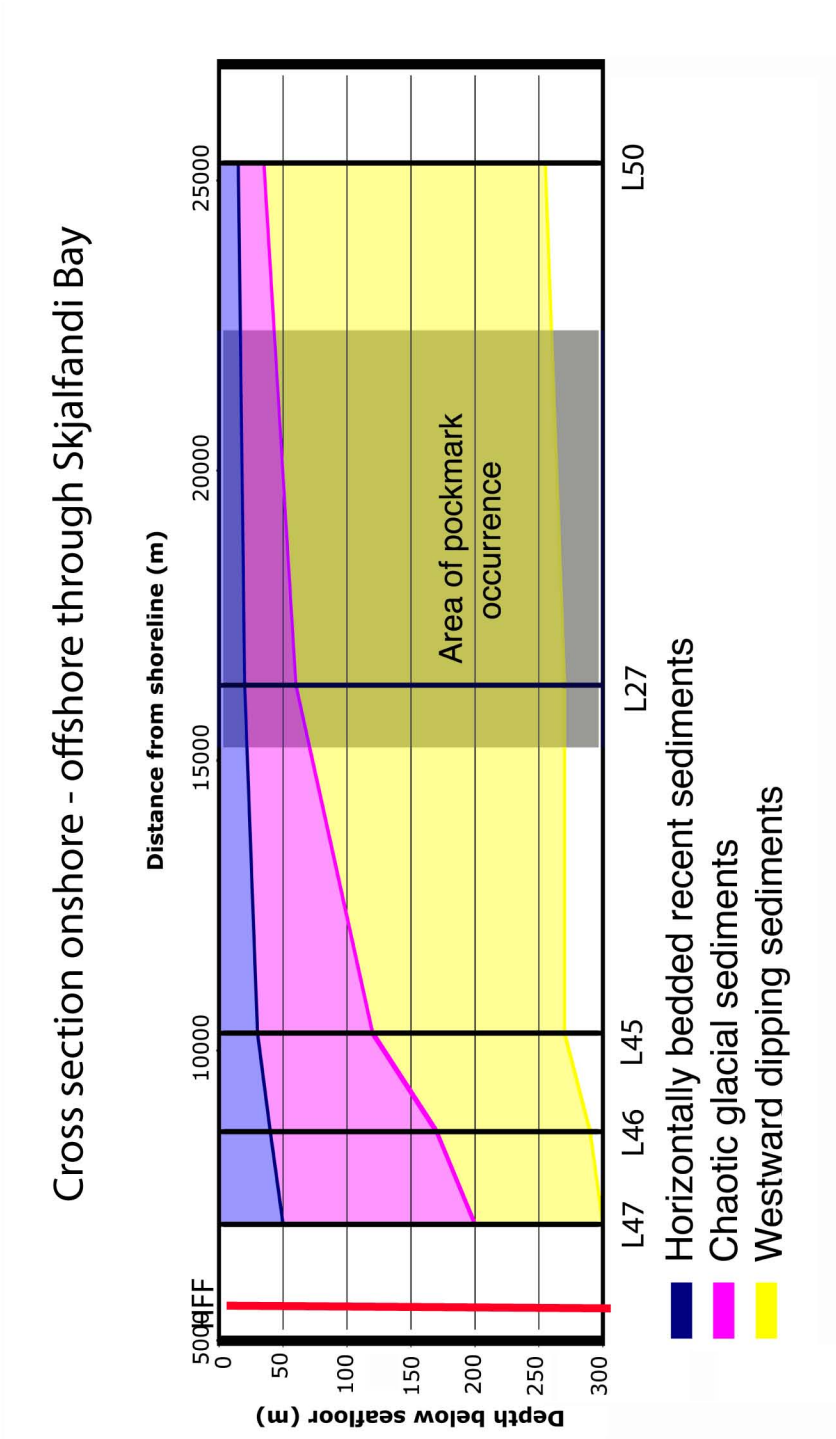


Figure 3.7

Sediment thickness variation S-N through Skjálfandi Bay. Pockmarks occur where the postglacial (recent) and glacial sediments are thin enough for the fluid to migrate to the surface, and where the sediments have been cut by the HFF, creating a fluid pathway along the fault plane.

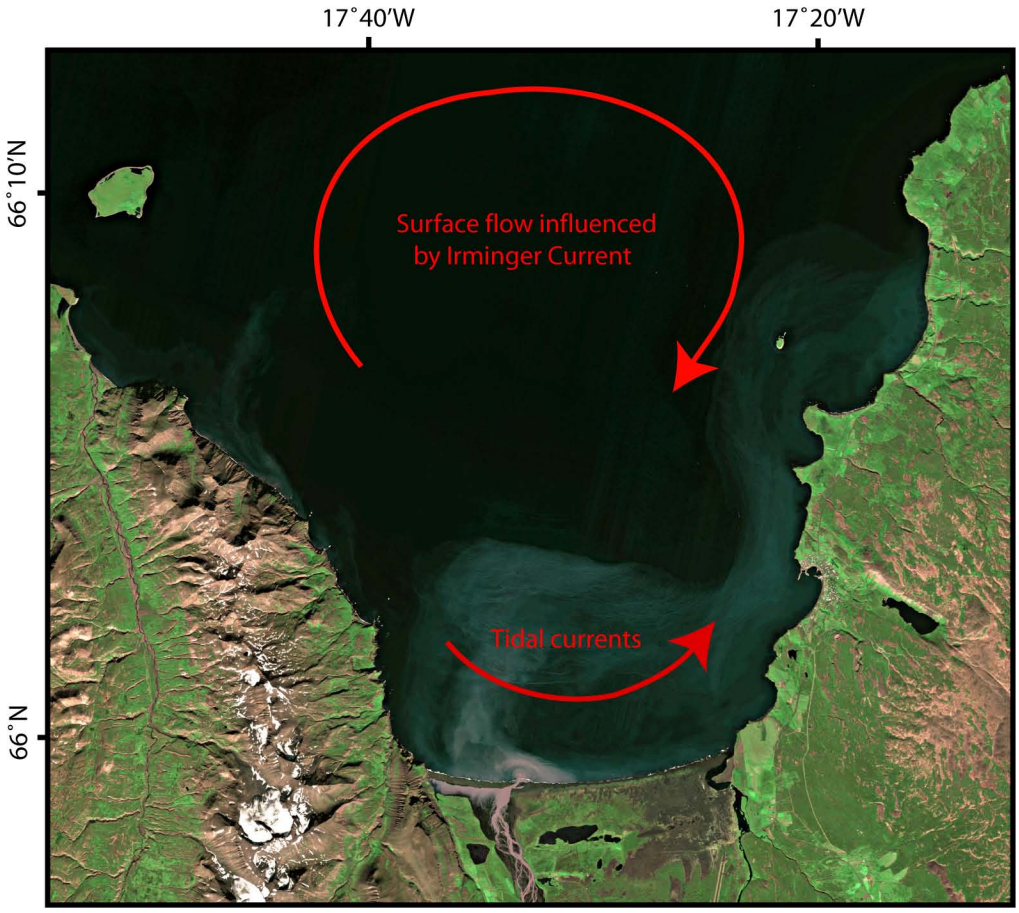


## Figure 3.8

SPOT image of Skjafandi Bay, showing the sediment input from Skjálfandafljót glacial river being transported anti-clockwise by the tides resulting in thicker sediment deposits in the southern portion of the bay.

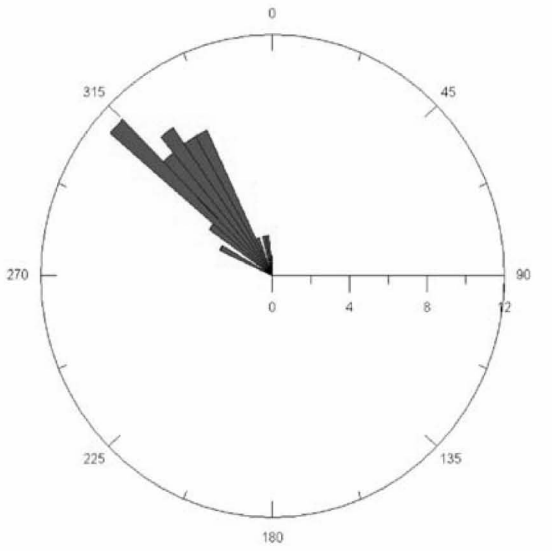


Pockmark Orientation
Western Skjáfandi Bay

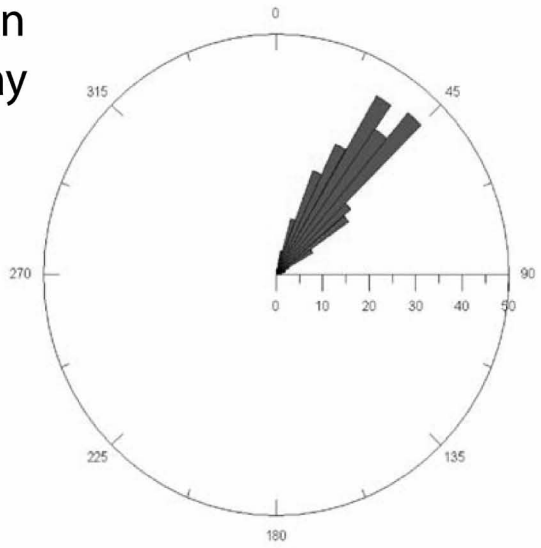


Pockmark Orientation
Eastern Skjáfandi Bay

Figure 3.9

Rose diagrams of the pockmark long axis orientation, NW-SE in the western half of Skjálfandi Bay and NE-SW in the eastern half of the bay. They are indicative of a clockwise bottom current circulating in the bay.

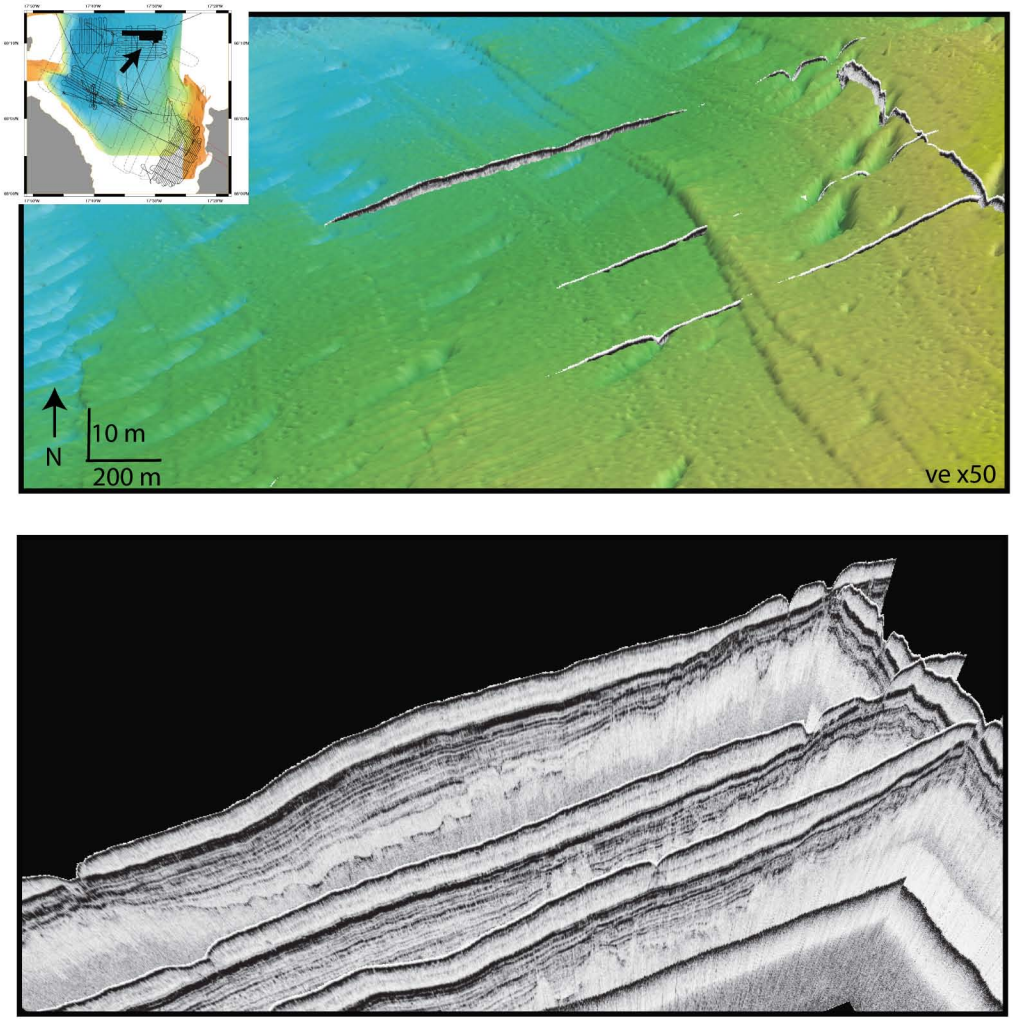


## Figure 3.10

Pockmarks long the uplifted northern block of the HFF occur in groupings. Sidescan data location indicated with the transparent grey box on the bathymetric data, seismic line location indicated with the white lines. Note in the bathymetric data the density of pockmarks close to the fault scarp and the paucity of the pockmarks further away.

On the right are the corresponding seismic lines, the two lines at the front on the image showing relic and current pockmarks on the hanging wall of the fault.

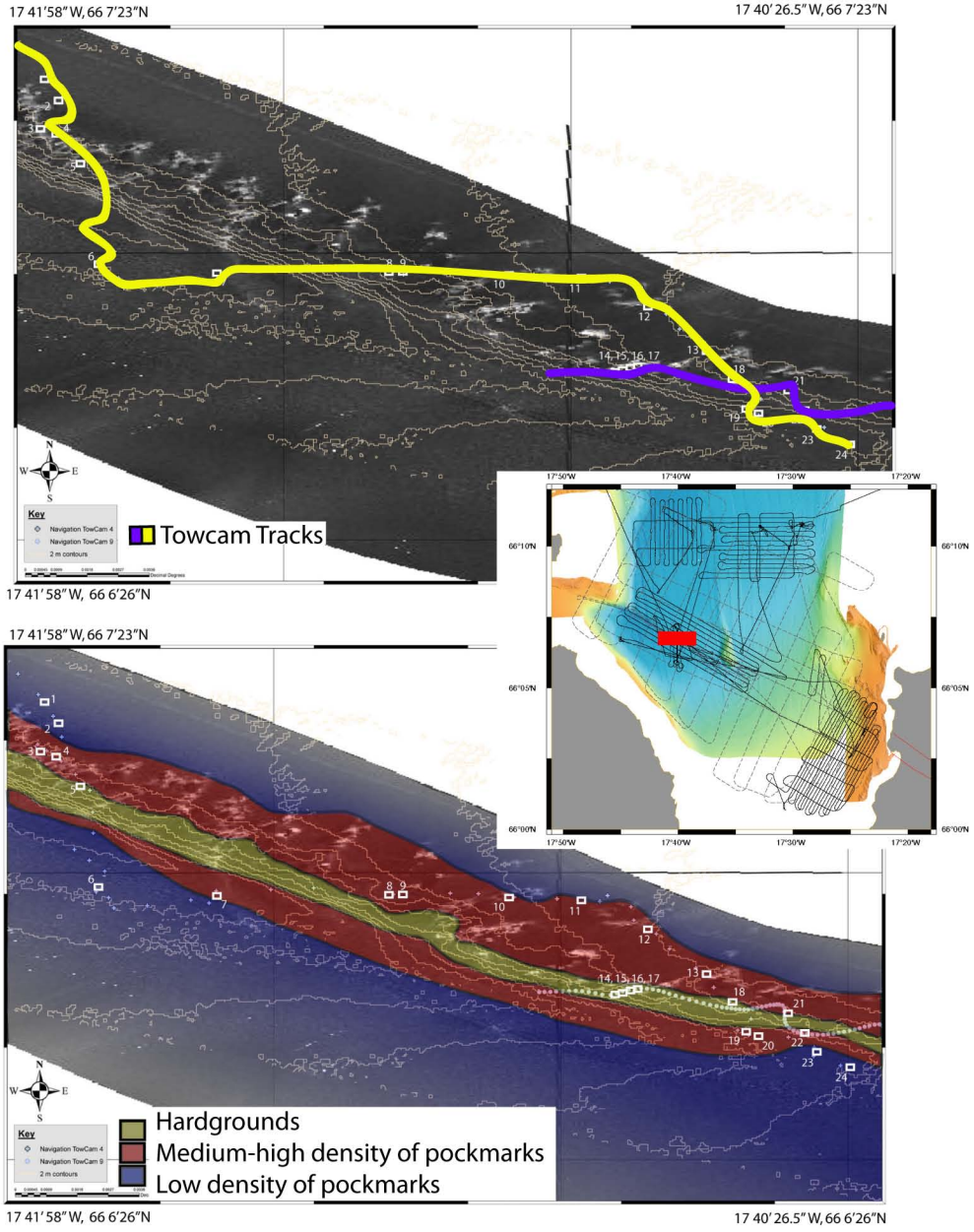


## Figure 3.11

Sidescan data, light areas high backscatter indicating rough seafloor in this case pockmarks. 2 m contours are superimposed on sidescan data highlighting the location of the fault scarp. The yellow and purple lines are navigation tracks of the towcam. Inset is the data coverage within Skjálfandi Bay, the location of the sidescan shown in red box. Below is the same sidescan data with the seafloor surface morphology indicated by color: Yellow = hardgrounds, fault scarp, Red = medium density of compound and unit pockmarks, increased diversity or density of various biota, Blue = no compound pockmarks and very few/no unit pockmarks, little to no faunal diversity. White numbered squares indicate the locations of bottom photos shown in Fig. 3.13.

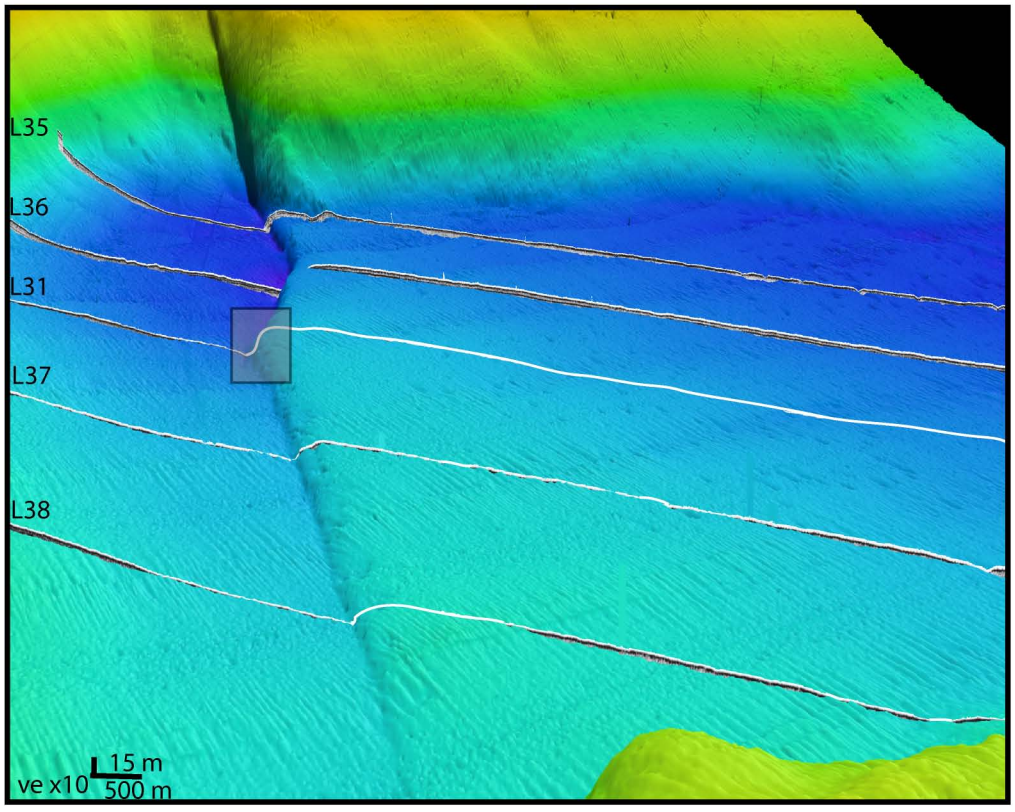


## Figure 3.12a

The SW corner of Skjálfandi Bay, (for location see Fig. 3.4) 3.12a is the bathymetric data and the white lines are the locations of the seismic data.

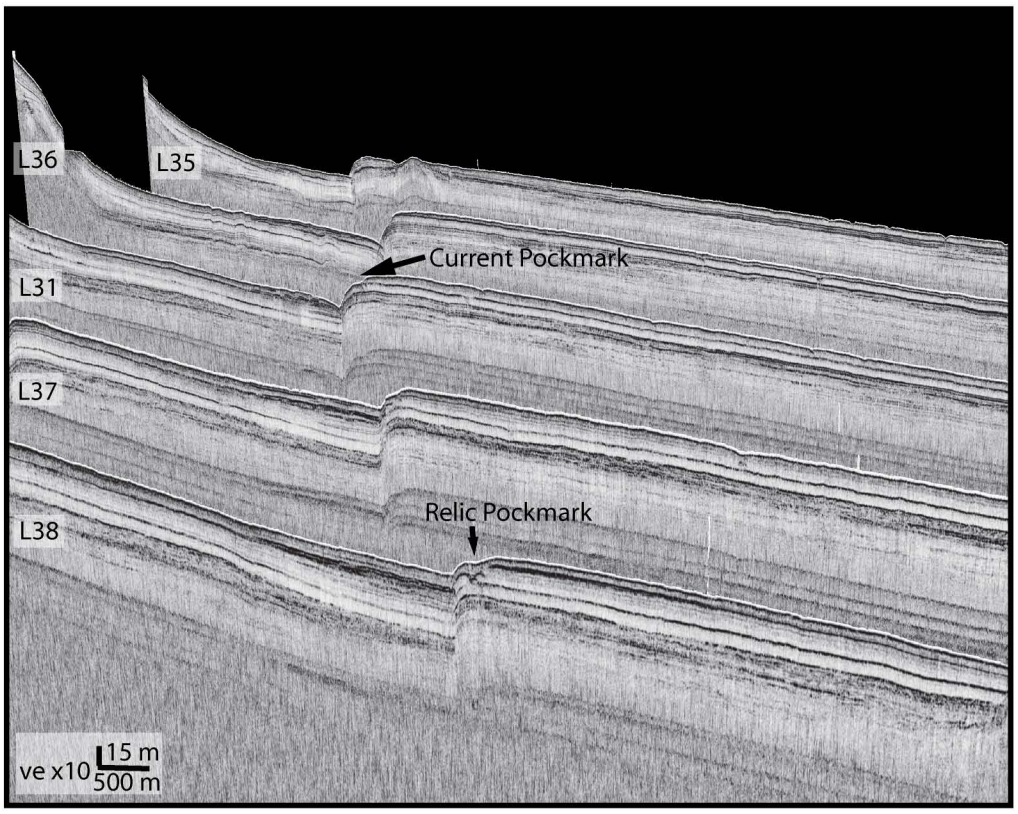


## Figure 3.12b

The SW corner of Skjálfandi Bay, (for location see Fig. 3.4) 3.12b shows a perspective view of the CHRIP data, linear distribution of pockmarks with some distributed gas in the sediments.

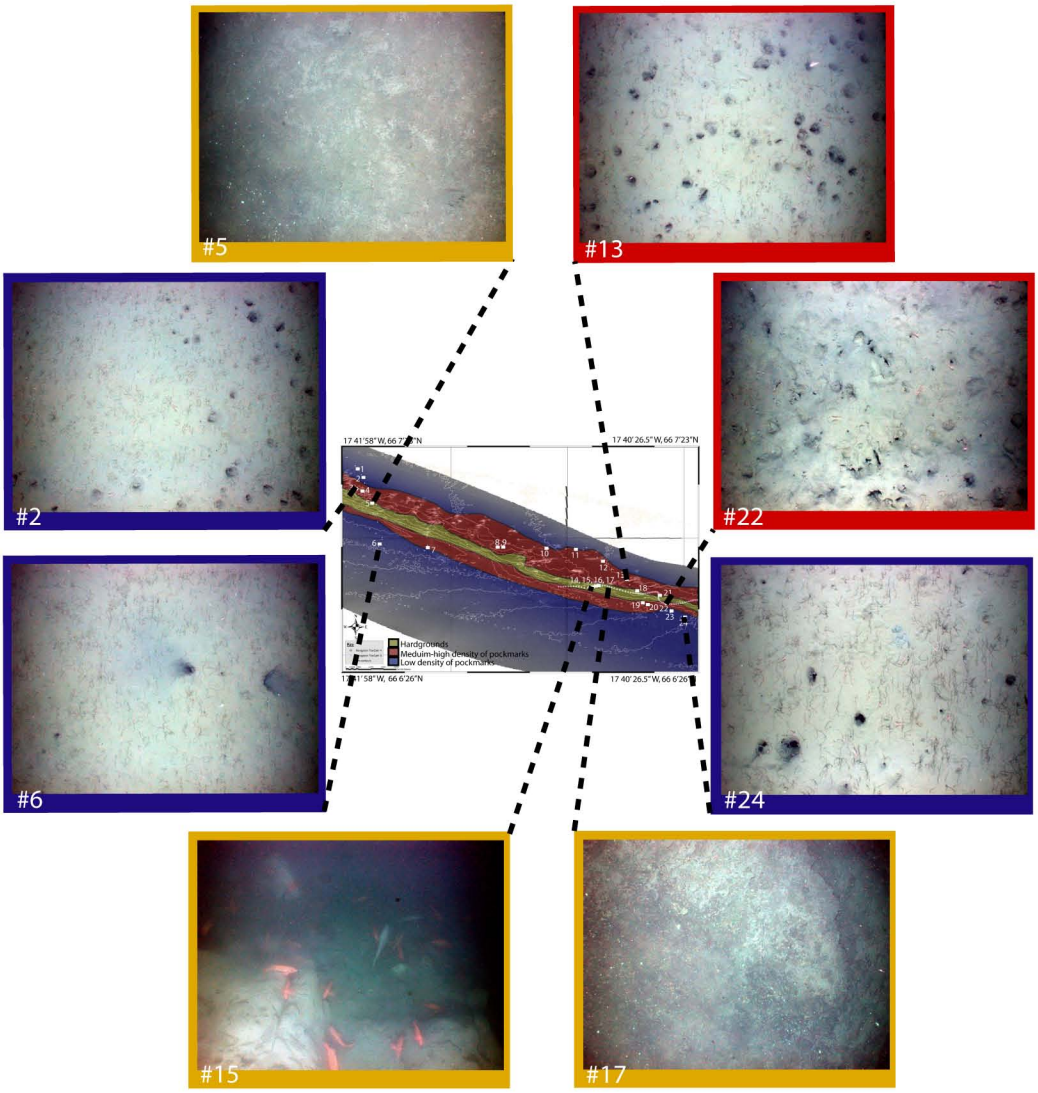


July 26, 2003, ~2.4 x 1.8 m

## Figure 3.13

Towcam photos of the seafloor, photo border correlates with substrate type: Blue are soft grounds with limited biota, Red indicate soft grounds with high density of large pockmarks and associated small pocks and increased biota density of burrowing shrimp, polychaetes and starfish. Yellow areas are hard grounds exposed by the fault scarp, no pockmarks and high densities of fish, soft corals, sea cucumbers, and urchins. Substrate characteristics clearly controls biota distribution. The differences in substrate are due to differences in fluid flow, associated with fault. Locations of the photos are indicated on inset location map.

## 3.8 REFERENCES

Billings A., Fornari D., 2002, New Towed Digital Deep Sea Camera and Multi-Rock Coring System: The WHOI TowCam, American Geophysical Union, Fall Meeting 2002, abstract #T11C-1263

Botz R., Winckler G., Bayer R., Schmitt M., Schmidt M., Garbe-Schönberg D., Stoffers P., Kristjansson J.K., 1999, Origin of trace gases in submarine hydrothermal vents of the Kolbeinsey Ridge, north Iceland, Earth and Planetary Science Letters, 171, 83-93

Chernova T.G., Roa P.S., Pikovskii Yu. I., Alekseeva T.A., Nath N.B., Rao R.B., Ch. M 2001, The composition and source of hydrocarbons in sediments taken from the tectonically active Andaman Backarch Basin, Indian Ocean. Mar. Chem. 75, 1-15.

Christodoulou D., Papatheodorou G., Ferentinos G., Masson M., 2003, Active seepage in two contrasting pockmark fields in the Patras and Corinth gulfs, Greece, Geo-Marine Letters, 23, 194-199.

Cohen, J. K., and J. W. Stockwell Jr., 1999, CWP/SU: Seismic Unix Release 33: A free package for seismic research and processing, software, Cent. for Wave Phenom., Colo. Sch. of Mines, Golden, Colo

Driscoll, N. W., Weissel J. K., Goff J. A., 2000, Potential for large-scale submarine slope failure and tsunami generation along the U.S. mid-Atlantic coast, Geology, 28, 406-410.

Dimitrov L., Woodside J., 2003, Deep sea pockmark environments in the eastern Mediterranean, Marine Geology, 195, 263-276.

Einarsson, P., 1991, Earthquakes and present-day tectonism in Iceland, Tectonophysics, 189, 261-279.

Fleischer P., Orsi T. H., Richardson M. D., Anderson A. L., 2001, Distribution of free gas in marine sediments: a global overview, Geo-Marine Letters, 21, 103-122.

Flóvenz, Ó. G., Sæmundsson, K., 1993, Heat flow and geothermal processes in Iceland, Tectonophysics, 225, 123-138.

Garcia S., Arnaud N.O., Angelier J., Bergerat F., Homberg C., 2003, Rift jump process in Northern Iceland since 10 Ma from 40Ar/39Ar geochronology, Earth and Planetary Science Letters, 214, 529-544.

Geptner, A. R., Richter B., Pikovskii Y. I., Chernyansky S. S., Alexeeva T. A., 2006 a, Polycyclic aromatic hydrocarbons as evidence of hydrocarbon migration in marine and lagoon sediments of a recent rift zone (Skjálfandi and Öxarfjördur), Iceland, Chemie der Erde, 66, 213-225.

Geptner, A. R., Richter B., Pikovskii Y. I., Chernyansky S. S., Alexeeva T. A., 2006 b, Hydrothermal polycyclic aromatic hydrocarbons in marine and lagoon sediments ar the intersection between Tjörnes Fracture Zone and recent rift zone (Skjálfandi and Öxarfjördur bays), Iceland, Marine Chemistry, 101, 153-165.

Gudmundsson A., 2000, Active fault zones and groundwater flow, Geophys Res Lett, 27, 2993-2996

Henkart, P., 2003, SIOSEIS, software, Scripps Inst. of Oceanogr., La Jolla, Calif. (available at http://sioseis.ucsd.edu).

Hill, J. C., Driscoll, N. W., Weissel J. K., Goff J. A., 2004, Large-scale elongated gas blowouts along the U.S. Atlantic margin, Journal of Geophysical Research, 109, B09101.

Hovland M., and Judd, A.G., 1988, Seabed Pockmarks and Seepages, 293pp., Graham and Trotman, Norwell Mass.

Hovland, M., Judd A.G., and King L.H., 1984, Characteristic features of pockmarks on the North Seafloor and Scotian Shelf, Sedimentology, 31, 471-480

Hovland, M., J. V. Gardner, and A. G. Judd (2002), The significance of pockmarks to understanding fluid flow processes and geohazards, Geofluids, 2, 127–136.

Josenhans, H.W., King L.H and G.B.J. Fader, 1978, A side scan sonar mosaic of pockmarks on the Scotian Shelf, Can. J. Earth Sci., 15, 831-840

Jónsson, S., and Valdimarsson, H., 2005, Recent developments in oceanographic research in Icelandic waters, Iceland - Modern Processes and Past Environments, Developments in Quarternary Science, 5, 79-92.

Judd A. G., 2003, The global importance and context of methane escape from the seabed, Geo-Marine Letters, 23, 147-154.

Judd A., Hovland M., 2007, Seabed Fluid Flow. 475pp., Cambridge University Press. ISBN-13 978-0-521-91950-3.

Kelley J. T., Dickson S. M., Belknap D. F., Barnhart W. A., Henderson M., 1994, Giant sea-bed pockmarks: Evidence for gas escape from Belfast Bay, Maine, Geology, 22, 59-62.

King L. H., MacLean B., 1970, Pockmarks of the Scotian Shelf, Bulletin of Geological Society of America, 81, 3141-3148.

Kvenvolden K.A., 1993, Gas hydrates – Geological perspective and global change, ,Rev. Gephys, 31, 173-187.

Norddahl, H., Pétursson, H. G., 2005, Relative sea-level changes in Iceland, new aspects of the Weichselian deglaciation of Iceland, in: C. Caseldine, A. Russel, J.

Hardardóttir, and O. Knudsen (Eds), Iceland: Modern Processes and Past Environments, Elsevier, Amsterdam, 2005.

Paull C. K., Hecker B., Commeau R., Freeman-Lynde R. P., Neumann C., Corso W. P., Golubie S., Hook J. E., Sikes E., Curray J., 1984, Biological Communities at the Florida Escarpment Resemble Hydrothermal Vent Taxa, Science, 226, 965-967.

Paull C. Ussler III W., Maher N., Greene H. G., Rehder G., Lorenson T., Lee H., 2002, Marine Geology, 181, 323-335.

Saemundsson K., 1974, Evolution of the axial rifting zone in Northern Iceland, Geol. Soc. of Am. Bull., 85, 495-504.

Riedel C., Schmidt M., Botz R., Theilen F., 2001, Grimsey hydrothermal field offshore North Iceland: Crustal Structure , faulting and related gas venting, Earth and Planetary Science Letters, 193, 409-421.

Voight, P.R., Gardener J., Crane K., Sundvor E., Bowles F., Cherkashev G., 1999, Ground Truthing 11- to 12-kHz sidescan sonar imagery in the Norwegian-Greenland Sea: part I: Pockmarks on the Vestnesa Ridge and Storegga slide margin, Geo Mar Lett, 19, 97-110.

Yun J. W., Orange D. L., Field M. E., 1999, Subsurface gas offshore of northern Claifornia and its link to submarine geomorphology, Marine Geology, 154, 357-368.

# Chapter 4

The geologic and tectonic evolution of the Tjörnes Fracture Zone

## 4.1 ABSTRACT

The Tjörnes Fracture Zone (TFZ), along northern Iceland, accommodates the deformation between the Kolbeinsey Ridge (KR) to the west and the North Volcanic Zone (NVZ) to the east. Nevertheless, much of our understanding of the deformation and evolution of the TFZ is based on onshore mapping and historic seismology. Here we present recently acquired high-resolution multichannel seismic (MCS) and swath bathymetry data that image the offshore deformation and help to define the evolution of this plate boundary. The MCS and bathymetry data reveal a complex history of deformation combining sinistral strike-slip faulting and block rotation with a minor component of deformation accommodated by extension across Eyjafjördur Skjálfandi and Öxarfjördur bays. On the basis of the geophysical and geological data, it appears the distributed deformation in the three basins (Eyjafjördur Skjálfandi and Öxarfjördur) occurs early on following a ridge jump back to the hotspot that occurred ~ 3 Ma ago. This phase of extension appears short-lived with ~3-6 km of extension distributed across all the three basins. As the NVZ becomes established, the distributed extensional deformation is replaced by dextral deformation forming the Húsavík-Flatey fault (HFF). A system of curvilinear faults connect the southern extent of the KR to the HFF in the west. The modern deformation along the HFF appears to die out to the east. As the NVZ propagates and the KR retreats northward

through time, some of the dextral strike-slip deformation is relayed north to the Grímsey Lineament (GL). The oblique trend of the GL also engenders a component of oblique rifting leading to a series of north-south trending volcanic constructs. GPS and earthquake data indicate that both the HFF and GL are actively deforming, which imparts a clockwise rotation for the intervening region reactivating the north-trending extensional faults with a bookshelf style of deformation.

## 4.2 INTRODUCTION

The northern Iceland margin records a complex interplay between tectonic deformation galciation and sea level fluctuations. The tectonic deformation is in large part within the Tjörnes Fracture Zone (TFZ), which is characterized by left-stepping, en-echelon NS-striking rift segments and a WNW-trending dextral (right-lateral) transform fault system connecting the North Volcanic Zone (NVZ) with the Kolbeinsey Ridge (KR) (Fig. 4.1). The TFZ is purported to have formed ~6-7 Ma ago as a result of an eastward jump of the axis of spreading in northern Iceland to its present position (Saemundsson, 1974; 1986). The ~150 km long (E-W) and ~70 km wide (N-S) TFZ lacks the clear topographic expression of typical oceanic fracture zones and is thus defined primarily by a region of high seismicity (Figs. 4.1 and 4.2). Small earthquake swarms are common within the TFZ making it the

most seismically active region in Iceland. Earthquake epicenters during 1983-2000 define two main seismic lineaments: the Húsavík-Flatey Fault (HFF) and the Grímsey Lineament (GL). Note the southern lineament, the Dalvík Lineament (DL), is the least seismically active. Two earthquakes (M6-6.5, Einarsson, 1986) near the eastern and western end of the HFF in 1872 caused severe damage in the village of Húsavík and on Flatey Island. In 1934 several buildings were damaged in a ~M6.3 earthquake on the DL, south of the HFF, and a M7 earthquake occurred offshore in the southwestern part of the TFZ in 1963 (Stefansson, 1966).

Accurate relative locations, focal mechanism studies, and detailed geological mapping show a distinct difference between the style of faulting along the HFF and the GL (Rögnvaldsson et al., 1998). The HFF is a well-developed right-lateral, strike-slip fault striking N60-65°W that can be traced from the western edge of the Holocene rift zone in northern Iceland for about 90 km to the [extinct?] southern end of the KR in the Eyjafjördur Basin (Fig. 4.2). The right-lateral displacement along the HFF prior to 1 Ma has been estimated up to 60 km resulting in a basement age difference of 5 Ma across the fault (Saemundsson, 1974). In recent years, most of the earthquake activity on the HFF has taken place at two locations; near its western end where it joins the Eyjafjördur Basin and some 40 km to the east where it intersects the east flank of the Grímsey platform, near Flatey Island. Focal

mechanisms indicate right-lateral, strike slip motion on a plane striking N122°E-N140°E, consistent with the WNW strike of the HFF (Rögnvaldsson et al., 1998). In contrast, focal mechanisms for earthquakes on the GL indicate left-lateral faulting on N-S trending fault planes with a considerable dip-slip component (Rögnvaldsson et al., 1998). This pattern has been interpreted as evidence of an oblique, en-echelon rift system, similar in some respects to the Reykjanes Peninsula, which marks the on land continuation of the Reykjanes Ridge in SW Iceland. The GL is believed to have formed during the last 1 Ma in response to the northward propagation of the NVZ beyond the HFF (Samundsson, 1986). Rögnvaldsson et al. (1998) proposed that continued northward propagation of the NVZ may lead to the extinction of the HFF.

While much of the Tjörnes fault system lies offshore, comparatively little mapping of this region has been conducted. McMaster et al. (1977) used single channel seismic reflection, gravity and magnetic data to define the major structural provinces within the TFZ. K. Gunnarsson of Orkustofnun (Iceland's National Energy Authority) has compiled single beam bathymetric data collected in this area by the Icelandic Hydrographic Survey, and interpreted 1100 km of multichannel seismic reflection data collected in 1978 and 1985 (Gunnarsson, 1998). His compilation shows that the TFZ is associated with some of the thickest sediments found on Iceland's insular shelf. These Plio-Pleistocene glacial sediments were deposited in N-S striking

grabens, including from west to east the Eyjafjördur, Skjálfandi Basin and Öxarfjördur basins. The thickest sediments (up to 4 km) are found on the inner shelf where the N-S trending Eyjafjördur and Skjálfandi grabens terminate against the HFF. Sediments between 1 and 2 km thick are present over a much wider area. Seismic reflection profiles across the southern part of Eyjafjördur graben near its intersection with the HFF reveal a faulting pattern that is typically listric within the sediments; faulting is seen in many places to extend up to the seafloor, forming escarpments as much as 10 m high (Gunnarsson, 1998). The overall pattern suggests a widening of the graben system south towards the HFF, where normal faulting appears to terminate against the strike-slip fault.

The only offshore location where sediments have been sampled to any significant depth is in a 554-m deep hole drilled on Flatey Island. This core sampled shallow water marine and coastal silts and sandstones characterized by repeated glacial regression/ transgression sequences, and two lava flows (Eiríksson et al., 1990). Shallow gravity cores taken in the Eyjafjördur Basin include fine-grained sediments with relatively high (up to 4%) total organic carbon content (Gunnarsson, 1998). The gravity cores reveal high sedimentation rates and contain sufficient fossil material to enable biostratigraphical zonation, C14 dating, and study of stable isotopes; they also contain discrete tephra horizons that may be linked to historical eruptions in

Iceland (PANIS Group, pers. comm., 2000). The basal sediments in this area are not more than 6 Ma old and the bulk of the sediments are believed to have accumulated over the past 2 Ma (Gunnarsson, 1998).

Here we present new multichannel seismics (MCS) and swath bathymetry data from the TFZ that places important constraints on the two tectonic models for the deformation and evolution of the region (Fig. 4.2). The very high Pleistocene-to-Recent sedimentation rates in this area provide an ideal "tape-recorder" of the tectonic evolution of the TFZ and the recent history of fault activity. Previous studies (Gudmundsson et al. 2006, Rögnvaldsson et al. 1998) suggest that both the KR and the NVZ are propagating volcanic segments, with the KR propagating south and NVZ propagating north. In this model the HFF has accommodated much of the deformation, with the GL and DL being nascent boundaries that will begin to accommodate additional deformation. In contrast our preferred model is that the KR is dying away to the south and migrating northward, with the DL only historically active and the GL becoming more active as the NVZ migrates to the north. To date most of the studies of the TFZ have been based on onshore geologic mapping and offshore seismicity. The data presented here provides important new constraints on the evolution of this region and allows us to test between these alternative tectonic models i.e. Gudmunsson (2006) versus Fenwick (accepted, Marine Geology). In addition the recently acquired MCS data

places important constrains on the distribution and thickness of glacial sediments deposited in the three north-south trending basins. We will first describe the tectonic deformation of the region and then the geologic and sediment history.

Our overarching scientific objectives were:

(1) determine the current location and history of strike-slip movement along the offshore portion of the Húsavík -Flatey (HFF) fault

(2) estimate the amount of extension across the Eyjafjördur graben (the southern extension of the Kolbeinsey Ridge), the Skjálfandi Bay and Öxarfjördur Bay in order to determine how strain has been accommodated in the TFZ over the past 6 Ma.

### 4.2.1 Transform faults and fracture zones

In oceanic crust the fracture zone marks both the active and fossilized transform segment, while the active faulting area between the spreading segments is known as the transform fault (Collette 1979, Tucholke and Schouten 1988). Fracture zones consist of highly faulted oceanic crust and highly metamorphosed serpentine (Searle 1986, Auzende et al 1989) and persists as features across the oceanic crust recording the position of spreading/transform segments at the time of formation. A complete history of the segment can be obtained by studying the whole length of the fracture

zone. Migration of spreading segments along a plate boundary with the associated migration of transform faults is attributed to flow in the subaxial asthenosphere moving the locus of spreading (Johnson and Vogt 1973, Schouten et al 1985).

As propagation of the rift segments continues, sections of one plate can be transferred to the other; this is recorded in the orientation of magnetic lineations in the crust. Stability of these features is largely dependant on their length, when transform faults are > 30 km they are permanent features of the rift/ridge system and are considered true transform faults, while at < 30 km they seem to be somewhat persistent features although not necessarily stationary (Tucholke and Schouten 1988, Kleinrock and Bird 1994, Behn and Lin 2000).

The exact age difference across the fracture zone is dependant on the offset of the ridge segments; consequently there can potentially be an observable difference in seafloor depth between the two sides (Menard and Atwater 1969). This difference is a function of the square root of the age of the seafloor (Parsons and Sclater 1977) and barring thermal resetting will persist through the life of the oceanic crust. As the distance between the two spreading centers increases so does the height and age differential across the fracture zone and the system trends to a more orthogonal geometry.

Transform faults are mainly orthogonal to the spreading centers but they can and do form at high angles, if this is the case the system will change to a more stable orientation (Thompson and Melton 1972, and Taylor et al 1994). With ridge-transform-ridge systems that have a small offset (< 1-2 my, < 20 km at average spreading rates) the geometry becomes more oblique with shallower nodal basins and may develop structures oblique to plate motion (Collette et al 1978, Fox and Gallo 1984, Macdonald 1985, Tucholke and Schouten 1988).

Northern Iceland provides us an ideal opportunity to study the evolution of a transform fault driven by ridge jump and propagation. Migration of the North American–European plate boundary westward across the Icelandic plume results in repeated rift jumps maintaining the spatial relationship between the active spreading zone and the plume. The deformation in Iceland appears to be accommodated by both oblique-slip and strike-slip faults, which may be the result of the anomalously thick basaltic crust (21 km thick at sea level, Darbyshire et al 2000) due to the high magmatic production from the plume.

### 4.2.2 Rift jump and extension

Northern Iceland has experienced numerous rift jumps as well as northward propagation of the NVZ, which has imparted a complex spatial and temporal deformation pattern. Understanding this evolution is the motivation behind this study. The rift jumps and eastward migration of the NVZ through time is controlled by the location of the Icelandic hotspot. Iceland is part of the Mid Atlantic Ridge (MAR) system and the style changes demonstrably due to the excess volcanism. Away from Iceland to the north and south as the volume of melt diminishes, the ridge comprises a sequence of offset ridge segments (Pálmason and Saemundsson 1974). Spreading in the North Atlantic started at 55-60 Ma with the intrusion of the North Atlantic Large Igneous Province- the remnants of which is the Icelandic Plume. The plume has been imaged, using seismic velocities, to a depth of 400 km (Wolfe et al 1997). Identified in both ICEMELT and HOTSPOT seismic experiments there appears to be a cylindrical velocity anomaly from 200-400 km depth, and from 200 km to the base of the crust there appears to be a horizontal plume head. The North American–European plate boundary is moving westward with respect to the plume head. According to the HS3-NUVEL1A model the Eurasian plate is moving at 14 mm/yr N218ºE, while the American plate is moving at 27 mm/yr N257ºE with the difference in plate movement being accommodated by spreading. This westward migration of the central rifting axis results in the locus of spreading getting spatially dissociated from the plume head. While volcanic activity may continue on the old spreading center for a period of time

depending on the volume of magma stored in the crust, eventually the spreading center will jump eastward back to the plume. On the basis of magnetic anomalies there has been at least two eastward jumps of the spreading center back to the plume in the last 15 Ma.

To the west of the present Icelandic spreading axis, the two previous spreading axes can be identified in the geologic record. Identifying the rift jumps locations through time enables us to investigate how the fracture zone responds and new ones form. The oldest known rift jump, the Northwestern Rift Zone, is now predominantly below sea level to the northwest of Iceland indicated by a 14.9 Ma unconformity in the northwestern peninsular (Hardarson et al 1997). The Skagafjördur Rift was active (8-3Ma) in concert with the most recent rift the North Volcanic Zone (NVZ) for 5-5.5 Ma until extension was fully transferred to the NVZ at 3 Ma (Saemundsson 1978, Garcia et al., 2003). The rift from the central volcano Hofsjökull north towards Skagafjördur is still active but is not accommodating any of the plate motion at the present time (Sigmundsson 2006).

At 3 Ma when spreading was fully transferred to the present NVZ some of the deformation between the Skagafjördur rift and the NVZ appears to be accommodated by extension in three offshore basins; Eyjafjördur, Skjálfandi, and Öxarfjördur. It appears as if the NVZ (including the Manareyjar Ridge) are

migrating to the north, partially transferring strain from the HFF to the GL, at present deformation across both lineaments is about equal. A visual inspection of the seafloor bathymetry shows that the three basins in our study area are deeper and better defined than others on the Icelandic margin.

### 4.2.3 Sedimentation along the northern margin

Sedimentation rates on the northern Icelandic margin are predominantly linked to the glacial cycle: birth, growth, and retreat. During the last glacial period, the whole land mass was covered in glaciers from 120-70 ka until it retreated at 10 ka. Ice flows were directed to the coast from the main central glacier (Fig. 4.3) until the Pleistocene when the glacial retreat left behind local minor ice centers, which greatly diminished the sediment yield to the margin (Einarsson, 1991). At the last glacial maximum (LGM), the coastline extended farther offshore approximately defined by the 100 m isobath. During the Kópasker interstadial (13-12.3 ka), marine sediments were deposited in NE and W Iceland. At around 12 ka, the Álfanes cold spell, when the ice sheets had retreated to the approximate location of the present coastline there was a brief growth phase of the glaciers filling the bays. This increase of the glacial extent dammed the local drainage creating a large lake, draining to the north over Flateyjarskagi Peninsular (Einarsson 1991). During another brief warming spell, the Allerød period, more marine sediments were deposited in the coastal margins. The final cooling spell increased the glaciers one final time, allowing

the tongues of the glaciers along the northern coast to extend to the ocean again, retreating finally around 10 ka. Subsequently, the location of the coastline has tracked the isostatic rebound and rising sea level.

The glacial sediments that are deposited in the marine environment are primarily from the growth and retreat phases and historically have not been studied in detail. Sediments are sequestered a distance away from present shorelines due to higher sea level than during the last glacial maximum (LGM). Sedimentation occurred at the edges of grounded ice sheets extending out into the ocean, and from catastrophic floods sourced from glacial lakes and jökulhlaups (Fig. 4). At ice sheet margins there are three primary types of sedimentation differentiated by the local of the glacier itself: temperate, subpolar, polar (Ashley & Smith 2000). In all these locals the initiating stage is the ice sheet melting, either releasing ice-rafted debris from a calved iceberg, or detritus melting out of the base of the floating tongue. In comparison there will be only small amounts of sediment accumulation beneath grounded glaciers as sediment reworking and transport are the primary processes occurring there. In the marine deposits there may be limited amounts of sorting resulting from different settling rates but in general the sediment will look very similar to land based tills (Sugden & John 1976). Rates of glacial sedimentation vary widely and depend on the rate and mode of ice wastage and the detrital content of the ice. To gather precise information on the rate of

sedimentation cores of the sediment are taken and a time scale is obtained through radiometric dating of organic debris.

Pleistocene/Holocene sediment deposition has been greatly influenced in northern Iceland by the episodic input of jökulhlaups and glacial lake drainage. The largest glacial river in Iceland, Jökulsá á Fjöllum, flows from the northern edge of the Vatnajökull ice cap to Öxarfjördur Bay, the river Skjálfandafljót flows from the northwest side of Vatnajökull across a large flood plain and then into Skjálfandi Bay, while the river Fnjóska flowing into Eyjafjördur Bay is sourced near Vatnajökull and Hofsjökull ice cap (Fig. 4.2). There have been two catastrophic floods (8-9 ka, 2-2.5 ka) that have eroded significant areas downstream (Waitt 2002) along with 10 historically recorded floods between 1477 and 1902-3 (Ísaksson 1985). The ice edge that at 10.5 ka extended into Öxarfjördur Bay was 70 km upstream by 9.6 ka and from there retreated to its present extent quickly. Jökulsá drains along the active rift, consisting of active lava flows and vent cones. During the catastrophic floods, the discharge rates were so high that not only were the glacial drift sediments removed, but basalt was sculpted into incipient scablands and fluted shapes. The peak discharge of the most recent catastrophic event at 2-2.5 ka is estimated to be 0.4-0.5 million $m^3/s$, in comparison peak spring discharge presently is 400-1000 $m^3/s$ (Waitt 2002). Melt generated by subglacial eruptions can be up to 14 times the volume of the lava: 0.5 $km^3$ lava = 7 $km^3$

melt water (Gudmundsson et al 1997). Jökulhlaups have significant impacts on the stratigraphy observed offshore; eroding large amounts of sediment off the shallow shelf and depositing it farther offshore (Uchupi et al 2001). If sufficient material is remobilized during one or more of these events the sediment record can be reworked and overprinted. Such deposits usually have a chaotic internal acoustic character that limits penetration and imaging of deeper layers. Nevertheless, the rapid sedimentation rates in regions that are not over printed provide a high fidelity recorder of tectonic deformation.

## 4.3 DATA ACQUISITION AND COVERAGE

Data presented here was collected by a high-resolution seismic systems; a portable High-Resolution Multichannel Seismic Acquisition System (MCS) in 2001 and multibeam swath bathymetry in 2002 and 2003 (Fig. 4.4). The Lamont High-Resolution system is a portable multichannel seismic profiling system designed to image sediment structure to depths of more than 1 km depth with a vertical resolution of 2-5 m. The data was acquired while the ship was running at 5 knots to minimize engine noise in the data while maximize data coverage, figure 4 details the data used in this paper. The system consists of a 210 cubic inch Gas Injection (GI) gun by Seismic Systems Inc., a 600 m long ITI streamer with 193 hydrophones in 48 groups with a 12.5 m group interval and an OYO DAS-1 digital acquisition system. An

air-cooled Price A-35 compressor can fire the GI gun at a shot interval of approximately 5 s (12.5 m). A Sun-based shipboard system running SIOSEIS was used to produce near-real-time brute stacks of each line. These brute stacks were invaluable in assessing data quality and in making a preliminary interpretation of the deformation in the HFF.

Owing to favorable weather conditions throughout the cruise, more extensive reflection coverage was obtained than originally planned, a total of 1600 km acquired across the three bays (Eyjafjördur, Skjálfandi, and Öxarfjördur). Here, we present MCS data from the Eyjafjördur Basin and Skjálfandi Basin, processed using the SIOSEIS (Henkart, 2003) and Seismic Unix (Cohen and Stockwell, 1999) processing software packages.

## 4.4 THE TJÖRNES FRACTURE ZONE

### 4.3.1 Faulting and sediment characteristics

Extension is accommodated across a variety of faults in the three basins, along north-trending oblique-slip faults with both a normal and strike-slip component that bound the edges of the basins. The strike-slip faults are orientated predominantly NW-SE, many of the NS oriented oblique-slip faults are manifested in the bathymetry, which facilitates tracing the faults throughout the seismic grid (Figs. 4.4, 4.5, and 4.6). The offset on the N-S faults is

greatest in regions of greatest earthquake activity: southern Eyjafjördur and northern Skjálfandi bays (Fig. 4.2). Basin bounding N-S faults offset the seafloor and are thus geologically active throughout all three basins. Basin asymmetry and dip of the sedimentary sequences suggest that the basin bounding faults are segmented and switch polarity along strike (Fig. 4.5).

In southern Eyjafjördur Bay, however, the active faults may be the southern extension of the Kolbeinsey Ridge as the fault system becomes curvilinear and merges with the HFF (Fig. 4.5). Numerous faults are observed in L19-L22 and have varying amounts of offset, the greatest ~10 m, is on L19. L20 and L21 have small divergent sediment wedges against the main scarp, implying syntectonic deposition (Driscoll and Hogg, 1995). Note that the small graben observed in the bathymetry and in the MCS data in the Eyjafjördur Basin dies away toward the south approaching the HFF. In fact, the polarity of the faults appears to change from L21 where it westward-dipping to L22 where the faults all appear to have an eastward component of dip (Fig. 4.5). South of the HFF, the amount of faulting and offset markedly diminishes consistent with the observed pattern of historic earthquake activity (Fig. 4.6). In this region glacial scour and sediment bypass has created a large hiatus with only a thin veneer of modern sediment mantling at least pre-LGM deposits, the sequences beneath the angular unconformity could in fact be substantially older as there is no drilling data available. Given the paucity of sediment it is

difficult to define the deformation history in this region, however, the surficial sediment along the fault does not exhibit divergence and rotation, which suggests it is post-tectonic deposition. Figure 7 (a, b, c, and d) shows the seismic profiles with large vertical exaggeration to highlight the fault architecture as well as the variability in the sediment carapace from south to north. The central graben imaged in Fig. 5 is within the larger basin Eyjafjördur basin structure shown in L21 (Fig. 7a), the basin exhibits slight asymmetry with the main basin bounding fault along the western side of the basin. Moving northward to L19 (Fig. 7b) the central graben becomes more pronounced with larger offsets on the graben bounden faults. The age and activity on these faults observed on L19 and L21 are difficult to constrain because of glacial erosion and sediment bypass on this portion of the margin, note the pronounced truncation observed just beneath the sea floor L19. Conversely, the fault history and offset is better recorded to the north in L16 and L12 (Fig. 7c and 7d respectively) by the overlying sedimentary sequences that are offset at the sea floor. The thickness and offset observed in the green unit can not be simply explained by dip-slip offset on the fault structures suggesting that there is a strike-slip component on the north-south trending basin faults (Fig. 7c and d). Finally the subtle basin asymmetry diminishes northward approaching L12 (Fig. 7d).

In the southern portion of Eyjafjördur basin a pronounced angular unconformity with marked truncation at or near the sea floor (Fig. 7a, b). In L16 (Fig. 7c) a layer with chaotic acoustic character mantles this angular unconformity and has wedge shaped internal acoustic geometry. Northward on L12 (Fig. 7b) an acoustically laminated unit (yellow sequence) is observed overlying the angular unconformity and is beneath the acoustically chaotic green unit. In L12, however, there appears to be wedge shaped geometries in the upper section of the green unit (shot point 2000). The uppermost pink unit exhibits lateral thickness variability from north to south and does not mimic or parallel the underlying reflectors (Fig. 7a-d).

In northern Skjálfandi Bay the increased fault activity and offset appears to increase approaching the GL (Fig. 4.8). Along L3 the sea floor is offset along a number of the fault strands and is coincident with the region of dense historic earthquake activity. Farther south, the north-south trending faults do not appear to offset the sea floor (Fig. 4.8, and 4.9). There is little to no deformation observed along L47 as it is in close proximity to and parallel to the HFF. In the center of the bay along L50 there is a slight increase in fault deformation, but the historical seismic activity is low in this region (Figs. 4.2, 4.8, and 4.9). Some of the faults on L50 reach the seafloor, but most do not with only minimal offset of the truncated horizon (purple reflector). To the north, L7 obliquely intersects the GL and there are currently active faults that

show growth along with magmatic intrusions in the seismically active region and there is clear offset of the sea floor to the south of the crossing with L3 (Fig. 4.10). In the swath bathymetry, rough sea floor is observed along the eastern portion of the Skjálfandi Basin and has a hummocky acoustic character in the MCS data (Fig. 4.8). In the south of Skjálfandi Bay, basin architecture is defined by distributed deformation that becomes more asymmetric to the north approaching the GL and regions of greater water depth.

Similar to the sediment distribution patterns observed in Eyjafjördur, the post LGM sediment thickness systematically increases to the north (Fig. 4.10, Fenwick et. al. accepted). The Marion Dufresne core (MD992275) also shows thickness variability in the Holocene greater to the north and thinning southward.

In southern Öxarfjördur Bay there is significant historic earthquake activity (Fig. 4.11) but little evidence for modern deformation in the surfical sediment. The acoustically laminated flat lying sediments that infill Öxarfjördur Bay are not offset by fault deformation (Fig. 4.11). In the region with high seismic activity near the eastern end of L60, 61, 63 (Fig. 4.2) there is little to no deformation observed in the surfical sediments. Often a disconnect exists between modern seismicity patterns and faults and offset observed on

geologic timescales. So this lack of observed deformation and offset in the sediment record may reflect different timescales of observation. There are some active faults at the eastern edge of the Öxarfjördur Basin but most do not offset the sea floor. The most recent sediments to infill the basin are laminated transparent sediments, similar to the transparent Holocene sediments identified around the Icelandic margin.

A truncation surface is observed in all three basins (purple horizon Fig 4.5, 4.7a-d, 4.8, 4.10, 4.11 and 4.12) and separates modern sediments near shore (i.e. pink unit) and glacial derived sediments offshore from the underlying truncated and deformed units (Fig. 4.12). In Eyjafjördur, Öxarfjördur and Skjálfandi bays the sediment that overlies the truncation surface is acoustically laminated with only a few chaotic layers. Sediment thickness above the angular unconformity (purple horizon) first diminishes northward to a minimum and then thickens seaward reaching a maximum thickness within the basin. At the mouth of the Eyjafjördur Bay there is a fault controlled half graben that acts as a sediment trap for recent river derived sediments (Fig. 4.6). As you move farther off shore (Fig. 4.7a-d) there is an increase in deformation and additional sediment above the truncation surface (Fig. 4.7c, d).

## 4.5 DISCUSSION

### 4.3.2 Tectonic Evolution

There are two end member tectonic models for the evolution of the Tjörnes Fracture Zone, Gudmundsson 2006 proposes that the HFF has been in existence for the last 9 Ma and has accommodated up to 60 km of dextral transform parallel displacement. Various estimates have been made of the amount of displacement accommodated within the Tjörnes Fracture zone, ranging from 5-60 km (Bergerat et al., 2000, Anglier et al., 2000, Fjäder et al., 1994, Gudmundsson et al., 1993, Jancin et al., 1985, Saemundsson 1974, Tryggvason 1973). Most estimates are based on the assumption that all of the extension is on the HFF strike-slip faults. In the Gudmundsson model because the HFF is either parallel or perpendicular to the near by ridge segments, he predicts that the NVZ is propagating north and the KR has been propagating south during the last 1Ma. If correct his model predicts that the GL and DL are new tectonic features formed as a consequence of this ridge propagation. The other model (Fenwick et. al. accepted) predicts that the NVZ is propagating north and the KR is withdrawing to the north through time. This age progression model predicts that the DL is the southern boundary to the distributed extension that occurred in response to the completed rift jump at approximately at 3Ma. The DL could also accommodate some dextral strike-sip deformation however onshore evidence of large deformation is not

observed (Gudmundsson 2006). The HFF has been active since 2.5 Ma and accommodates the deformation between the southern KR and the NVZ, with continued propagation of the NVZ to the north deformation is now also being accommodated on the GL (Fig. 4.13).

The style and magnitude of the Eyjafjördur basin diminishes markedly south of the intersection of the central graben with the HFF (Fig. 4.5 and 4.6). Furthermore the historic earthquake activity is predominantly observed along the HFF and GL with a dearth of activity observed on the DL. The upper sediment layers observed in the Eyjafjördur Bay south of the HFF are not deformed or offset, which is not consistent with a southward propagating KR, these observations suggest that there is no southward propagation of the KR.

In Eyjafjördur, Skjálfandi and Öxarfjördur basins (e.g. Fig. 4.5, 4.8, and 4.9) the predominant fault trend is NNE. In our model the extensional deformation occurs shortly after the completed rift jump with distributed extension between the northern extent of the NVZ and the southern extent of the KR. As the NVZ became established the deformation evolved into a dextral strike-slip domain, exhibiting some similarities with ridge transform style of deformation. With time the NVZ continued to propagate north and now some of the deformation is accommodated on the GL. Modern GPS data (Geirsson et al. 2006) shows the deformation is evenly distributed across both

the GL and HFF, which is constant with our conceptual model. The orientation of and segmented nature of the GL result is distributed extension and volcanic activity (Fig, 4.2, 4.11, and 4.12). As the NVZ migrated north and the deformation is accommodated between the HFF and GL the north trending normal faults have been reactivated as sinistral oblique faults, similar to bookshelf faulting models developed for migrating transform faults along mid ocean ridge systems (Fig. 4.14, Phipps Morgan & Kleinrock 1991, Wetzel et al 1993). In such a model the extensional deformation occurred early on with the dominant style of deformation being associated with dextral strike-slip deformation along the HFF and GL.

As the MCS data only penetrated on the order of 0.5 km, it placed little constraints on total crustal thinning. To place some simple constraints on the magnitude of distributed extension between the southern KR and NVZ we used a simple isostatic model with no flexural strength to estimate the magnitude of extension. On the basis of a reference column at sea level, we can estimate the amount of extension from the observed water depth in the basins (Figs. 4.13 and 14; Driscoll et al., 1989), because at some depth we predict there will be no lateral pressure gradients. Assuming a starting thickness and measuring a profile of bathymetry a stretching factor can be determined (Fig 4.14). In an effort to quantify the amount of extension taking place on we performed a basic isostatic analysis of a series of E-W trending

along 66.5˚, 66.4˚, 66.3˚, 66.2˚N from 16.5ºW to 19.2ºW (dotted red lines, Fig. 4.4). Based on the bathymetry, a crustal reference thickness of 21 km at sea level (Darbyshire et al., 2000) and following the method of Driscoll et al. (1989) a stretching factor or amount of extension was determined for each of the profiles (Fig. 4.14, Table 1).

Given a profile length of 125 km and an average crustal thickness across the profile of 20 km, the 2.4-5.2% thinning calculated would be equal to 3.0-6.5 km of extension across the length of the profile. If each basin is taken independently extension is unequally divided between them, with the largest percentage extension in Eyjafjördur Basin at around 7%, ~2 km, to the least in Öxarfjördur Basin at 2%, ~0.5 km (Table 1).

Table 4.1

| **All basins** | | | | |
|---|---|---|---|---|
| | basin width km | Ave crustal km | % thinning | Extension km |
| 66.5 | 125.0 | 20.5 | 2.4 | 3.0 |
| 66.4 | 125.0 | 20.2 | 3.8 | 4.8 |
| 66.3 | 125.0 | 20.1 | 4.3 | 5.4 |
| 66.2 | 125.0 | 19.9 | 5.2 | 6.5 |

| **Eyjafjördur** | | | | |
|---|---|---|---|---|
| | basin width km | Minimum crustal km | % thinning | Extension km |
| 66.5 | 31.7 | 19.5 | 7.2 | 2.3 |
| 66.4 | 38.3 | 19.8 | 5.6 | 2.2 |
| 66.3 | 33.5 | 19.7 | 6.1 | 2.0 |
| 66.2 | 17.5 | 20.2 | 3.8 | 0.7 |

| **Skjálfandi** | | | | |
|---|---|---|---|---|
| | basin width km | Minimum crustal km | % thinning | Extension km |
| 66.5 | 32.4 | 19.8 | 5.5 | 1.8 |
| 66.4 | 31.2 | 20.2 | 3.6 | 1.1 |
| 66.3 | 30.6 | 20.4 | 3.1 | 0.9 |
| 66.2 | 30.1 | 20.4 | 2.7 | 0.8 |

| **Öxarfjördur** | | | | |
|---|---|---|---|---|
| | basin width km | Minimum crustal km | % thinning | Extension km |
| 66.5 | 23.4 | 20.1 | 4.3 | 1.0 |
| 66.4 | 21.0 | 20.2 | 4.0 | 0.8 |
| 66.3 | 26.7 | 20.2 | 3.6 | 1.0 |
| 66.2 | 22.5 | 20.5 | 2.2 | 0.5 |

Given that the spreading rate has stayed relatively constant through time at approximately 1 cm/yr, the measured of 3-6.5 km of extension suggests that the phase of distributed deformation was short-lived being approximately 0.5 Ma. As the NVZ became established we predict that the style of deformation changed from distributed extension to predominantly dextral strike-slip deformation. With continued northward propagation of the NVZ dextral strike-slip deformation migrated north to the GL, at present based on modern GPS measurements it appears that both the HFF and the GL are actively deforming. This deformation imparts a clockwise rotation in the TFZ and reactivates the north trending normal faults as oblique sinistral strike-slip faults (Fig. 4.14). This reactivation makes the normal faults and basin extension appear to be active as they offset the sea floor. The orientation of the GL is oblique to the HFF and engenders regions of extension and consequent volcanic activity. Through time we predict that the deformation along the HFF will diminish in concert with an increase in deformation along the GL.

### 4.3.3 Depositional history

The sediment record along the northern Icelandic margin records the waxing and waning of ice sheets. A consistent depositional pattern is observed in all Eyjafjördur, Skjálfandi, Öxarfjördur basins (e.g. Fig. 4.5, 4.7, and 4.11). A prominent angular unconformity is observed in all of the basins that is

interpreted to record glacial scour and erosion associated with the LGM. It is possible that given the strong truncation surface, the high rate of sedimentation sourced from the Jökull and the catastrophic floods that have occurred in the last 9 ka that the sedimentological record has been erased in this basin. The catastrophic floods at 8-9 ka, 2-2.5 ka had potential to erode significant amounts of sediments offshore and certainly did onshore, up to 30 m of basalt in places. This removal of sediment in the near shore would interrupt the tape recorder of time that we usually regard the sediment succession to be.

The most recent Holocene sediment is found across all the basins with varying thickness, it has a transparent acoustic character with occasional laminations. Older Holocene/Pleistocene sediments are more chaotic and exhibit a higher degree of deformation. The thickness of the deposits is controlled by the interaction of the sediment supply and the accommodation space. These in turn are influenced by glacial erosion, tectonic deformation and sea level. In Eyjafjördur Bay the extent of the glacier can be located between L16 and L17, as south of L16 the data shows only the truncation surface created during the LGM, and L16 and north there are chaotic deposits that exhibit characteristics typical of glacial mouth deposits and lobe switching.

Near shore only modern river derived sediments are observed above the angular unconformity. Their pattern suggests they were deposited by current controlled processes, the depositional of pattern of the modern sediments neither mimics nor obscured the underlying geometry suggesting that these deposits are current controlled, their thickness diminishes offshore to a minimum before once again thickening. Two new depositional packages are observed off shore (Fig. 4.7b and c) the basal package (green unit) has chaotic internal structure that up section shows wedging that is interpreted to be the edges of lobes. There appears to be evidence of lobe switching which would be consistent with emplacement just seaward of the grounded ice sheet (Fig. 4.15).

Continuing offshore a more laminated acoustic unit is observed and might be the distal package associated to the proximal glacial deposits imaged in Fig. 4.7c, with increasing distance from the grounding line of the ice sheet the chaotic acoustic character of the stratigraphy diminishes (Fig. 4.7c and 4.7d). Independent evidence for the grounding line of the ice sheet (Hubbard et al., 2006) is consistent with the distribution of sediment distribution and bypass observed in Eyjafjördur, Skjálfandi, Öxarfjördur bays.

## 4.4 CONCLUSIONS

This increasing spatial separation between the extension on land and the MAR gives rise to repeated rift jumps, creating new transform fault/accommodation zones. In the Tjörnes Fracture Zone there are two main active faults oblique to the spreading segments connecting the southern portion of the Kolbeinsey Ridge and the northern portion of the North Volcanic Zone. The Husavik-Flatey Fault curves north into the southern KR in Eyjafjördur Bay and south into the Theistareykir Fissure Swarm, the Grímsey Lineament to the north of the HFF connects to the southern portion of the KR, crosses the Manareyjar Ridge and then connects to the North Volcanic Zone. Areas of highest seismic activity lie along the GL where there is increased volcanic activity (between Manareyjar Ridge and KR) where the GL joins the NVZ and where the HFF curves into the KR.

Based on geophysical data acquired offshore in northern Iceland and onshore mapping we have developed a conceptual model for the tectonic evolution of the TFZ. Building on the results of Fenwick et al. (accepted), we present a conceptual model that helps explain the temporal and spatial distribution of deformation.

- Distributed extensional deformation in the Eyjafjördur, Skjálfandi, and Öxarfjördur basins along north trending fault systems occurs early on after a rift jump occurs. Through time as the boundary between the American and Eurasian plates migrates away from the hotspot the rift axis continues to jump eastward to an area of low strength. The DL appears to be the southern limit of this distributed extension, which may explain the minor dextral strike-slip offset observed along the lineament (Gudmundsson 2006). As the nascent ridge segment becomes organized the distributed extension is replaced by dextral strike-slip deformation.

- We predict that the HFF fault system postdates the distributed extensional deformation. Modern earthquake seisimcity and GPS data suggest that the HFF is still active. The deformation along the HFF seems more intense in the western region where it curves into the southern extent of the KR, and diminishes eastward as it approaches the town of Husavik. Sea floor offset is observed along much of the HFF system.

- With continued propagation of the NVZ, some of the dextral strike-slip deformation has been transferred to the GL. The Grímsey Lineament connects the North Volcanic Zone, Manareyjar Ridge and the

Kolbeinsey Ridge. Regions of high seismic activity are where the Grímsey Lineament connects with the North Volcanic Zone and between Manareyjar Ridge and Kolbeinsey Ridge – an area of increased volcanism. This northward migrating transform zone has imparted a clockwise rotation that has reactivated the normal faults in a bookshelf style of deformation.

- The stratigraphic sequences observed offshore predominantly reflect glacial processes. The truncation surface observed in Eyjafjördur, Skjálfandi, and Öxarfjördur basins records glacial erosion as the ice sheet extended north across the region. During ablation sediment units were deposited offshore that have no equivalent units on shore. The emplacement history of the sediment accounts for much of the acoustic character fop the sediments observed along the margin.

In summary the TFZ has migrated north through time as a consequence of the northward propagating NVZ and the northward withdrawal of the KR. We have developed a new model that suggests in the early stages of deformation following the ridge jump the deformation appears to be more distributed and exhibit similarities to continental rifting. As the rift is established the dextral strike-slip fault deformation develops and the system exhibits more of the a ridge-transform–ridge architecture.

Studying this continually evolving system allows us the opportunity to better understand the complicated nature of evolving transform faults. In the Tjörnes Fracture Zone there appears to have been an initial stage of extension accommodation more in line with continental style accommodation zones: graben faulting with normal faults accommodating portions of the extension. This appears to have been followed and overprinted by more traditional oceanic transform faulting, with the development of the HFF and then subsequently with the northward propagation of the North Volcanic Zone the Grímsey Lineament.

## 4.5 ACKNOWLEDGEMENTS

This research was supported by a grant from the National Science Foundation, University of Iceland Research Fund and the Iceland Geosurvey.

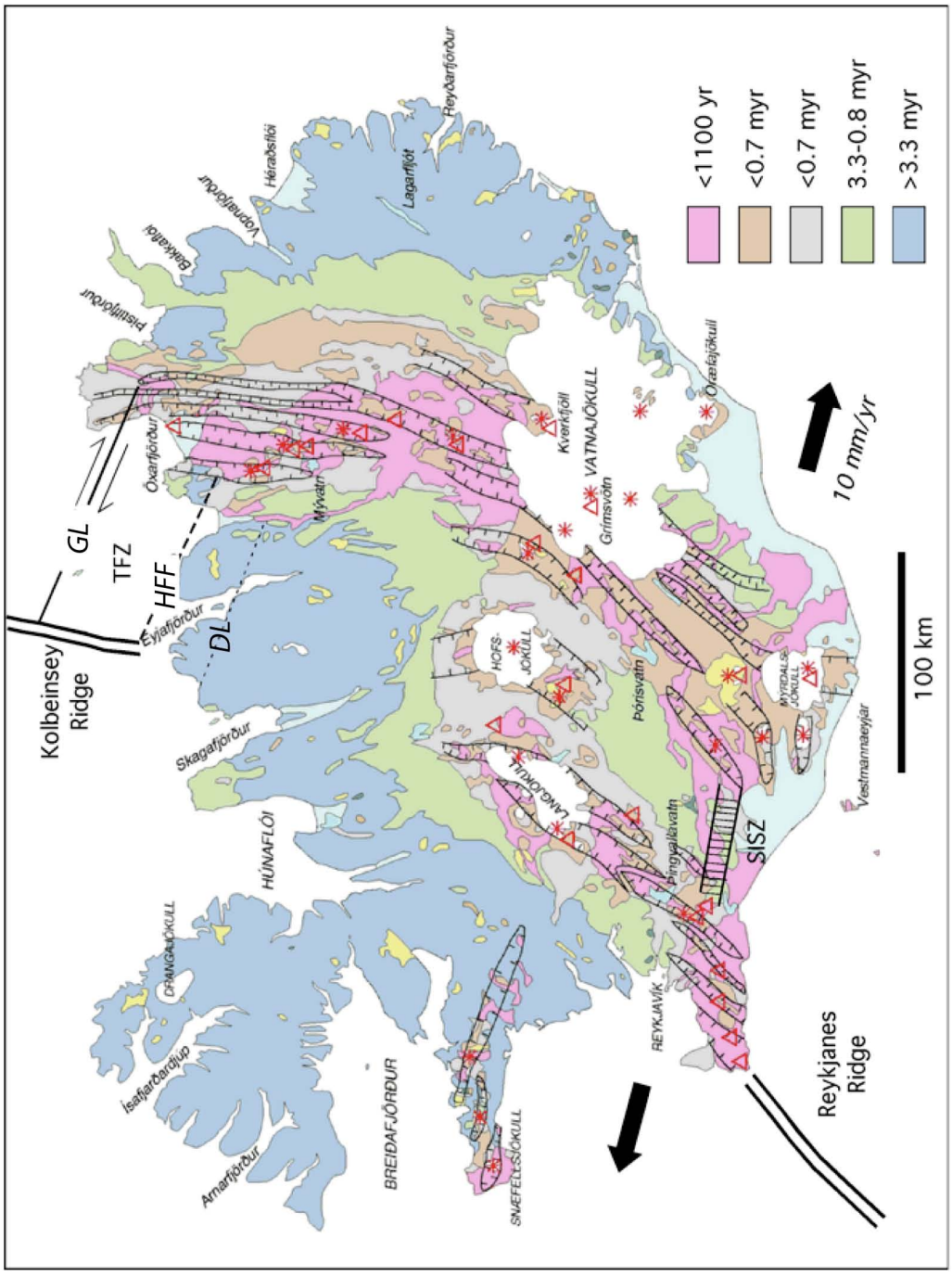


Figure 4.1

Geologic map of Iceland with active rifting, seismic and fault zones indicated. Ages of the bedrock are indicated by the colors. The Tjörnes Fracture Zone (TFZ), Grímsey Lineament (GL), Húsavík-Flatey Fault (HFF), Dalvík Lineament (DL), South Iceland Seismic Zone (SISZ) are labeled.

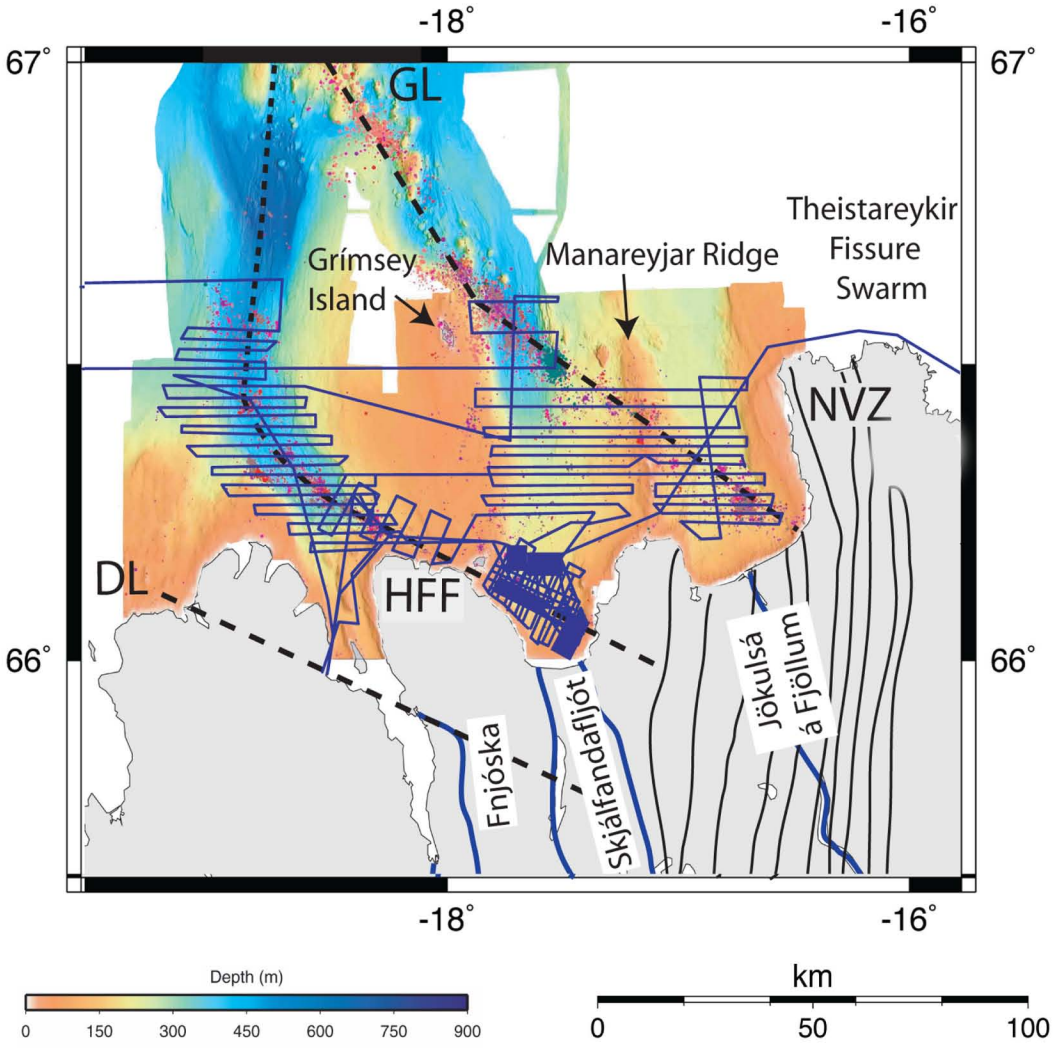


## Figure 4.2

Regional bathymetry along with data distribution: Dashed black lines are the location of the Grímsey Lineament, the Húsavík-Flatey Fault and the Kolbeinsey Ridge. Blue solid lines are the locations of multi channel seismic (MCS) and CHIRP lines. Onshore rivers are indicated in blue, and the North Volcanic Zone (NVZ) and Theistareykir Fissure swarm are shown by solid black lines. Earthquake epicenter distribution is shown with the colored clusters, note the focused occurrence along the western end of the HFF where it curves into the KR and along the GL.

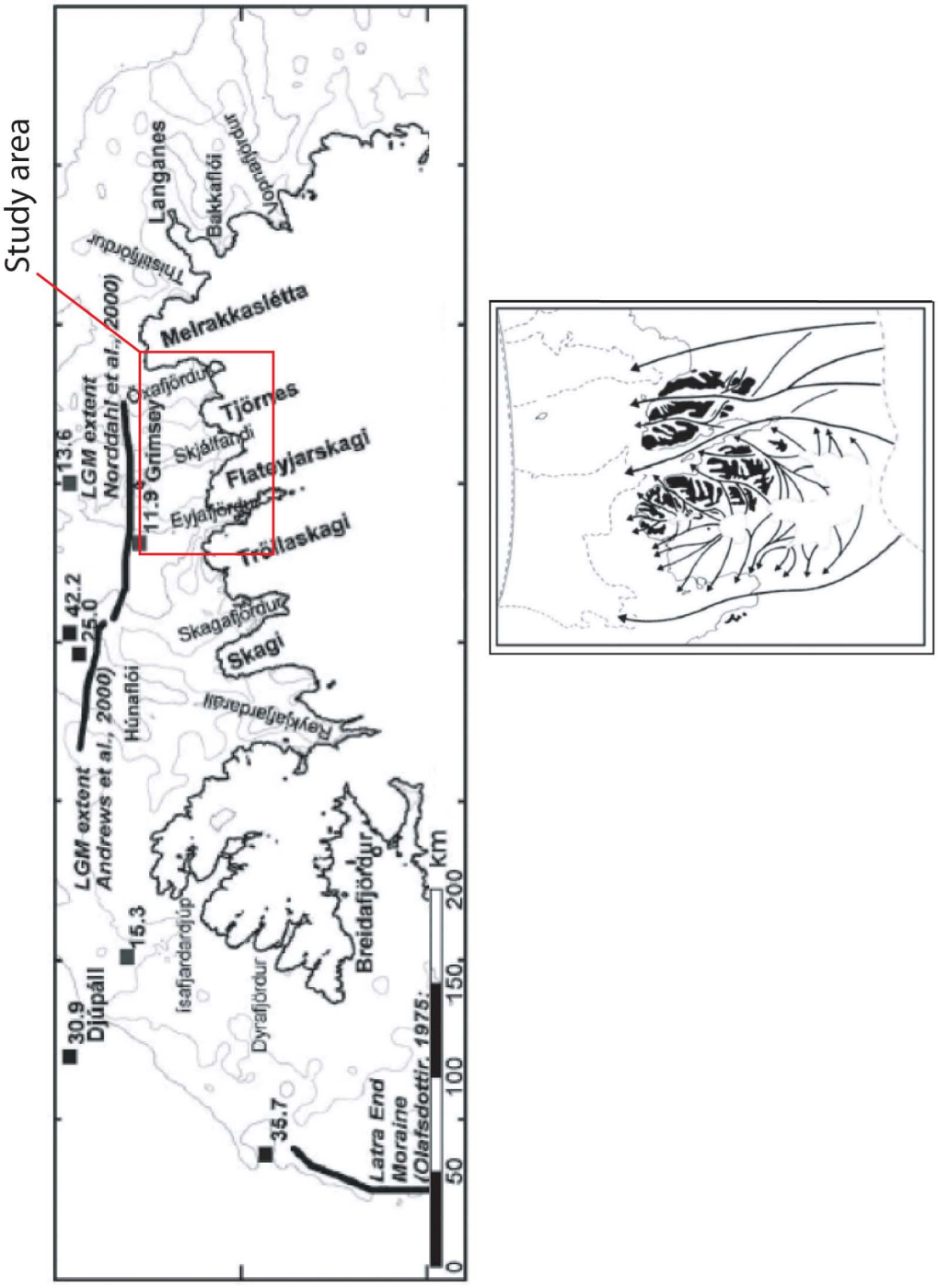


Figure 4.3

Mapped glacial extent around Iceland and ice flow patterns from the last glacial maximum modified from Hubbard et al 2006.

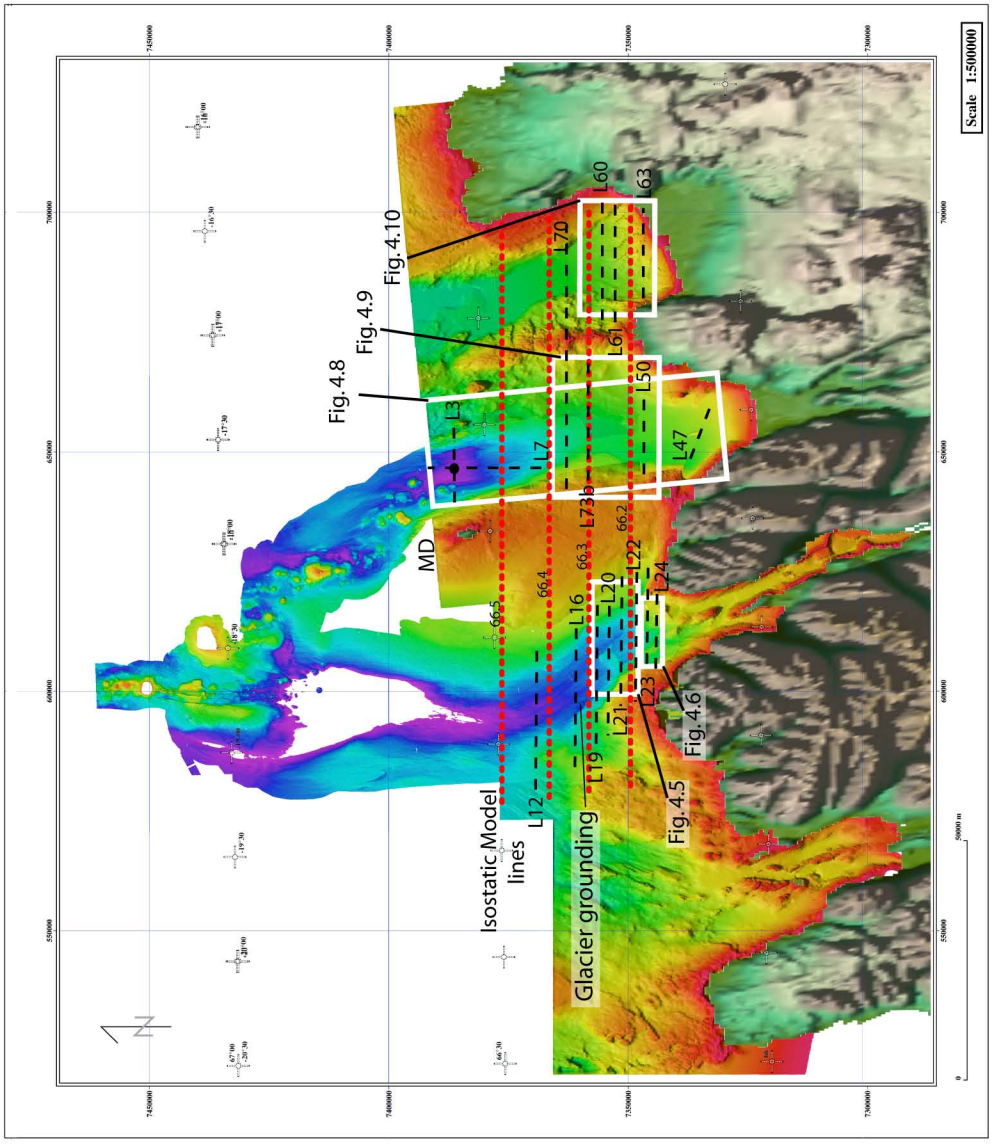


## Figure 4.4

Regional bathymetry along with data distribution. Solid black lines are the location of the Grímsey Lineament, the Húsavík-Flatey Fault and the Kolbeinsey Ridge. Dashed black lines are the locations of multichannel seismic lines shown in the paper, red dashed lines are the locations of the isostatic model profiles. The extent of the galciation during the LGM in Eyjafjördur Bay is shown by the fine red dashed line just south of L16. The white boxes indicate the locations of Figures 5, 6, 8, 9, and 11. MD is the location of the Marion Dufresne core (MD992275) at the crossing of L3 and L7.

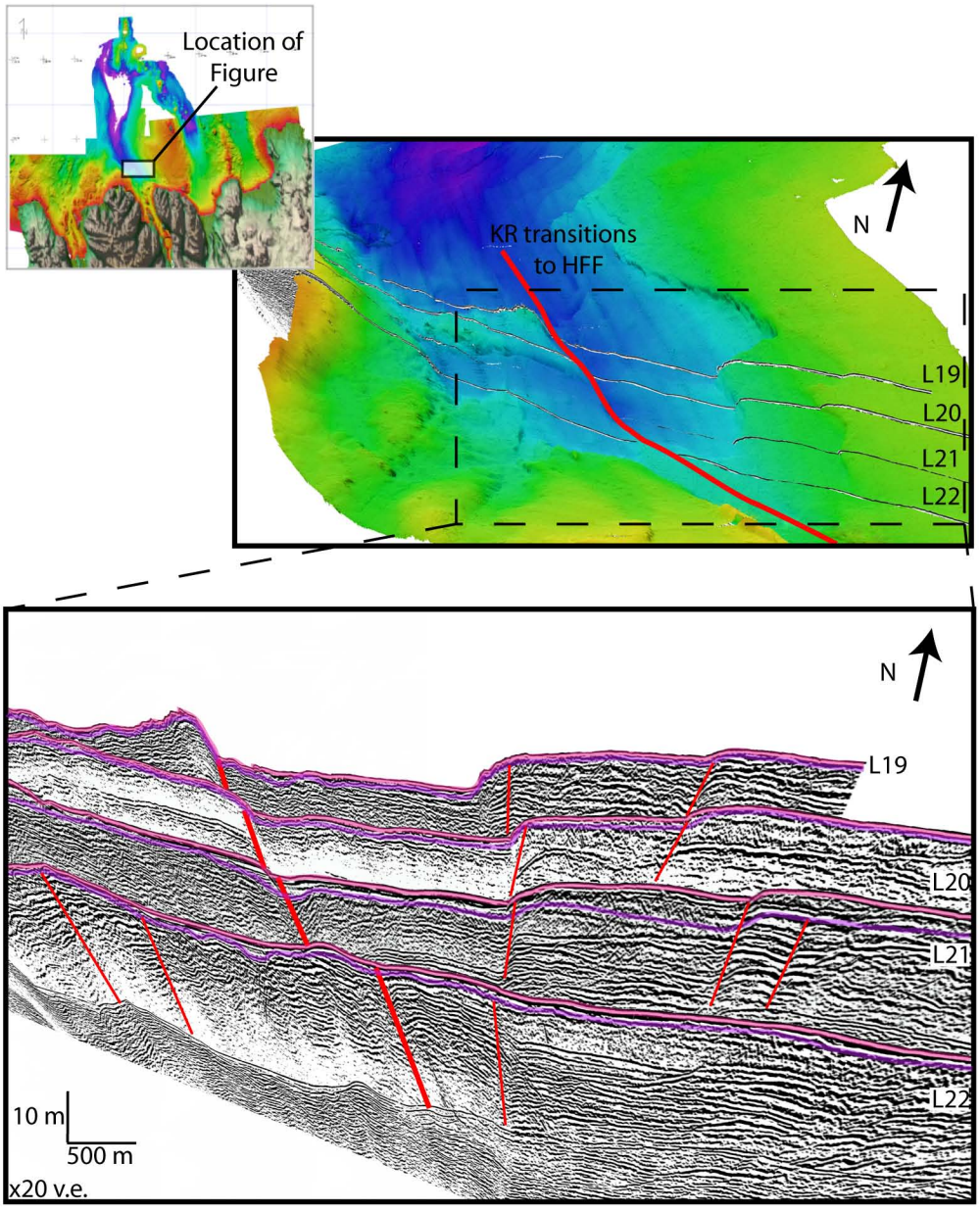


## Figure 4.5

Seismic data located in southern Eyjafjördur Bay, L19 - L22. The KR transition to the HFF is shown in red on the bathymetry, and thick red on the seismic data. The pink lines on the seismic data indicate the top of the Holocene sediments while the purple line indicates the truncation surface created at the LGM.

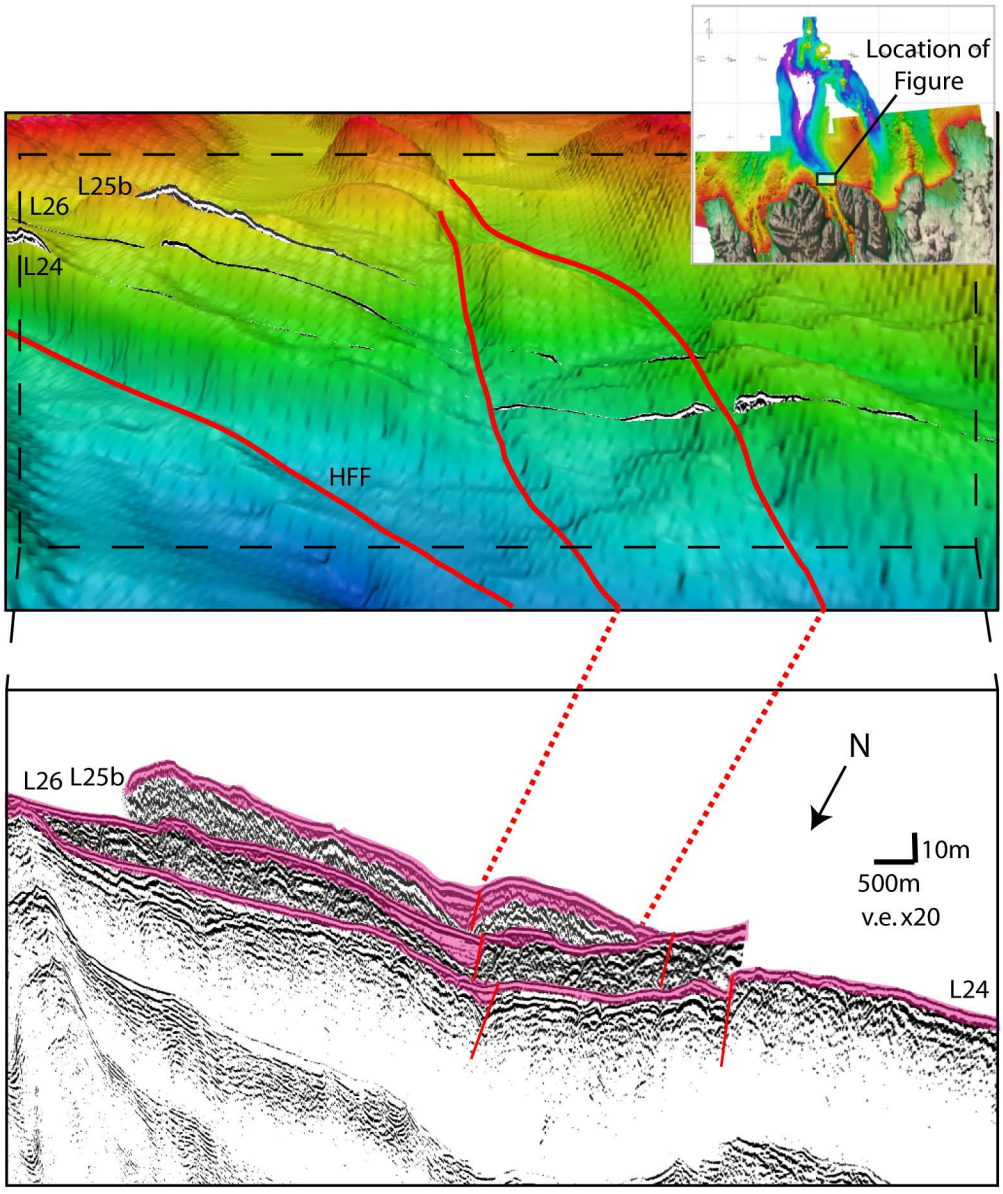


## Figure 4.6

MCS data located in the mouth of Eyjafjördur bay, Holocene sediment highlighted in pink, illustrating the infilling of the fault controlled structures south of the HFF and close to shore.

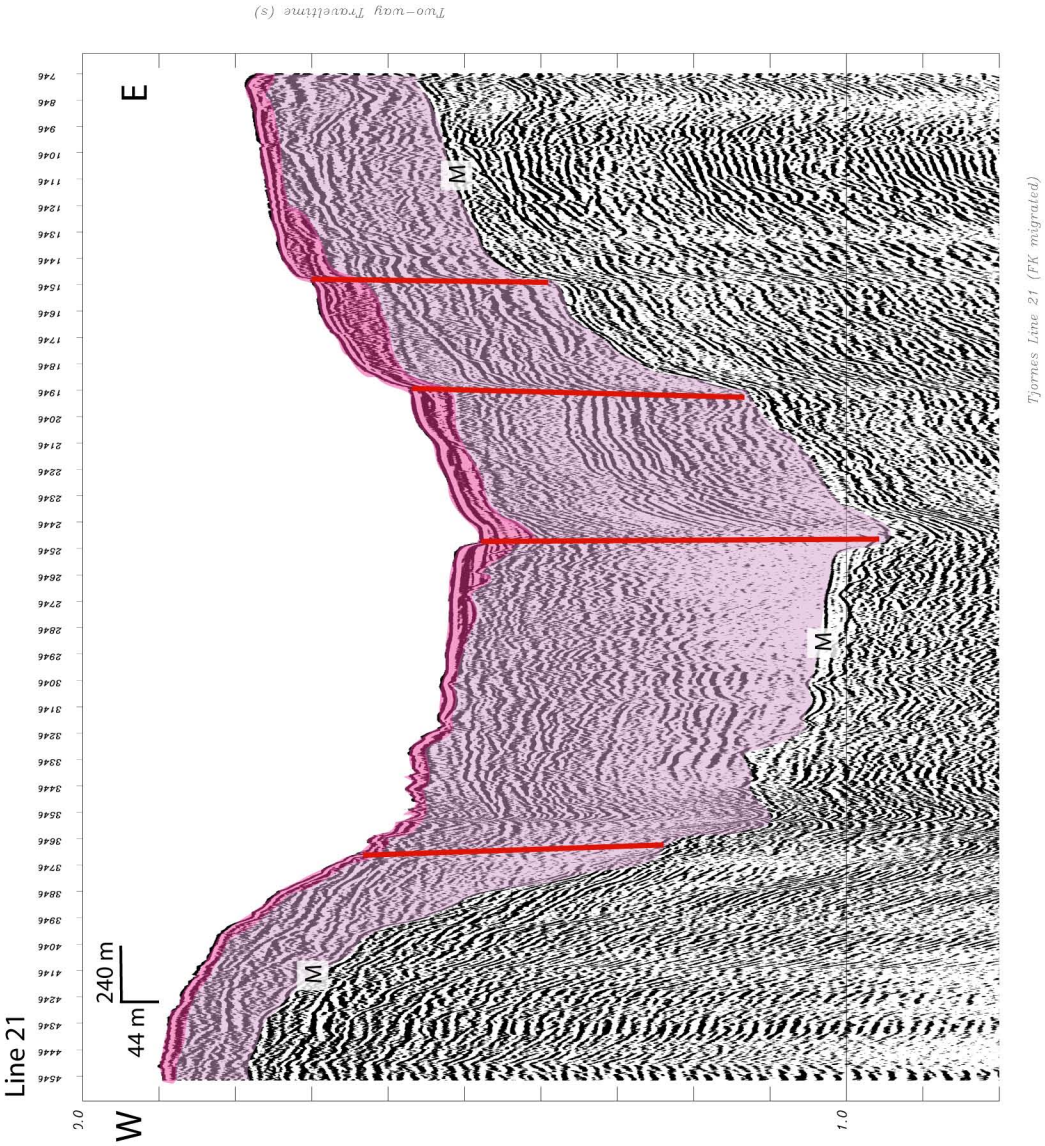


## Figure 4.7a

MCS data within Eyjafjördur Bay, for locations see Figure 4.6, a) through d) are located progressively farther north. Pink indicates Holocene/Pleistocene sedimentation above the truncation surface created at the LGM, purple indicates sediment below the truncation surface. Green and yellow indicate glacial sediments deposited at the edge of the glacier, M indicates the multiple.

a) L21; close to shore with four active faults cutting the seafloor. The greatest offset is seen in the center of the bay as this is the HFF.

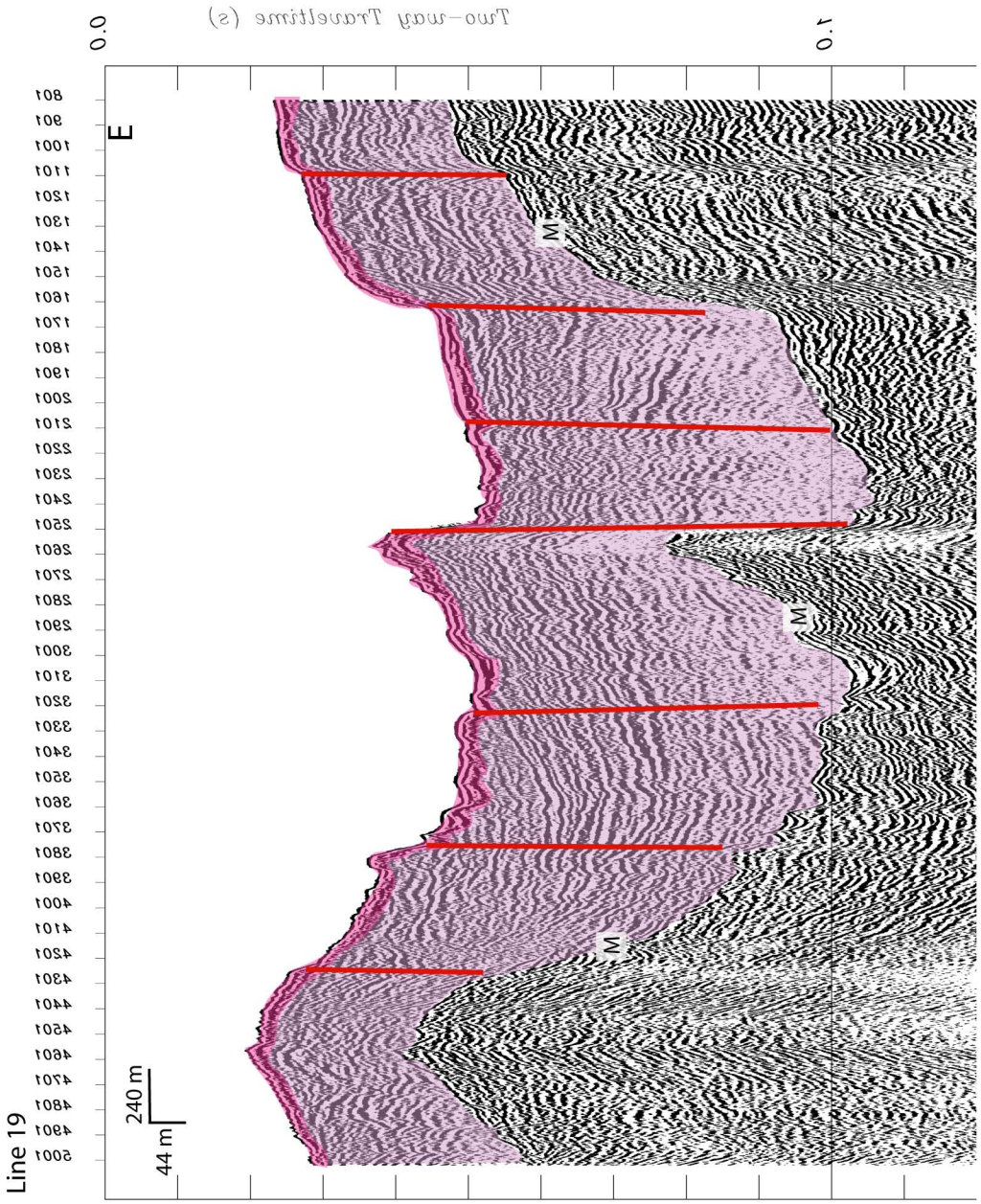


Figure 4.7b

MCS data within Eyjafjördur Bay, for locations see Figure 4.6, a) through d) are located progressively farther north. Pink indicates Holocene/Pleistocene sedimentation above the truncation surface created at the LGM, purple indicates sediment below the truncation surface. Green and yellow indicate glacial sediments deposited at the edge of the glacier, M indicates the multiple.

b) L19; more active faults, but the most active one is still the HFF. The large relief in this profile coincides with the reorientation of the fault to a more northerly orientation

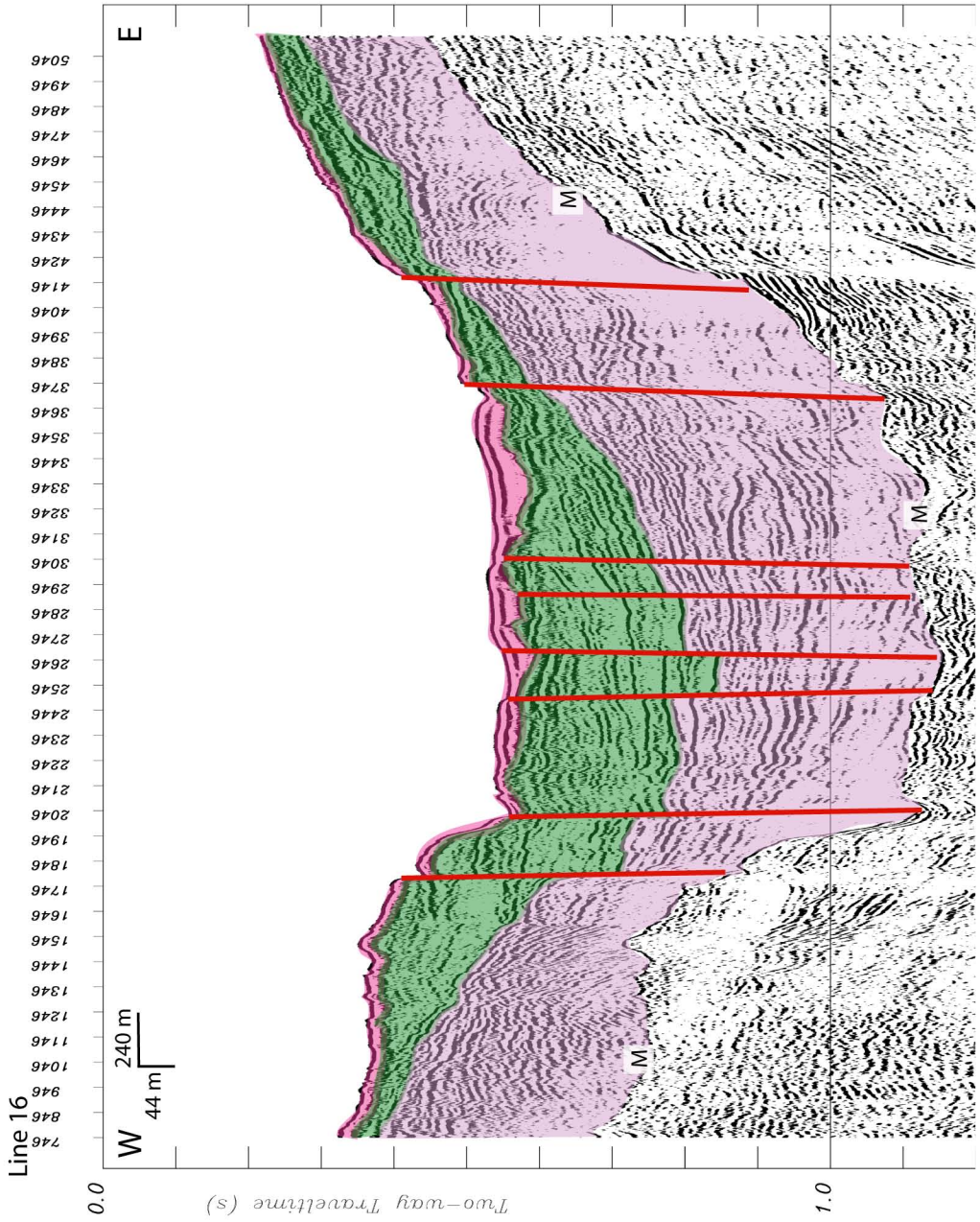


Figure 4.7c

MCS data within Eyjafjördur Bay, for locations see Figure 4.6, a) through d) are located progressively farther north. Pink indicates Holocene/Pleistocene sedimentation above the truncation surface created at the LGM, purple indicates sediment below the truncation surface. Green and yellow indicate glacial sediments deposited at the edge of the glacier, M indicates the multiple.

c) L16; Green sediments deposited at the margin of the glacier, some indications of lobe switching observed. Significant offset seen on the active faults with differences in acoustic character indicating some component of strike slip movement.

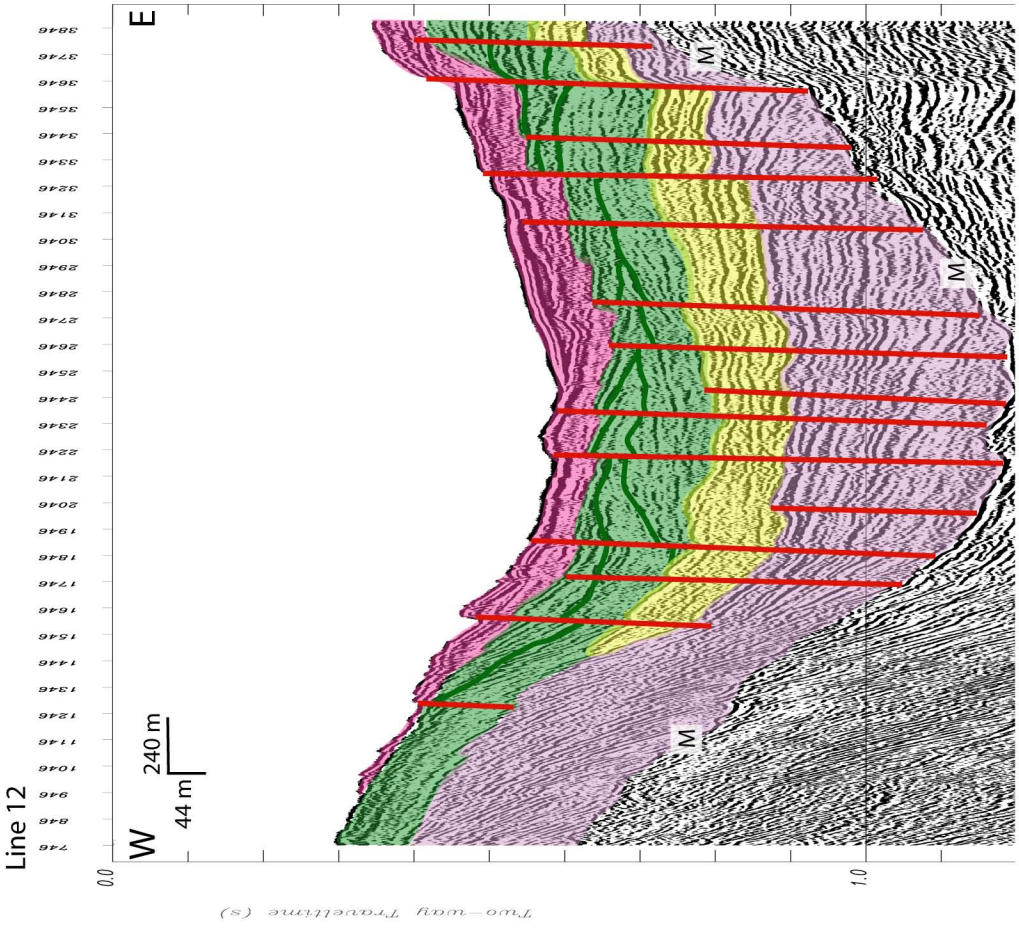


## Figure 4.7d

MCS data within Eyjafjördur Bay, for locations see Figure 4.6, a) through d) are located progressively farther north. Pink indicates Holocene/Pleistocene sedimentation above the truncation surface created at the LGM, purple indicates sediment below the truncation surface. Green and yellow indicate glacial sediments deposited at the edge of the glacier, M indicates the multiple.

d) L12; northern most line with green lobe switching layer (indicated by darker green lines) and a chaotic layer, perhaps a jökulhlaup deposit underlying it.

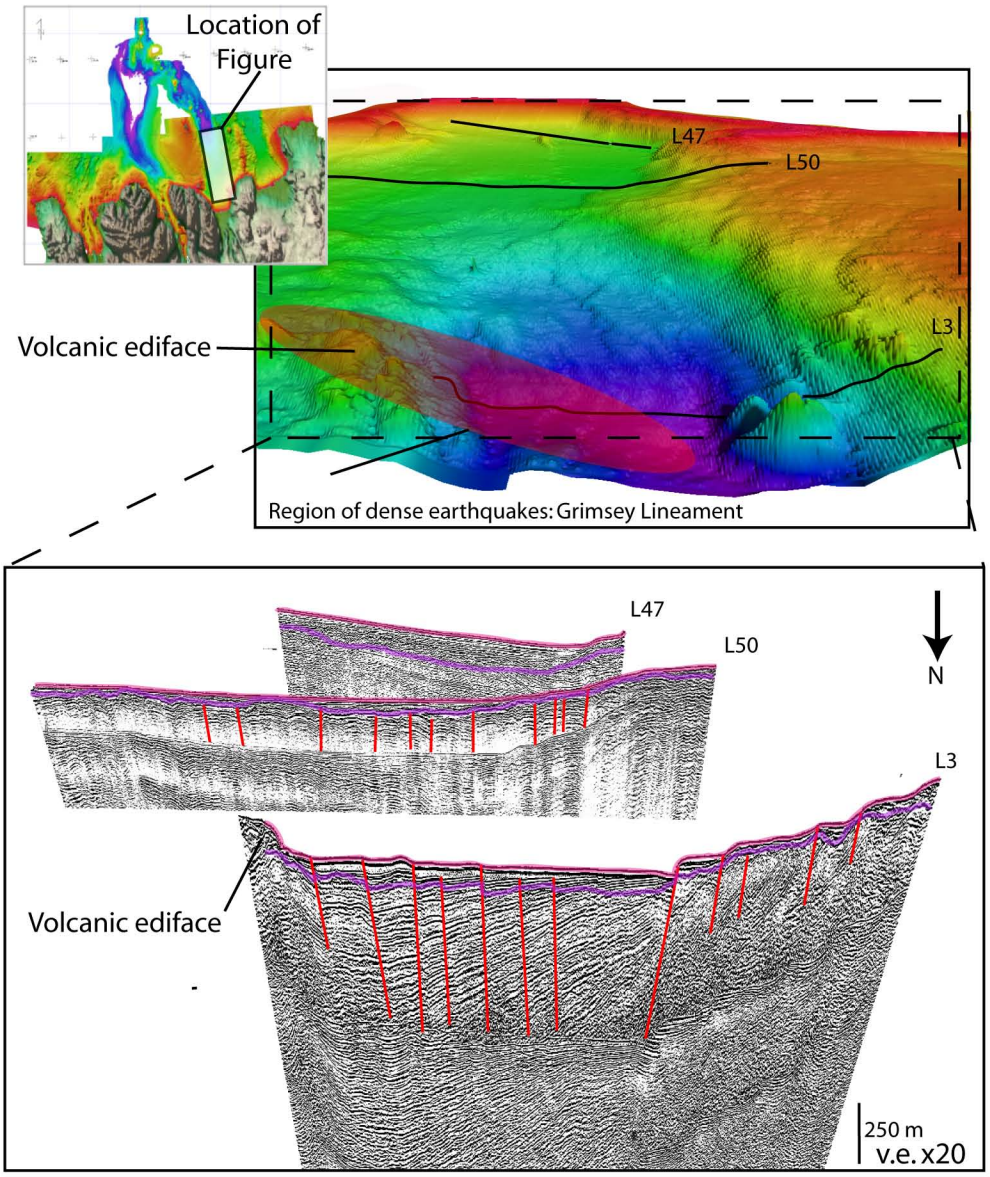


## Figure 4.8

L47, 50, 3 are located in the southern middle and northern Skjálfandi Bay. The southern most line has little deformation, the central line has a limited amount of older deformation and the northern line crosses the GL, and has significant deformation. The faults are largely active to the seafloor and there are differences in acoustic character across the faults that suggest a component of strike-slip offset.

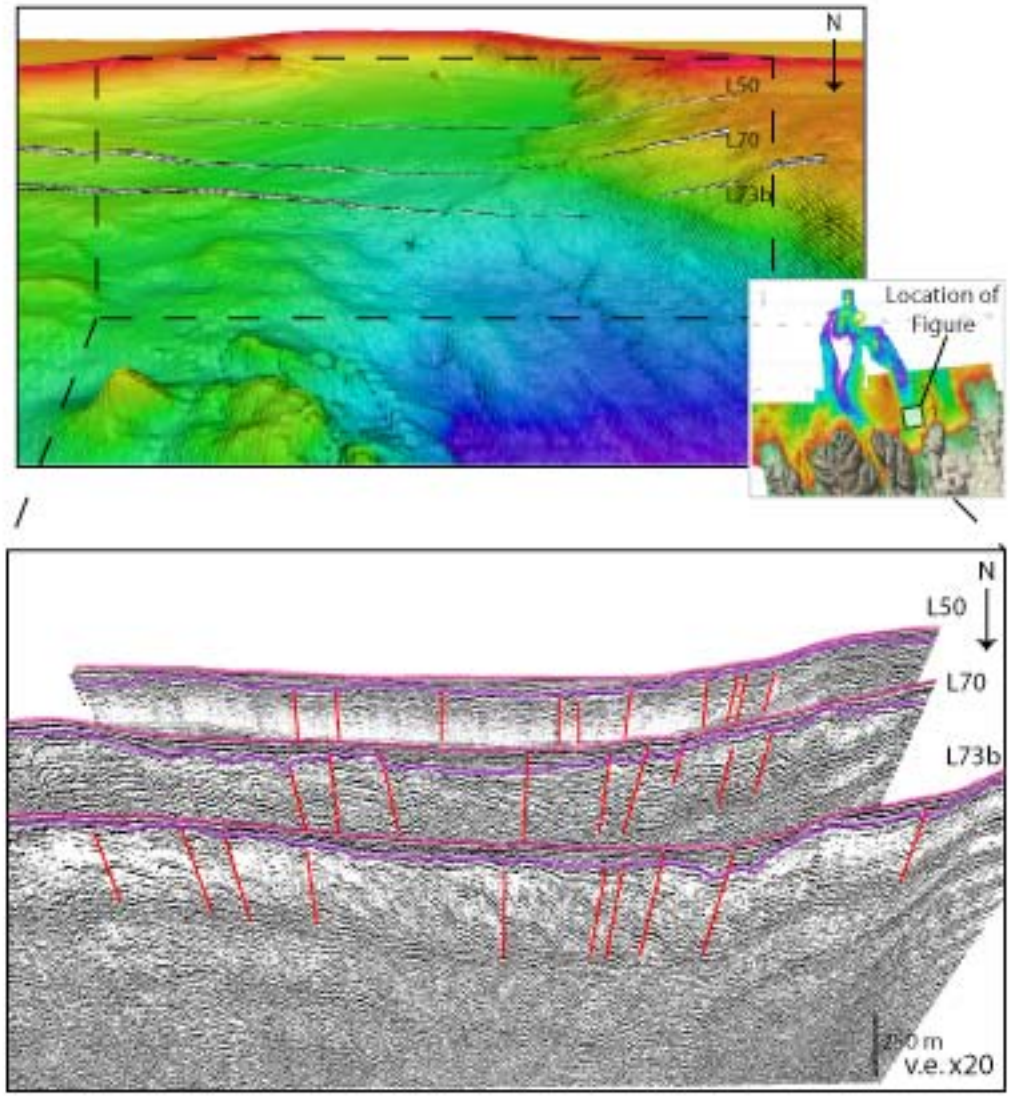


## Figure 4.9

Seismic from central Skjálfandi Bay away from the GL or the HFF. Faulting and deformation is limited but increases to the north closer to the GL. Numerous inactive faults do not cut through the truncation surface. The locations of the seismic data are shown in the bathymetric data, with red lines indicating faults in the data, the pink line on the seismic data indicate the top of the Holocene sediments while the purple line indicates the truncation surface created at the LGM.

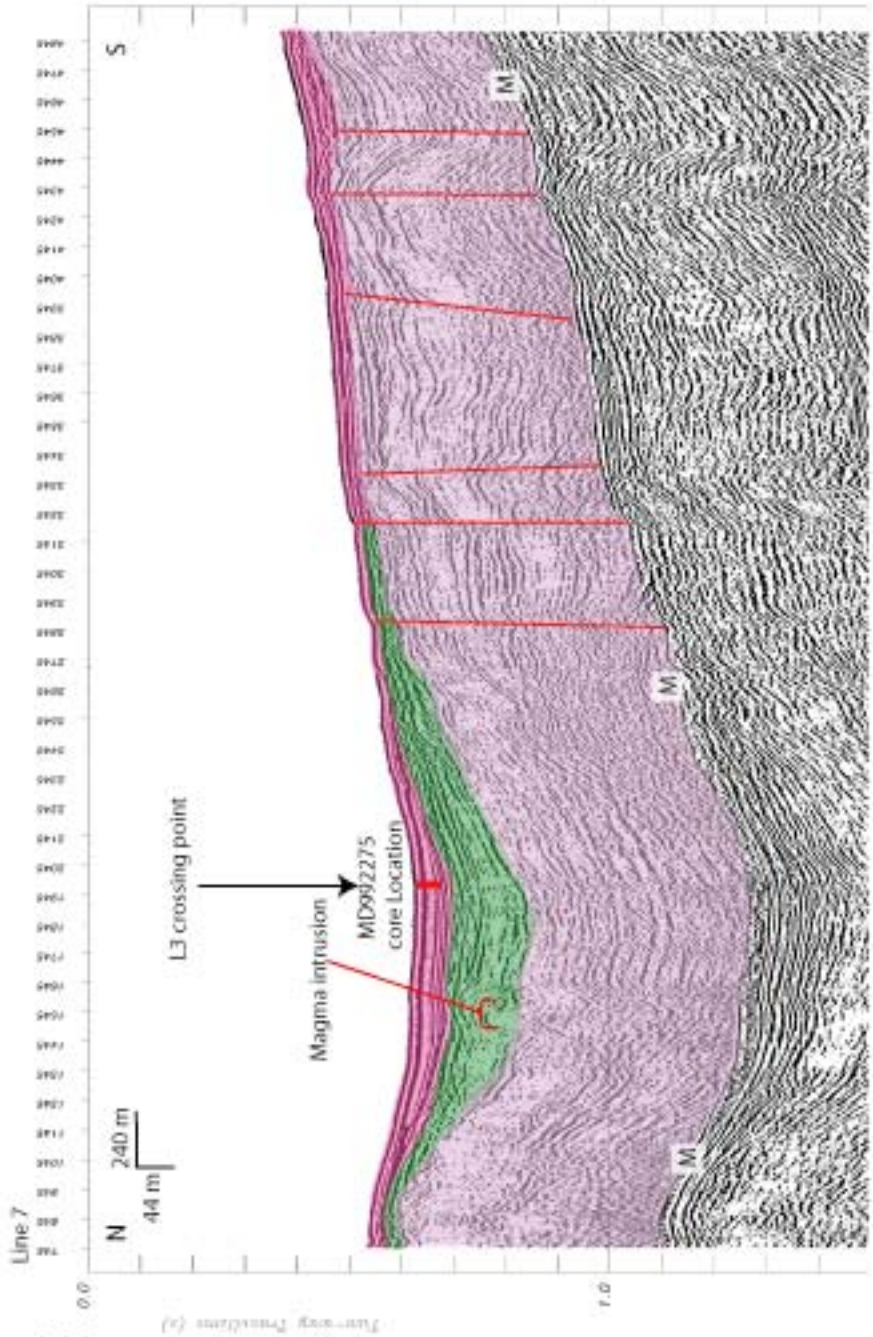


## Figure 4.10

Line 7 runs N-S through northern Skjálfandi bay crossing the GL. The truncation surface deepens into the basin, at the base of the stratigraphic successions deposited at the edge of the glacier. A magamatic intrusion may be imaged at depth within the GL. The locations of the seismic data are shown in the bathymetric data, with red lines indicating faults in the data, the pink lines on the seismic data indicate the top of the Holocene sediments while the purple line indicates the truncation surface created at the LGM.

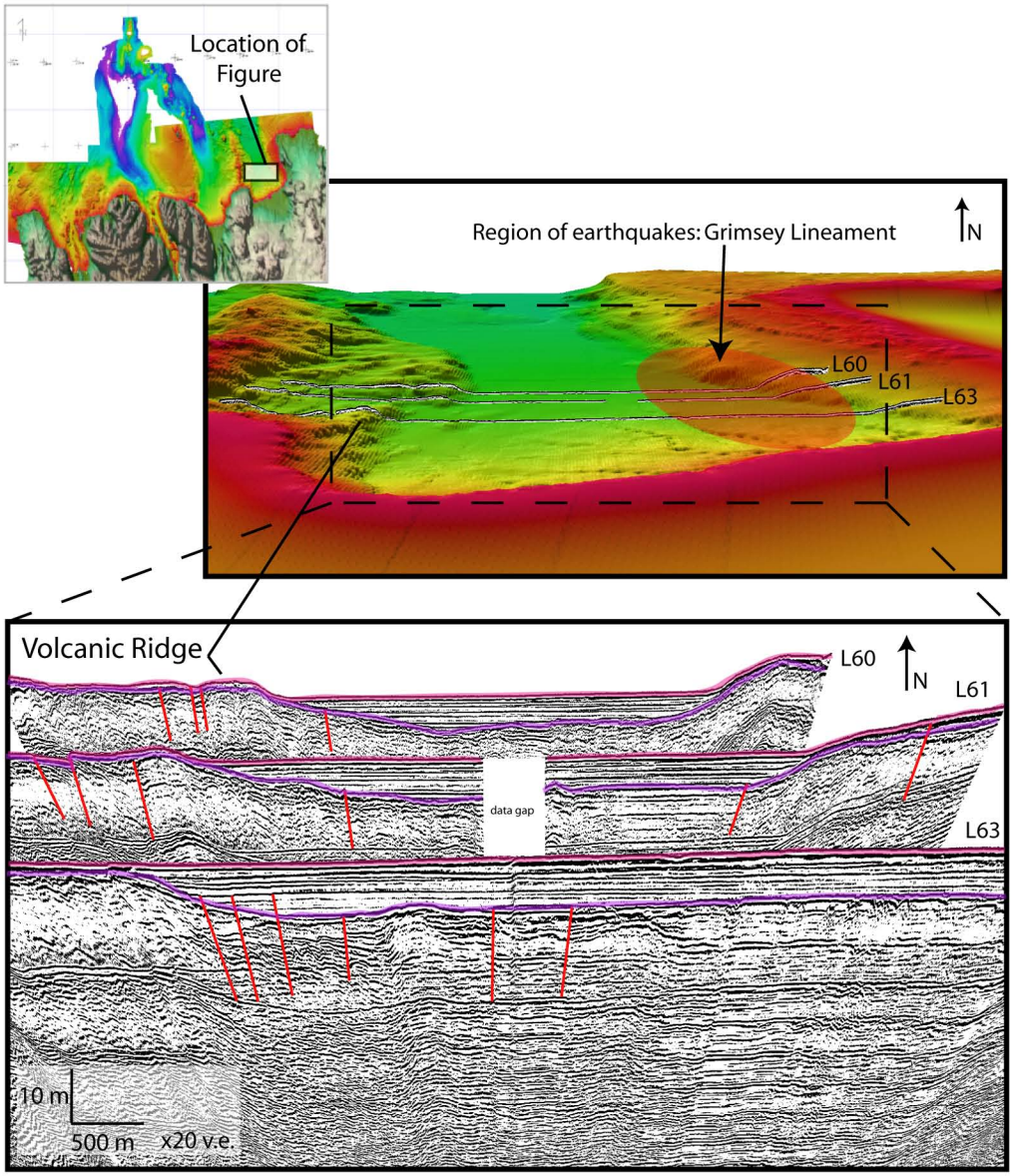


## Figure 4.11

Lines in southern Öxarfjördur Bay crossing the eastern edge of the GL, some limited faulting is observed in the area of high earthquake activity. The locations of the seismic data are shown in the bathymetric data, with red lines indicating faults in the data, the pink lines on the seismic data indicate the top of the Holocene sediments while the purple line indicates the truncation surface created at the LGM.

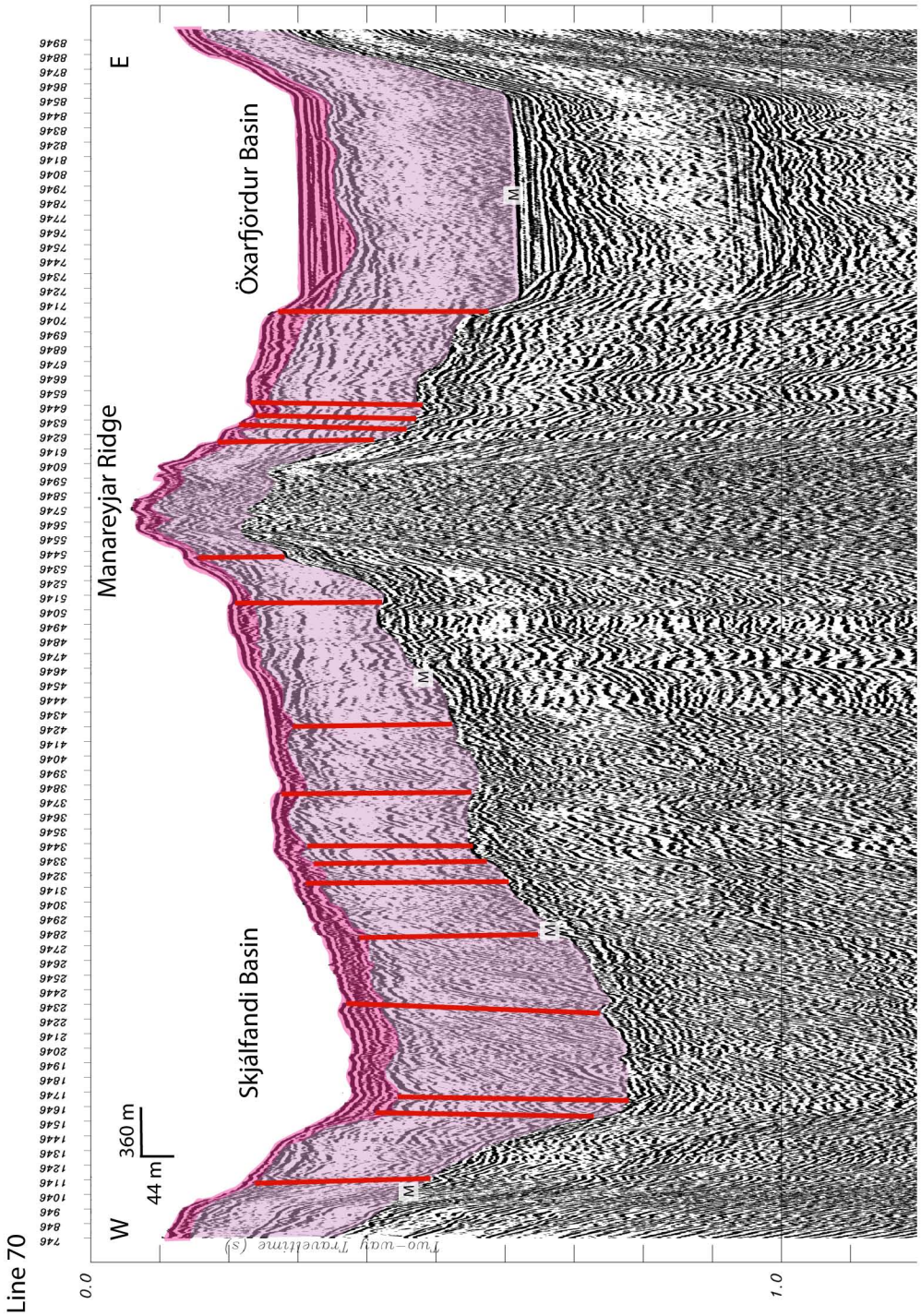


## Figure 4.12

MCS data L70, crossing both Skjálfandi and Öxarfjördur bays showing the volcanic constructs and laminated sediments infilling the Öxarfjördur Bay.

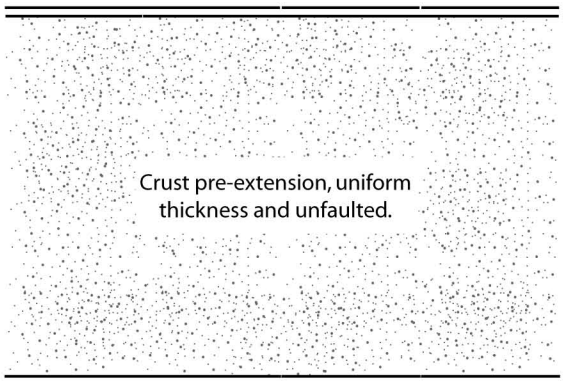


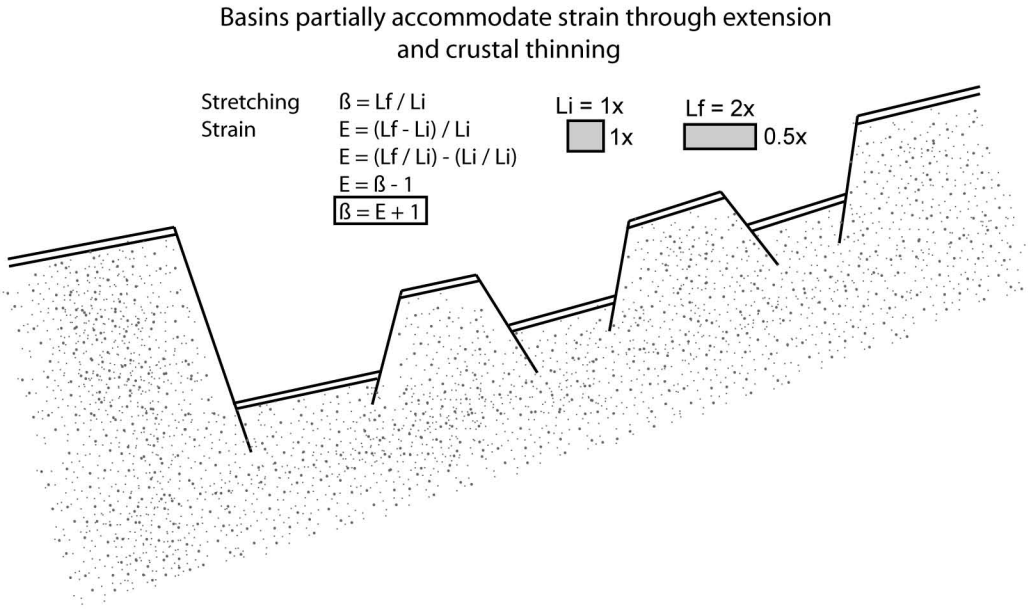


## Figure 4.13

Basin extension accommodates strain through faulting and crustal thinning. Down dropped basins are common. Stretching is a measure of the ratio of the final length to the initial length, and strain is a measure of the change in length to the initial length.

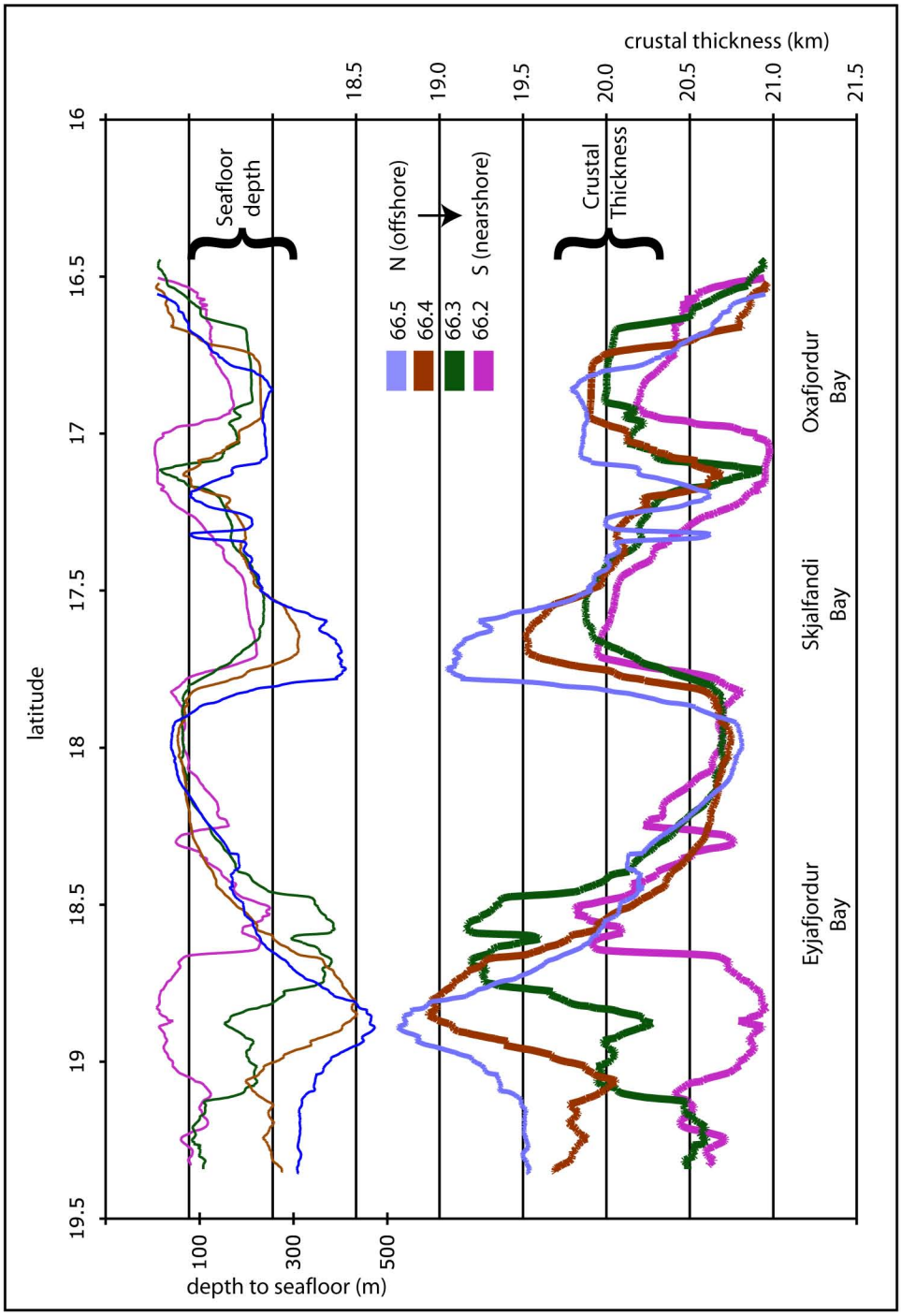


Figure 4.14

Crustal thickness based on bathymetry and local isostasy: Lightweight lines are the bathymetry from the different profiles, and the heavy lines are the crustal thickness calculated based on these profiles. Extension estimates are shown in Table 4.1.

A.

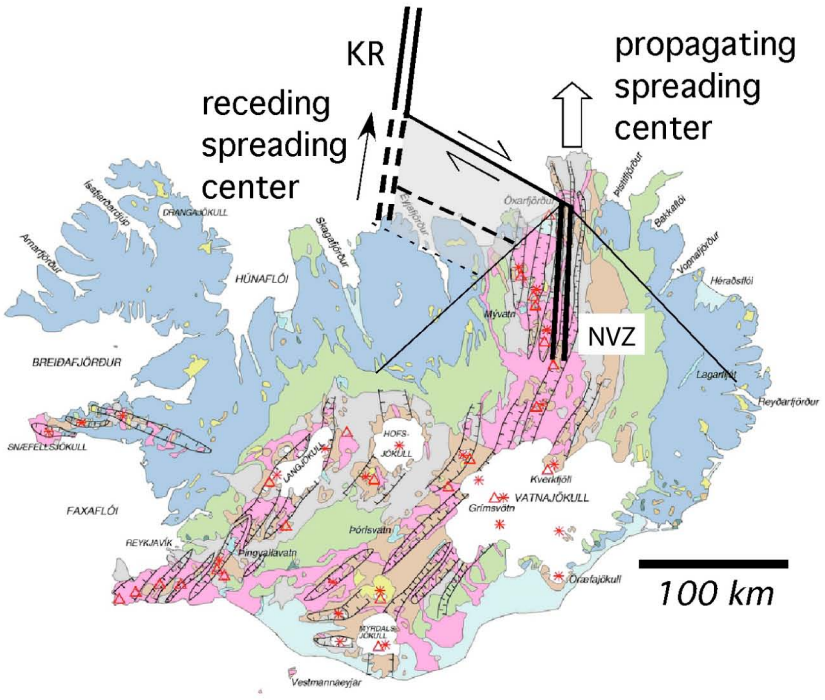


B.

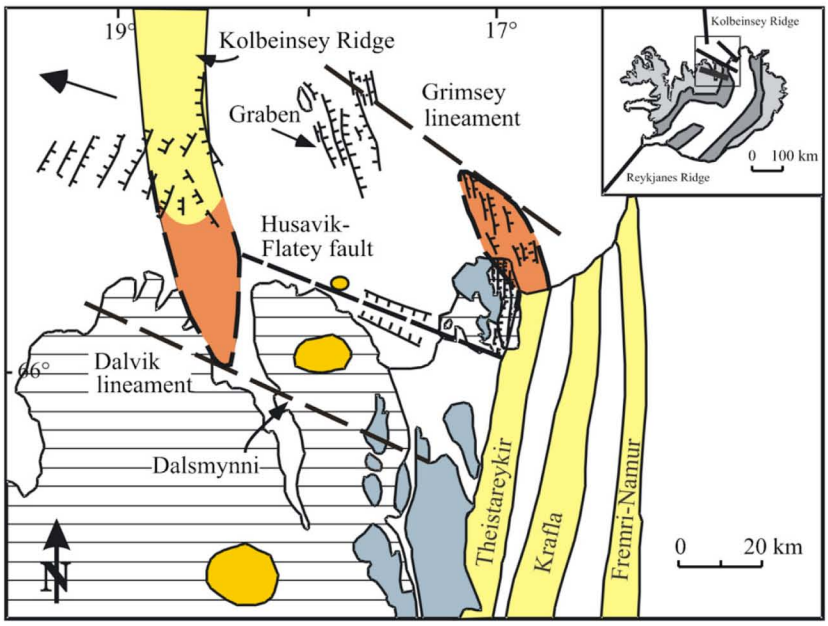


## Figure 4.15

Two hypotheses for the tectonic evolution of the TFZ;

a) Migrating fracture zone, driven by the northward propagation of the NVZ and northward retreat of the KR. Activity progressively transferring from the DL to the HFF to the GL.

b) Microplate rotation as the NVZ propagates north and the KR propagates south. Activity presently focused on the HFF, and transferring both to the GL and the DL.

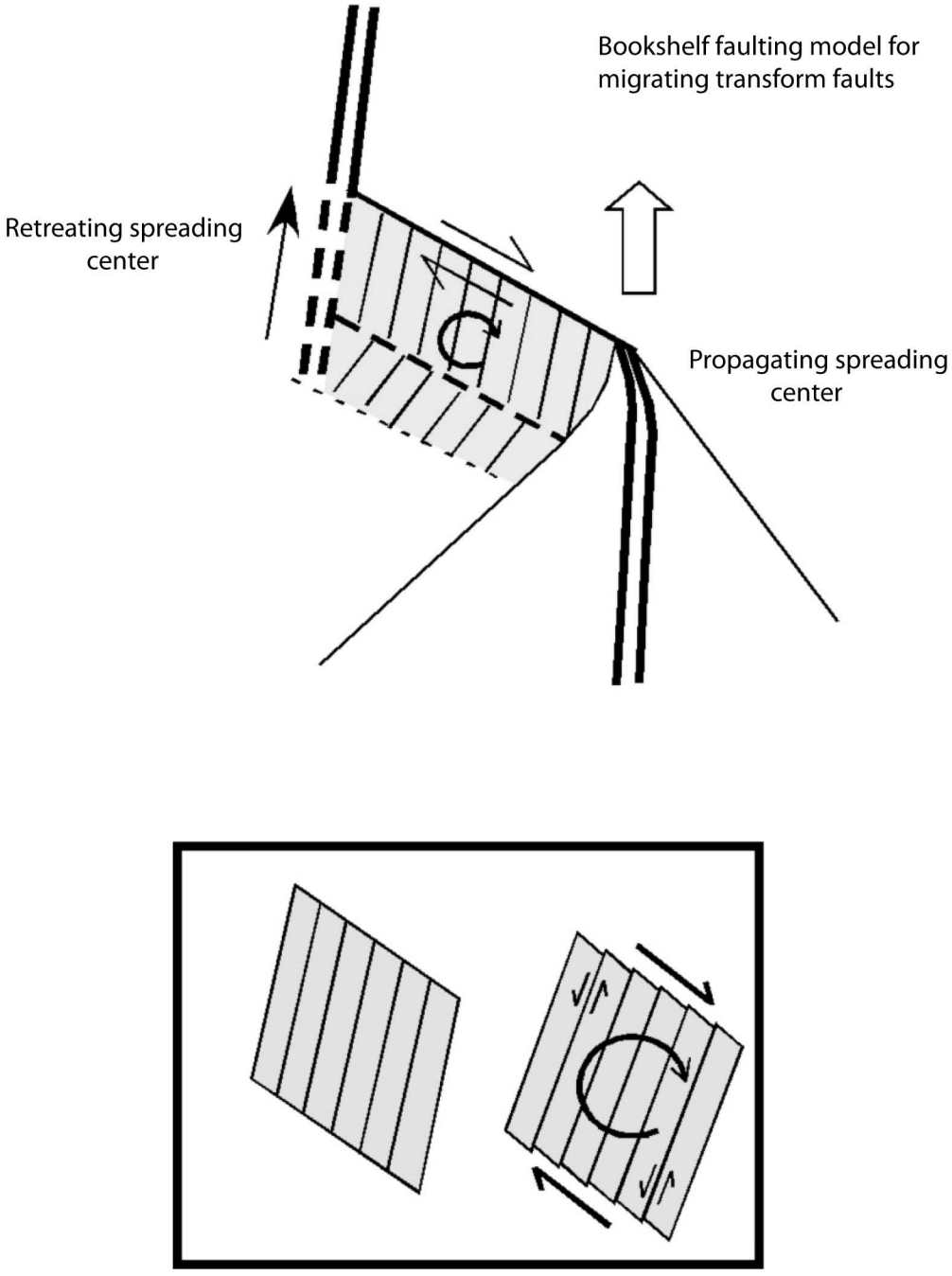


Figure 4.16

Bookshelf faulting model for migrating transform faults modified from Phipps Morgan & Kleinrock, 1991; Wetzel at al 1993

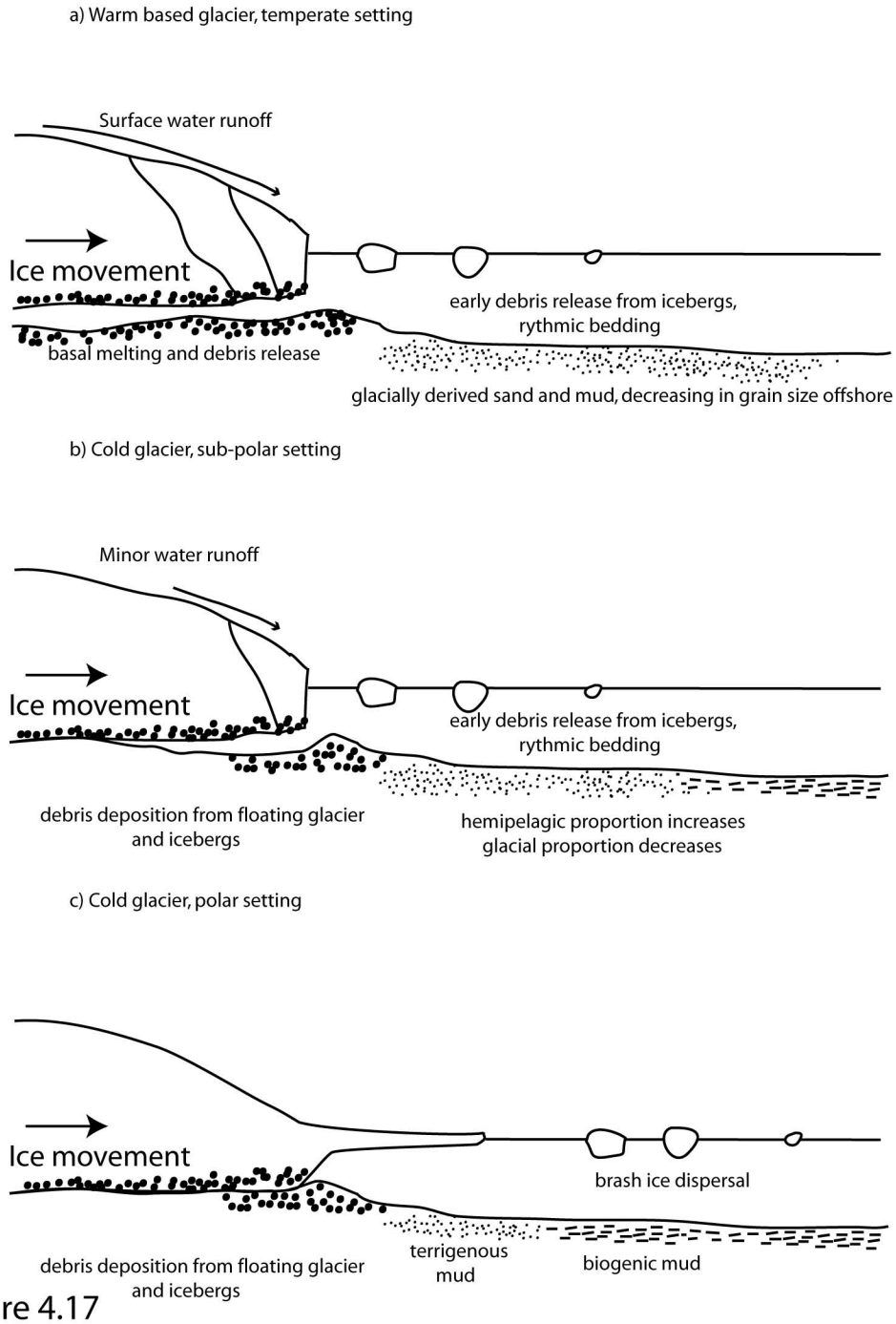


Figure 4.17

Sedimentation patterns and mechanisms seen on glacial edges. a) warm temperate glacier; generally floating glacier with limited sedimentation beneath from melting with rhythmically bedded terrigenous sand and mud. b) cold glacier, sub polar setting; some grounded glacier along with some floating near the edge, with rhythmically layered sediments with a proportion biogenic in origin. c) cold glacier, polar settings; fully grounded glacier with brash ice dispersed sediment deposition and a large component of biogenic sediments.

## 4.8 REFERENCES

Anglier J., Bergerat F., Homberg C., 2000, Variable coupling across weak oceanic transform fault, Flateyjarskagi, Iceland, Terra Nova, 12, 97-101.

Ashley, G.M., Smith, N.D., 2000, Marine seimentationi at a calving glacier margin, GSA Bulletin, v. 112 no.5, 657-667

Auzende, J.-M., Bideau D., Bonatti E., Cannat M., Honnorezparallel J., Lagabrielle Y., Malavieille J., Mamaloukas-Frangoulis V., and Mevel C., 1989, Direct observation of a section through slow-spreading oceanic crust, Nature, 337, 726-9

Bergerat F., Angelier J., Homberg C., 2000, Tectontic analysis of the Húsavík-Flatey (northern Iceland) and mechanisms of an oceanic transform zone, the Tjörnes Fracture Zone. Tectonics, 19, 1161- 1177.

Bosworth, W., 1985. Geometry of propagating continental rifts. Nature 316, pp. 625–627.

Cohen, J. K., and J. W. Stockwell Jr., 1999, CWP/SU: Seismic Unix Release 33: A free package for seismic research and processing, software, Cent. for Wave Phenom., Colo. Sch. of Mines, Golden, Colo.

Collette, B.J., 1979, Thermal contraction joints in spreading seafloor as an origin of fracture zones, Nature, 251, 299-300.

Darbyshire, F.A., Priestley, K.A., White, R.S., Stefánsson, R., Gudmundsson, G.B., Jakobsdóttir, S.S., 2000, Geophysical International, vol. 143, no. 1, 163-184

Driscoll, N.W., Karner, G.D., Weissel, J.K., and the Shipboard Scientific Party, 1989. Stratigraphic and tectonic evolution of Broken Ridge from seismic stratigraphy and Leg 121 drilling. In Peirce, J., Weissel, J., et al., Proc. ODP, Init. Repts., 121: College Station, TX (Ocean Drilling Program), 71–91. doi:10.2973/odp.proc.ir.121.104.1989

Einarsson, P., 1991, Geology of Iceland, Mál og menning, Reykjavik

Fenwick, R., Brandsdóttir, B., Driscoll, N., Detrick, R., Kent G., Accepted, Tectonic Deformation on the Husavik-Flatey Fault, Northern Iceland, Marine Geology.

Fjäder K., Gudmundsson A., Forslund T., 1994, Dikes, minor faults and mineral veins associated with a transform fault in North Iceland, Journal of Structural Geology, 16, 109-119.

Fox P. J., Gallo D. G., 1984, A tectonic model for ridge-transform-ridge plate boundaries: implications for the structure of oceanic lithosphere, Tectonophysics, vol. 104, 205-242

Hardarson, B. S., Fitton, J. G., Ellam, R. M., and Pringle, M. S., 1997, Rift relocation: A geochemical and geochronological investigaion of a palaeo-rift in northwest Iceland, Earth and Planetary Science Letters, 153, 181-196.

Henkart, P., 2003, SIOSEIS, software, Scripps Inst. of Oceanogr., La Jolla,Calif. (available at http://sioseis.ucsd.edu).

Hieronymous, 2004 C.F. Hieronymous, Control on seafloor spreading geometries by stress- and strain-induced lithosphere weakening, Earth Planet. Sci. Lett. 222 (2004), pp. 177–189.

Hubbard, A., Sugden, D., Dugmore, A., Norddahl, H., Pétursson, H.G., 2006, A modeling insight into the Icelandic Last Glacial Maxium ice sheet, Quaternary Science Reviews, 25, 2283-2296.

Ísaksson, S.P., 1985, Stórhlaup, Í Jökulsá á Fjöllum a fyrri hluta 18. aldar, Natturufraethingurinn, 54, 165-191

Kusznir N.J., and Egan, S.S. , 1989 Simple-shear and pure-shear models of extensional sedimentary basin formation: application to the Jeanne d'Arc

basin, Grand Banks of Newfoundland. American Association of Petroleum Geologists Memoir 46 (1989), pp. 305–322.

Garcia S., Arnaud N.O., Angelier J., Bergerat F., and Homberg C., 2003, Rift jump process in Northern Iceland since 10 Ma from 40Ar/39Ar geochronology, Earth and Planetary Science Letters, 214, 529-544.

Gibbs A. D., 1984, Structural evolution of extensional basin margins, Journal of the Geological Society, v. 141, 609-620.

Gudmundsson, M.T., Sigmundsson F., Björnsson, H., 1997, Ice-volcano interaction of the 1996 Gjálp subglacial eruption, Vatnajökull, Iceland, Nature, 389, 954-957.

Gudmundsson A., Brynjolfsson S., Jonsson M.T., 1993, Structural analysis of a transform fault-rift zone junction in North Iceland, Tectonophysics, 220, 205-221.

Jancin M., Young K.D., Voight B., Aronson J.L., Saemundsson K., 1985, Stratigraphy and K/Ar ages across the west flank of the northeast Iceland axial rift zone, in relation to the 7 Ma volcano-tectonic reorganization of Iceland, J. Geophys. Res., 90, 9961-9985.

Vogt P. R., and Johnson G. L., 1973, Magnetic Telechemistry of Oceanic Crust, Nature 245, 373-375.

Kearney P., and Vine F.J., (1996) Global Tectonics, Blackwell Science.

Lavier L. L., and Buck W. R., 2002, Half graben versus large-offset low-angle normal fault: Importance of keeping cool during normal faulting, Journal of Geophysical Research, 107, 2122.

Macdonald K, Luyendyk B. P., 1985, Investigation of faulting and abyssal hill formation on the flanks of the East Pacific Rise (21°N) using ALVIN, Marine Geophysical Researches, 515-535.

Menard, H. W., (1964) Marine Geology of the Pacific, McGraw-Hill, New York

Menard, H. W., and Atwater, T.,1969, Origin of fracture zone topography, Nature, 222, 1037-40.

Morley C. K., 1995, Rift Structure: Models and Observations: Developments in the structural geology of rifts over the last decade and their impact on hydrocarbon exploration, Geological Society, London, Special Publications, 80, 1-32.

Parsons B., and Sclater J.G., 1977, An analysis of the variation of ocean floor bathymetry and heat flow with age, Jouranl of Geophysical Research, 82, 803-27.

Pockalny R. A., Detrick R. S., Fox, P. J., 1988, Morphology and tectonics of the Kane Transform from Sea Beam bathymetry data, Journal of Geophysical Research, 93, 3179-3193.

Rosendahl B. R., 1987, Architecture of Continental Rifts with Special Reference to East Africa, Annual Review of Earth and Planetary Sciences, 15, 445-503.

Saemundsson K., 1974, Evolution of the axial rifting zone in Northern Iceland, Geol. Soc. of Am. Bull., 85, 495-504.

Saemundsson K., 1978, Fissure Swarms and Central Volcanoes of the Neovolcanic Zones of Iceland. Geology Journal Special Issue, No. 10, 415–432.

Searle, R. C., 1986, GLORIA Investigations of Oceanic Fracture Zones: Comparative Study of the Transform Fault Zone,J. Geol. Soc. London 143 743–756.

Schouten H., Klitgord K. D., and Whitehead J. A., 1985, Segmentation of mid-ocean ridges, 317, 225 – 229

Sigmundsson F., 2006, Iceland Geodymanics, Crustal Deformation and Divergent Plate Tectonics, Springer.

Smith M., Mosley P., 1993, Crustal heterogeneity and basement influence on the development of the Kenya Rift, East Africa, Tectonics, 12, 591-606.

Sugden, D.E., John, B.S., 1976, Glaciers and Landscapes, Edward Arnold, ISBN 0 7131 5840 9

Sykes, L.R., (1967) Mechanism of earthquakes and nature of faulting on the mid ocean ridges, Journal of Geophysical Research, 72 , 2131-2153.

Taylor, B., Crook, K., Sinton, J., 1994, Extensional transform zones and oblique spreading centers, Journal of Geophysical Research, 99, 19707-18.

Thompson, G, and Melson, W. G., 1972, The petrology of oceanic crust across fracture zones in the Atlantic Ocean: evidence of a new kind of seafloor spreading, Journal of Geology, 80, 526-38.

Tucholke B. E., and Schouten H., 1988, Kane Fracture Zone, Marine Geophysical Researches, 10, 1- 39.

Tryggvason E., 1973, Seismicity, earthquake swarms, and plate boundaries in the Iceland region, Bull. Seis. Soc. Am. 63, 1327-1348.

Uchupi, E., Driscoll, N., Ballard R.D., Bolmer S.T., 2001, Drainage of late Wisconsin glacial lakes and morphology and late quaternary stratigraphy of the New Jersey-southern New England continental shelf and slope, Marine Geology, 172, 117-145.

Waitt, R.B., 2002, Great Holocene floods along Jökulsá á Fjöllum north Iceland, Spec. Pubs. Int Ass. Sediment, 32, 37-51.

Wilson, J.T., (1965) A new class of faults and their bearing on continental drift, Nature, 207, 343-7.

Wolfe, C-J, Bjarnason, I.T. VanDecar, J.C. and Salomon, S.C. (1997) Seismic structure of the Iceand mantle plume, Nature, 385, 245-247.

# Chapter 5

# Conclusion

pThis dissertation has presented a working model of the tectonic evolution of the Tjörnes Fracture Zone in Northern Iceland, and investigated the stratigraphic evolution of a tectonically and glacially active margin using the first comprehensive offshore data set for the region. This research examines how evolving fracture zone distributes deformation through time, creating new faults/lineaments and reactivating pre-existing structures. We also address the controls and influences on pockmark locations and morphology on the sea floor.

Studying this continually evolving system allows us the opportunity to understand better the complicated nature of evolving transform faults. In the Tjörnes Fracture Zone, there appears to have been an initial stage of extension accommodation more in line with continental style accommodation zones: graben faulting with normal faults accommodating the extension between the northern NVZ and the southern extent of the KR. This appears to have been followed and overprinted by more traditional oceanic transform faulting, with the development of the HFF and then subsequently with the northward propagation of the North Volcanic Zone, that is the Grímsey Lineament.

In Chapter 2, we present new evidence for the distribution of pockmarks in Skjálfandi Bay, and have a hypothesis for their distribution and consequent

morphology. Some insight has also been gained into the interaction between seafloor processes, such as tides and currents, and the expulsion of fluid/sediments giving rise to pockmark morphology. In the vicinity of the HFF, there is an observed increase in biology near the pockmarks and hard grounds exposed along the HFF that might be associated with increased nutrients being supplied by the fluid.

## 5.1 POCKMARK DISTRIBUTION AND SEAFLOOR MAPPING IN SKJÁLFANDI BAY

Pockmarks are increasingly being identified as common features along margins, CHIRP, MCS, bathymetry, side-scan sonar, and towcam pictures allow us to investigate the occurrence and limitations of their location and morphology. In Skjálfandi Bay, there are two primary locations where pockmarks are observed; offshore in a band ~15-22 km, and in close proximity to the HFF fault scarp along the western side of the bay. Pockmarks located along the fault plane are easily attributed to fluid migrating along the fault plane from depth, and the increase in faunal diversity on or near the pockmarks is likely to be from an increased nutrient flux as part of the fluid flow or detrital deposition in the pockmarks.

Pockmarks located in a band farther out in the bay occur where the recent and glacial sediments are thin enough to allow fluid migration from depth along westward dipping bedding planes; recent sediments are < 30 m thick and glacial sediments are < 50 m thick. They occur in a well-defined band within Skjalfandi Basin that we propose is determined by the interplay of the distribution of source material and the thickness of the overlying glacial sediments. The source for the fluid is thermogenic gases from depth, most likely sourced from the Tjörnes beds. The increased thermal gradient in this area allows organic material to reach the thermogenic “cracking” window at a shallower depth. The pockmarks have a very distinct morphology, in cross section they are “v” shaped and in plan view they are asymmetric. A “v” shaped cross section is indicative of an active pockmark; repeated blowouts keep the pockmark excavated and the walls steep, the asymmetry of the plan view morphology results from overprinting of the seafloor by currents. This focused fluid flow along the bedding planes results in linear pockmark chains that undergo subsequent modification by clockwise bottom currents. The orientation of the overprinted tail on the pockmarks indicated that the circulation is most likely associated with the North Irminger Current. The towcam images collected along the HFF and elsewhere in the bay indicate that fluid flow is still active. There is a higher faunal density within the large pockmarks. Some of the towcam photos captured small sediment expulsion

features around the smaller pocks, piles of sediment perhaps blown out from the pock. Fluid flow along transform faults is an important process, and appears to develop early on in the evolution of transform faults systems.

## 5.2 TECTONIC EVOLUTION OF THE TJÖRNES FRACTURE ZONE

This increasing spatial separation between the extension on land and the MAR gives rise to repeated rift jumps, creating new transform fault/accommodation zones. In the Tjörnes Fracture Zone there are two main active faults oblique to the spreading segments connecting the southern portion of the Kolbeinsey Ridge and the northern portion of the North Volcanic Zone. The Husavik-Flatey Fault curves north into the southern KR in Eyjafjördur Bay and south into the Theistareykir Fissure Swarm, the Grímsey Lineament to the north of the HFF connects to the southern portion of the KR, crosses the Manareyjar Ridge and then connects to the North Volcanic Zone. Areas of highest seismic activity occur along the GL between Manareyjar Ridge and KR, where the GL joins the NVZ, and where the HFF curves into the KR.

The initial phase of tectonic response from the rift jump appears to be distributed extensional deformation across the three basins (Eyjafjördur,

Skjálfandi, Öxarfjördur), along north trending normal faults. The DL appears to be the southern boundary of distributed deformation. As the NVZ becomes more organized the extensional deformation was replaced by dextral strike-slip faults giving rise to the HFF. The deformation along the HFF is ongoing, albeit decreased from the maximum that occurred in the Miocene. This decrease in activity is the result of the NVZ propagating past the HFF and transferring a portion of the deformation to the GL. Based on GPS data, the deformation is approximately equal between the HFF and the GL. This northward migration of the NVZ is accompanied by the northward retreat of the KR imparting a clockwise rotation that reactivates the N-S normal faults as oblique slip sinistral strike-slip faults in the manner of bookshelf faulting.

Research presented here provides illumination on the processes that occur during rift jumps and subsequent plate boundary development. Further work is needed to finalize this model by defining the deformation present on the GL. Furthermore, assessing the NW trending fabrics that are observed onshore and near shore would offer insights into the initial phases of extension.